Microtrons and Recirculators

Andreas Jankowiak
Institut für Kernphysik
Johannes Gutenberg – Universität Mainz

The CERN Accelerator School
Small Accelerators
31.05.2005

Contents

1) Definition of the subject: Recirculation ?

2) Introduction of the different types of accelerators (main part of the lecture)

a) Classical Microtron (concept of phase focussing)
b) Race-Track-Microtron (detailed longitudinal dynamic)
c) Recirculators (isochronous, independent orbit recirculation)

3) Further classification concerning Rf-systems

normal conducting (nc) $\leftrightarrow$ superconducting (sc) systems
continuous wave (cw) $\leftrightarrow$ pulsed operation

4) Bunch of examples - highlighting special applications, parameters or other interesting features

a) nc pulsed RTMs
Scanditronix 100MeV (DK), Eindhoven University 75MeV (NL), INP Moscow State University permanent magnet 70MeV (RUS)

Contents

4) continued ...

b) nc pulsed Recirculators
MIT Bates Linac (Middleton, USA), MAX-LAB New Injector (Lund, S)

c) cw RTMs
sc: MUSL, University of Illinois (Urbana-Champaign, USA)
and especially
nc: MAMI, University of Mainz (GER)
(detailed description, polytron excurse)

d) sc cw Recirculators
S-DALINAC, Technical University of Darmstadt (GER)
CEBAF, JLAB (Newport News, USA)

5) Energy Recovering Linacs

basic idea, JLAB IR Demo FEL, future projects

1) Recirculation

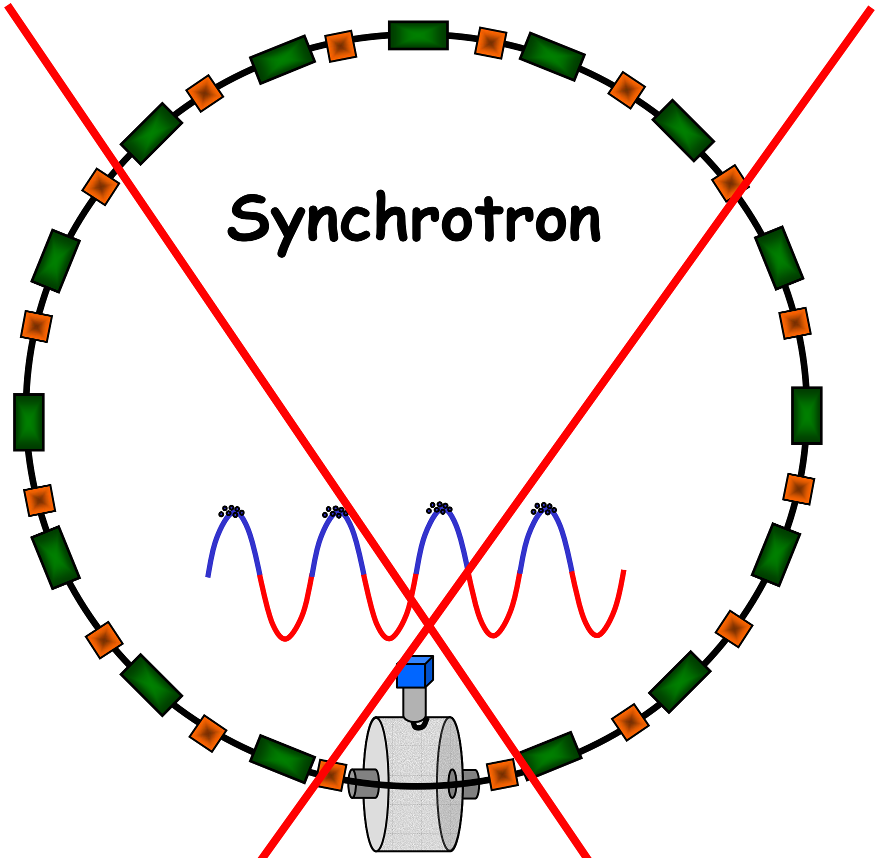

fixed orbit
number of turns: ~100.000
ΔE: ~100eV / turn
particles: e^-, e^+, p, ions, ...
pulsed operation

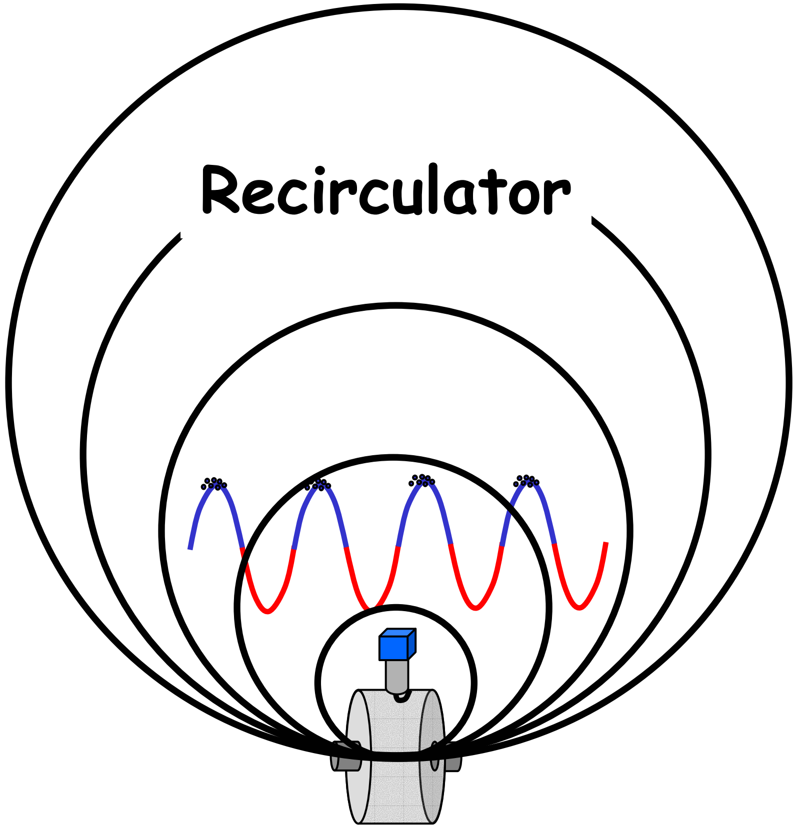

different orbits, fixed frequency
number of turns: 1 - ~100
ΔE: ~511KeV – some 100MeV / turn
particles: e^-
cw operation possible

2a) Classical Microtron [7,8]

First publication: V.I. Veksler 1944 [1] (idea mentioned by L.W. Alvarez 1939 and S. Schwinger 1945, micro(wave)tron named by L.I. Schiff [3]).

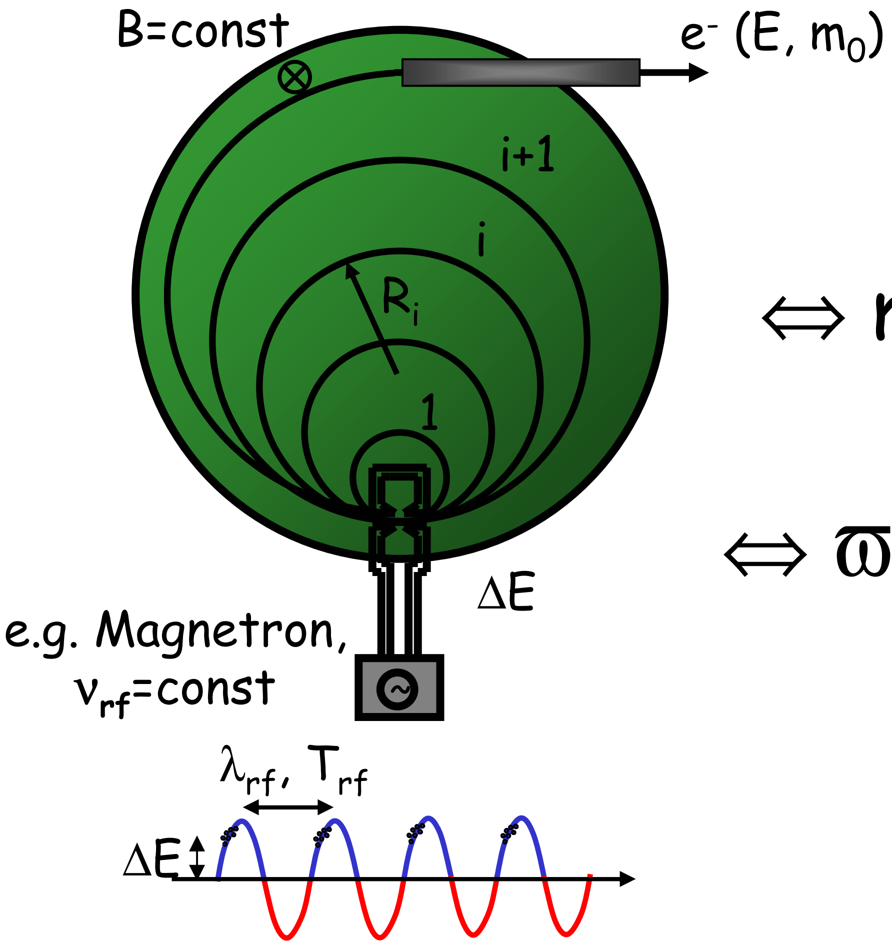

$$k_{rf} = \frac{2\pi}{\lambda_{rf}} \text{ wave number} \qquad k_{rf}\, z - \omega t$$

$$m \cdot \vec{R} \cdot \vec{\varpi}^2 = e \cdot \left(\vec{v} \times \vec{B}\right)$$

$$\Rightarrow m \cdot R \cdot \varpi^2 = e \cdot v \cdot B$$

$$\Leftrightarrow m \cdot \varpi^2 = e \cdot \frac{v}{R} \cdot B = e \cdot \varpi \cdot B$$

$$\Leftrightarrow \varpi = \frac{e \cdot B}{m} = \frac{e \cdot B}{\gamma \cdot m_0} = \frac{e \cdot c^2 \cdot B}{E}$$

$$\Leftrightarrow \boxed{T = \frac{2\pi}{e \cdot c^2 \cdot B} \cdot E}$$

note: $R = \dfrac{\beta \cdot E}{e \cdot c \cdot B}$

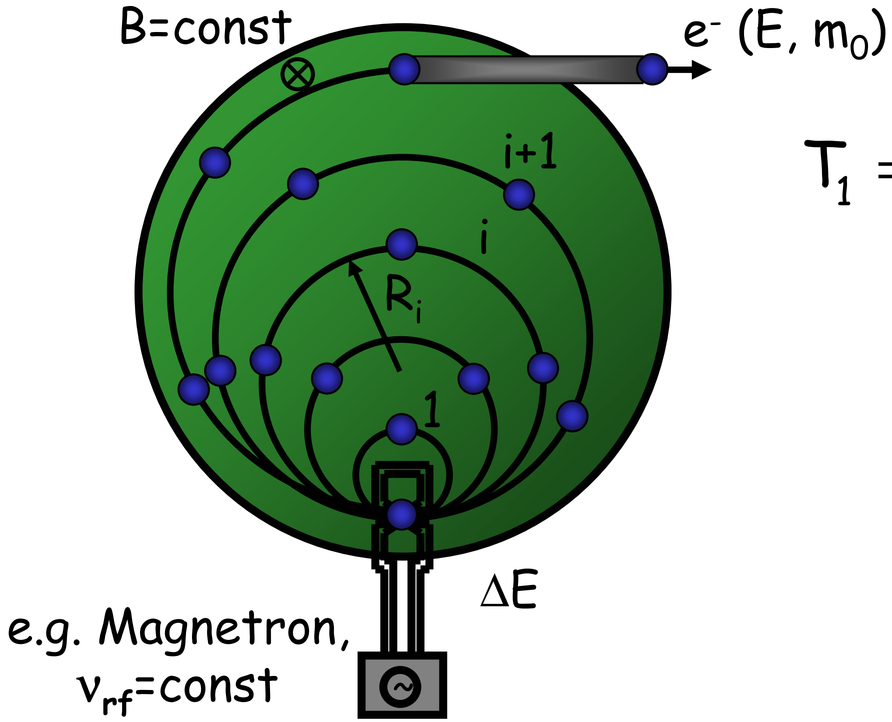

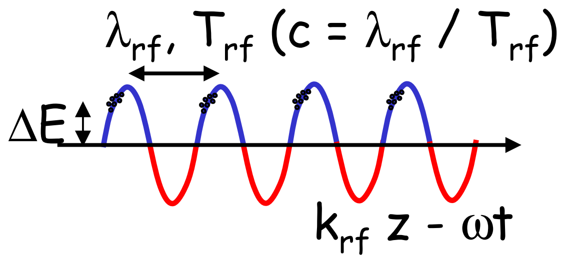

First turn:

$$T_1 = m \cdot T_{rf} = \frac{2\pi}{e \cdot c^2 \cdot B} \cdot \left(m_0 c^2 + f \cdot \Delta E \right) \quad (1)$$

rest energy of the electron: 511keV

Next orbits difference:

$$T_{i+1} - T_i = n \cdot T_{rf} = \frac{2\pi}{e \cdot c^2 \cdot B} \cdot \Delta E \quad (2)$$

(1) and (2):

$$\boxed{\Delta E = \frac{n}{m - n \cdot f} \cdot m_0 c^2 \qquad B = \frac{1}{m - n \cdot f} \cdot \frac{2\pi}{e \cdot c \cdot \lambda_{rf}} \cdot m_0 c^2 \qquad m,n \in \mathbb{N}}$$

<u>**first microtrons f=1**</u> (e^- starts with v = 0)

choice of m,n: - for compact design B should be as high as possible

$\rightarrow$ m - n = 1 and λ_{rf} as small as possible (high ν_{rf})

- ΔE should be as low as possible $\rightarrow$ n = 1

m=2, n=1 $\rightarrow$ ΔE=511keV (m=3,n=2 $\rightarrow$ ΔE=1022keV and so on !)

First realised microtron:
National Research Council, Ottawa, Canada, 1947 [5]

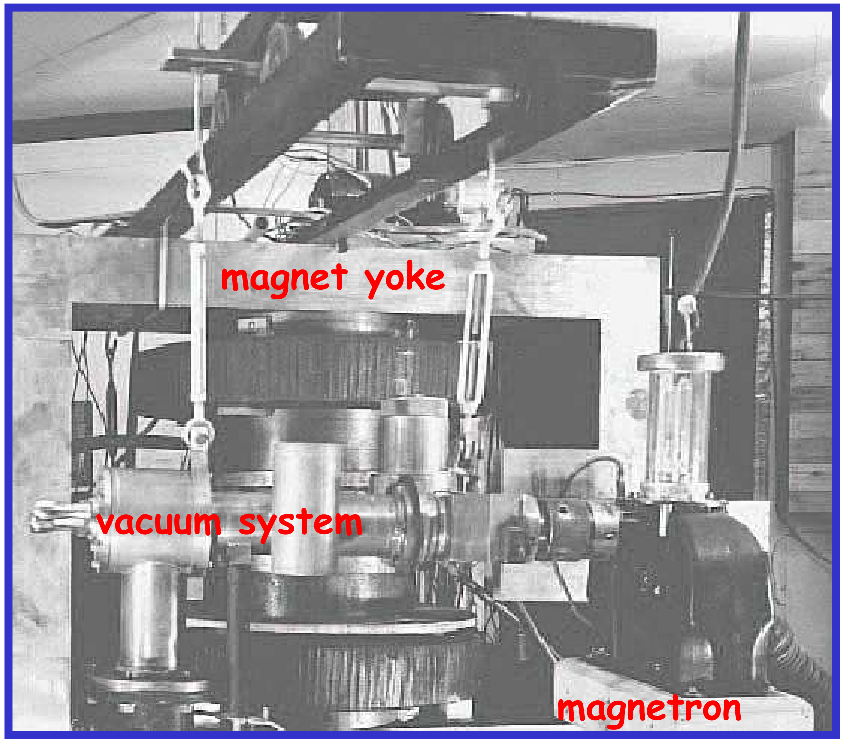

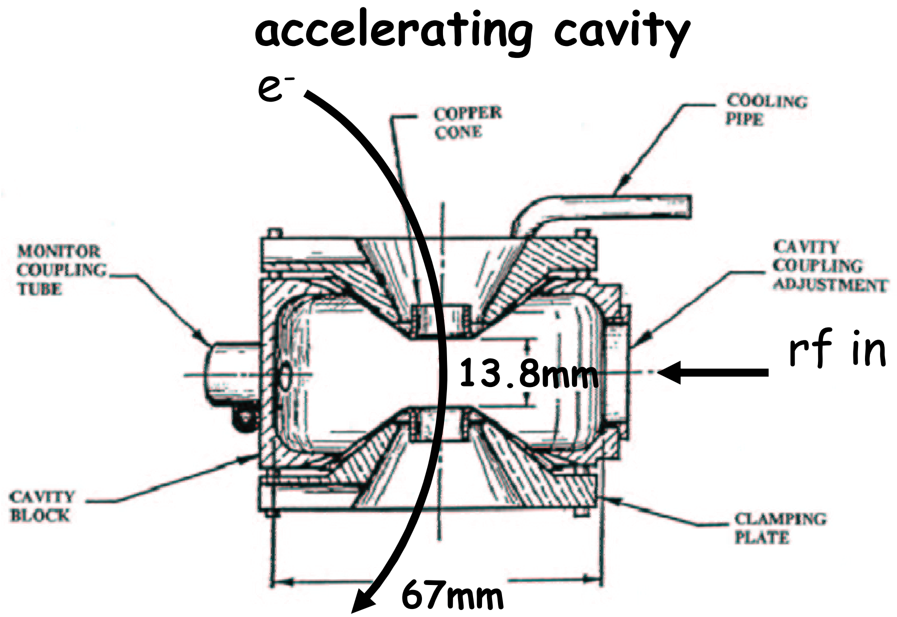

defines minimum pole width !

- m=2, n=1, f=1, ΔE=511keV, B=0.1T, 8 orbits, 4.6MeV, diameter of 8th turn = 0.305m
- magnetron power source (ν_{rf}=2.8GHz$\leftrightarrow\lambda_{rf}$=10.7cm, 300kW $\rightarrow$ only pulsed operation) (~ μs, ~100Hz)
- no "electron source", field emission e^- from cavity lips accelerated (after some improvements max. 3mA <u>pulse</u> current in the 7^{th} turn)
- no smooth variation of output energy possible !

Idea of V.N. Melekhin:
make use of f by clever injection mechanism ! [6]

thermionic electron source (e.g. LaB_6) in wall of flat, cylindrical cavity (allows also higher currents up to some 10 mA)

$$\Delta E = \frac{n}{m - n \cdot f} \cdot m_0 c^2$$

$$B = \frac{1}{m - n \cdot f} \cdot \frac{2\pi}{e \cdot c \cdot \lambda_{rf}} \cdot m_0 c^2$$

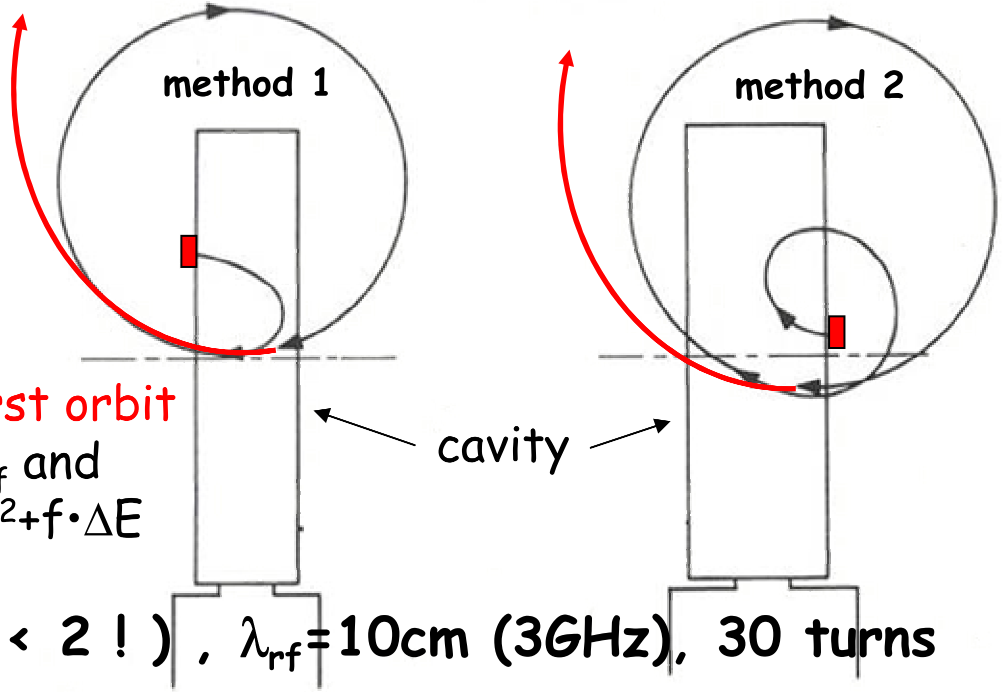

it follows the first orbit with $T_1 = m \cdot T_{rf}$ and e^- -energy: $m_0c^2 + f \cdot \Delta E$

e.g.: m=2,n=1, f=1.6 (f < 2 !) , λ_{rf}=10cm (3GHz), 30 turns

→ B=0.27T, ΔE=2.5·511keV=1280keV,
$2 \cdot R_{30}$=0.97m, E_{30}=38.8MeV

(with f=1: B=0.107, only E_{30}=15.8MeV)

By just changing B, a new regime of f is selected allowing for continuous variation of the output energy in the order of 2:1 !

Flerov Lab, JINR, Dubna, Russia

25MeV microtron,
vacuum chamber opened,
upper magnet pole removed

General remarks on microtrons:

- up to 44MeV realized (Ø=1.3m magnet)
- 100μA **average** beam current (much higher than e.g. a betatron)
- inherent low energy spread (see 2b)
- requires homogenous dipole field
- used for:
  nuclear physics, radiotherapy, injector for synchrotrons (Lund, Frascati, Wisconsin), irradiation, ...
- easy to operate, few components
- transversal focussing: by rf in the cavity, e.g. oval beam holes supply vertical focussing.

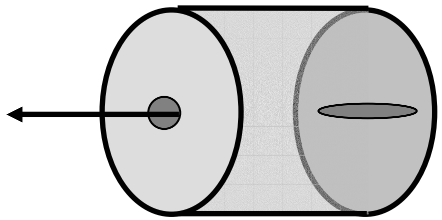

Longitudinal Phase focussing (here just schematic)

(independently formulated by V.I. Veksler [1] and E.M. McMillan [2])

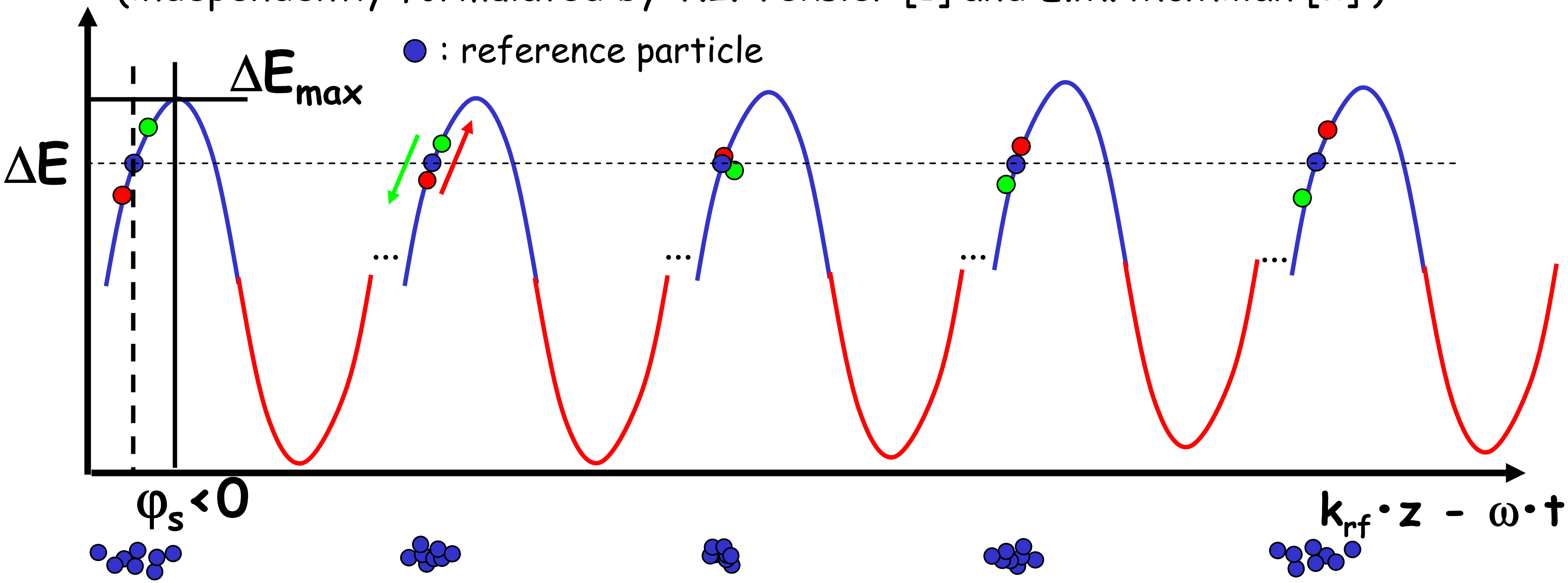

$$R = \frac{\beta \cdot E}{e \cdot c \cdot B}$$

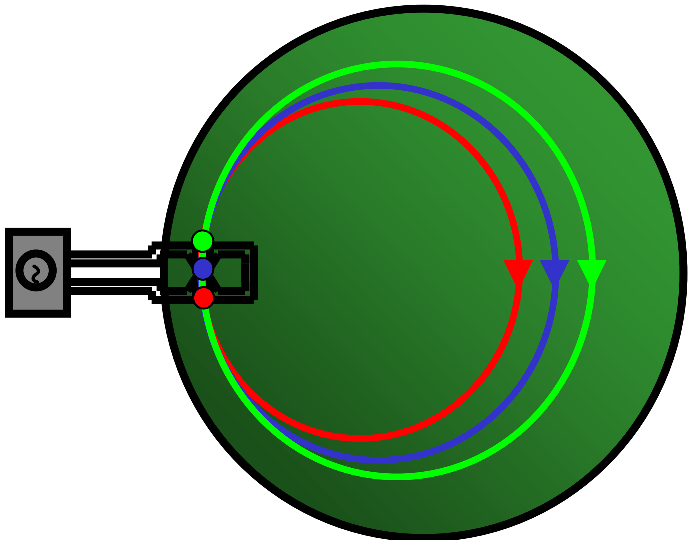

e.g. ● particle:

- arrives earlier,
- gains more energy
- has longer path lengths
- needs more time
- approaches reference particle

2b) Race-Track-Microtron

Suggested by J.S. Schwinger (1945), first proposals by E.M. Moroz [9] and A. Roberts [10], first realisation University of Western Ontario, Canada [11] (1960)

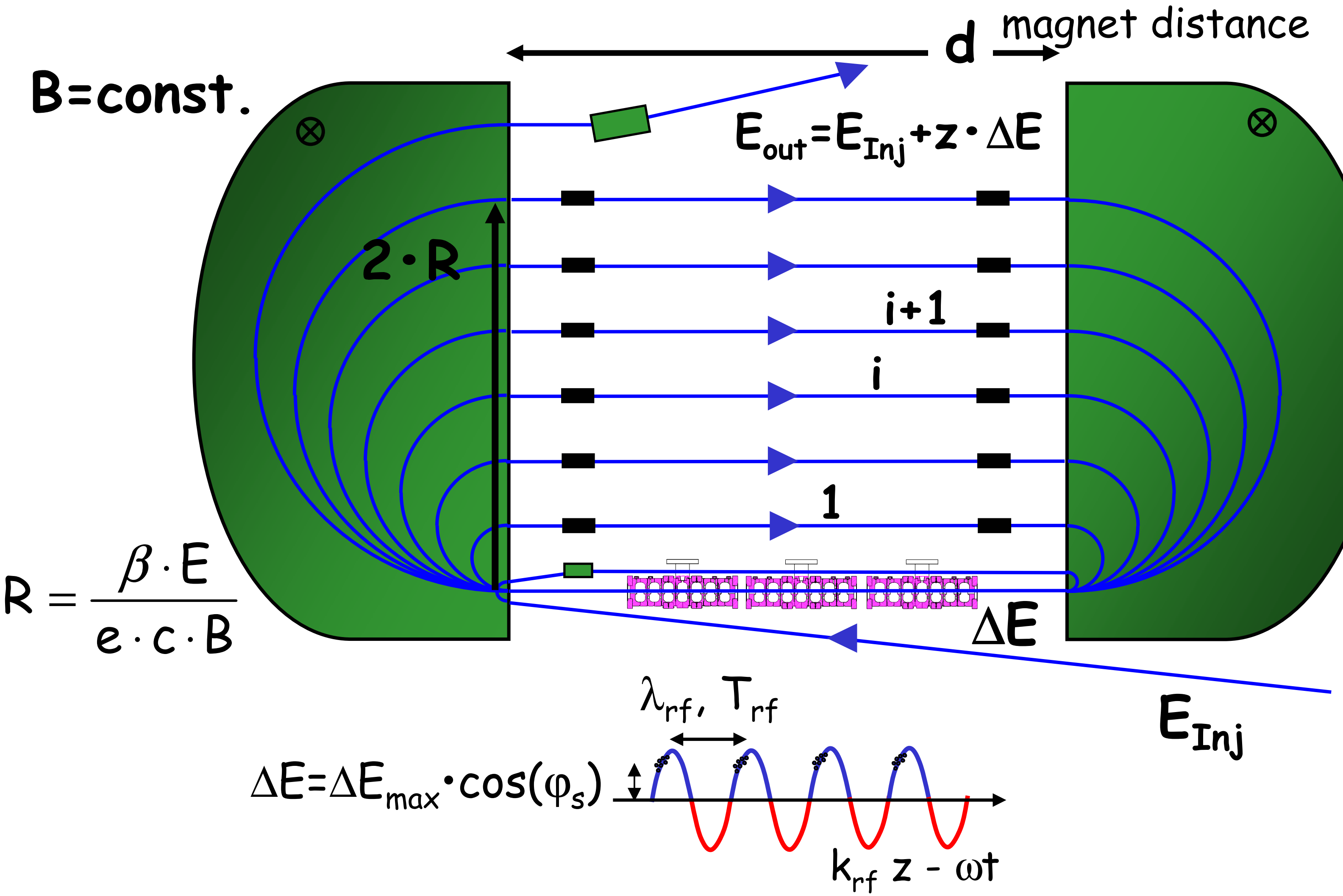

First complete turn (static coherence condition):

$$T_1 = \frac{2\pi}{e \cdot c^2 \cdot B} \cdot \left(E_{Inj} + \Delta E\right) + \frac{2 \cdot d}{\beta_1 \cdot c} = m \cdot T_{rf} \qquad | \cdot c \;\; (c = \lambda_{rf} / T_{rf})$$

$$\boxed{\frac{2\pi}{e \cdot c \cdot B} \cdot \left(E_{Inj} + \Delta E\right) + \frac{2 \cdot d}{\cancel{\beta_1} = 1} = m \cdot \lambda_{rf} \qquad (1)}$$

Next orbits difference (dynamic coherence condition):

$$T_{i+1} - T_i = \frac{2\pi}{e \cdot c^2 \cdot B} \cdot \Delta E + \frac{2 \cdot d}{c} \cdot \left(\frac{1}{\beta_{i+1}} - \frac{1}{\beta_i} \right) = n \cdot T_{rf} \qquad | \cdot c \;\; (c = \lambda_{rf} / T_{rf})$$

$$\boxed{\frac{2\pi}{e \cdot c \cdot B} \cdot \Delta E + 2 \cdot d \cdot \cancel{\left(\frac{1}{\beta_{i+1}} - \frac{1}{\beta_i} \right)}_{=0} = n \cdot \lambda_{rf} \qquad (2)}$$

$m, n \in \mathbb{N}$

For a given λ_{rf} and n eq. (2) defines the relation between ΔE and B. E_{Inj} or d can be selected to fulfil eq. (1). Necessary energy gain should be low $\rightarrow$ n=1 in most cases !
Other way round: $n \cdot \lambda_{rf}$ and d define the geometry. By varying B, ensuring that ΔE can be supplied and adjusting E_{Inj} , the output energy can be smoothly changed.

Some numbers according the term containing β: $2 \cdot d \cdot \left(\frac{1}{\beta_{i+1}} - \frac{1}{\beta_i} \right) = \delta d$

A) E_{Inj}=4MeV, ΔE=0.6MeV, d=1.67m, λ_{rf}=12.24cm (2.45 GHz):

1→2: δd=-4.6mm (δφ=-13.4°)
2→3: δd=-3.2mm (δφ=-9.4°, Δφ=-4.0°)
3→4: δd=-2.3mm (δφ=-6.9°, Δφ=-2.5°)

$$\delta\phi = 2\pi \cdot \frac{\delta d}{\lambda_{rf}}$$

$\beta_{4.6MeV}$=0.9938

B) E_{Inj}=12MeV, ΔE=6MeV, d=2m, λ_{rf}=10cm (3 GHz):

1→2: δd=-0.71mm (δφ=-2.5°)
2→3: δd=-0.33mm (δφ=-1.2°, Δφ=-1.3°)
3→4: δd=-0.18mm (δφ=-0.6°, Δφ=-0.6°)

β_{18MeV}=0.9996

C) E_{Inj}=180MeV, ΔE=7.5MeV, d=12.9m, λ_{rf}=12.24cm (2.45 GHz):

1→2: δd=-0.0072mm (δφ=-0.021°)
2→3: δd=-0.0064mm (δφ=-0.019°, Δφ=-0.002°)

$\beta_{187.5MeV}$=0.999996

- Low injection energies favour small magnet spacing d and large wave length (low frequencies, but big cavities; results in space problems)
- At energies above some 10MeV taking β=1 in most cases justified

Examples
(development of synchronous phase φ during acceleration)

RTM1, MAMI:
4MeV → 15MeV, 18 turns,
ΔE=0.6MeV, d=1.67m

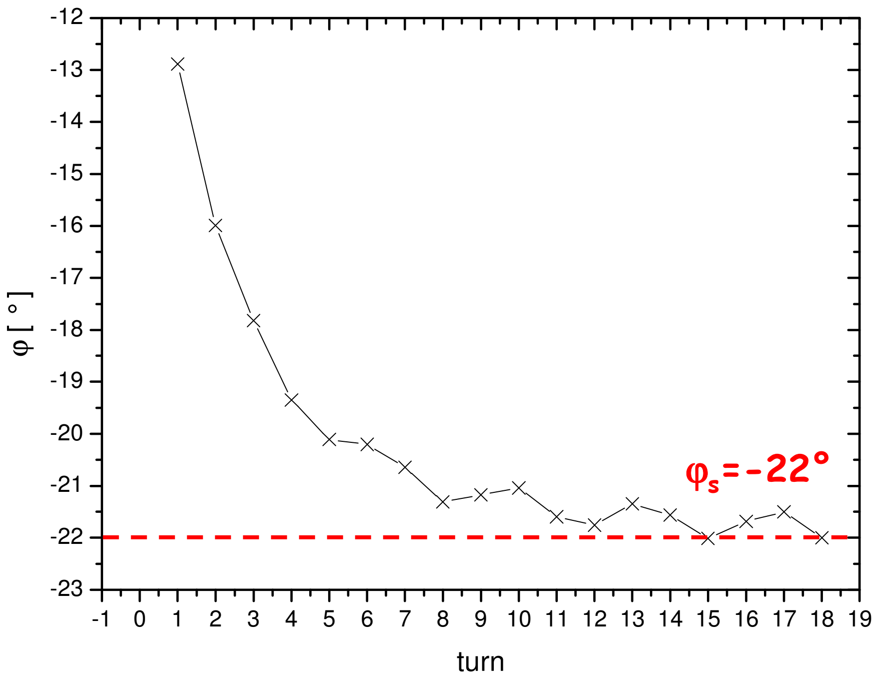

RTM2, MAMI:
15MeV → 180MeV, 51 turns,
ΔE=3.24MeV, d=5.60m

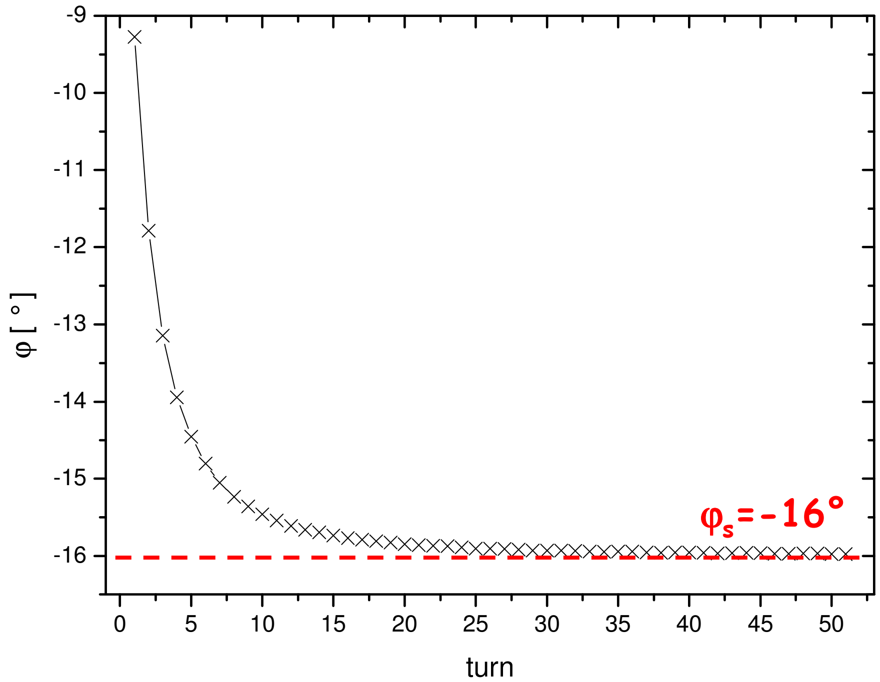

from now on β=1:

$$\frac{2\pi}{e\cdot c\cdot B}\cdot\left(E_{Inj}+\Delta E\right)+2\cdot d=m\cdot\lambda_{rf} \quad\wedge\quad \frac{2\pi}{e\cdot c\cdot B}\cdot\Delta E=n\cdot\lambda_{rf}$$

static coherence condition **dynamic coherence condition**

B=const.

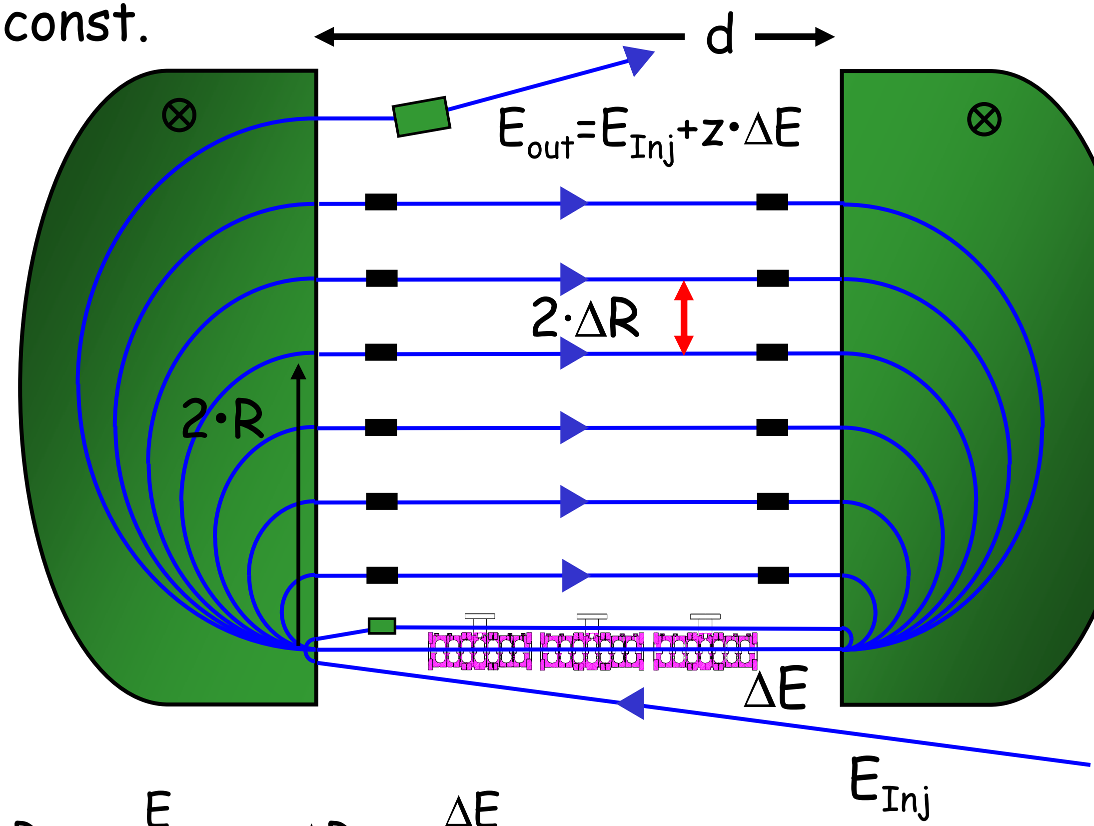

$$R=\frac{E}{e\cdot c\cdot B}\ ,\quad \Delta R=\frac{\Delta E}{e\cdot c\cdot B}$$

spacing of orbits:

$$2\cdot\Delta R=2\cdot\frac{n\cdot\lambda_{rf}}{2\pi}$$

e.g. n=1, λ_{rf}=12.24cm

$\rightarrow$ $2\cdot\Delta R$ = 39mm

take care of injection and first orbit:

beam must pass the linac sections !

Longitudinal Beam Dynamics of an RTM:

as usual describe all particles with respect to reference particle: $\begin{pmatrix} \delta\phi \\ \delta E \end{pmatrix}$

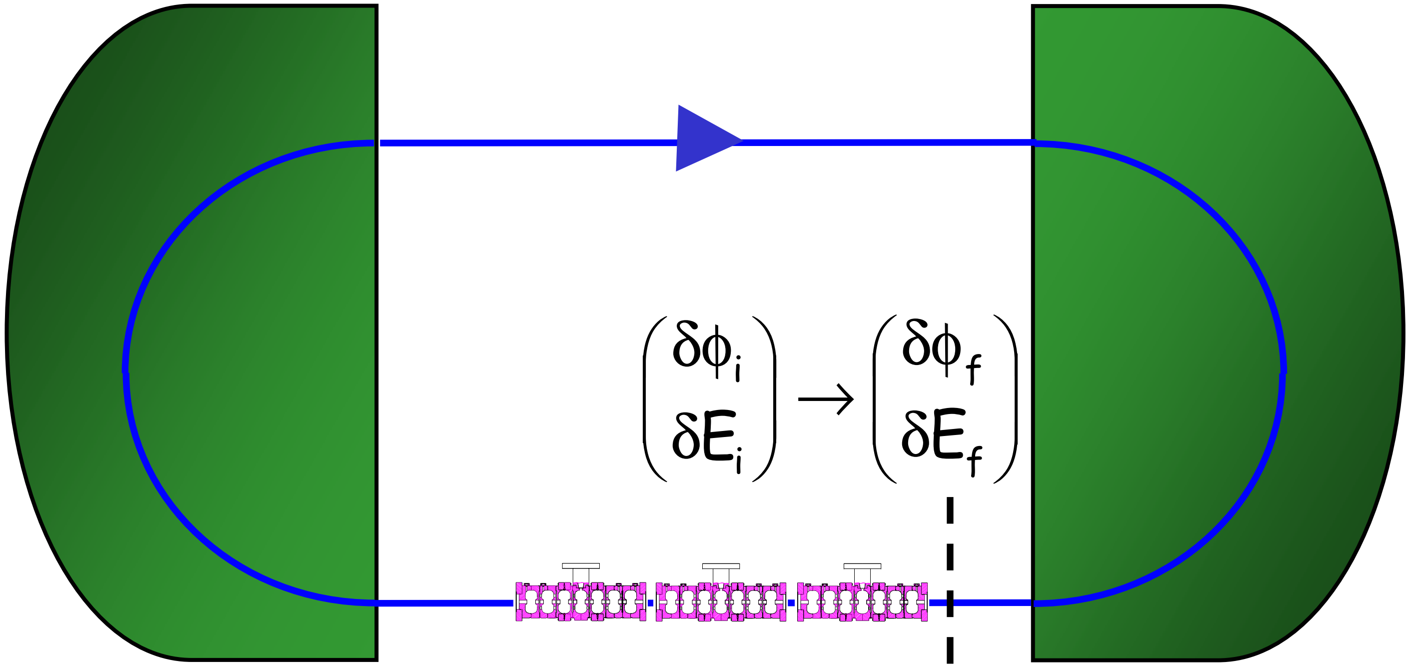

$$\frac{2\pi}{e \cdot c \cdot B} \cdot \Delta E = n \cdot \lambda_{rf} \qquad \Delta E = \Delta E_{max} \cdot \cos(\varphi_s)$$

Only two relevant elements for transformation:
one linac pass followed by one 360° recirculation through dipoles

One Linac pass:

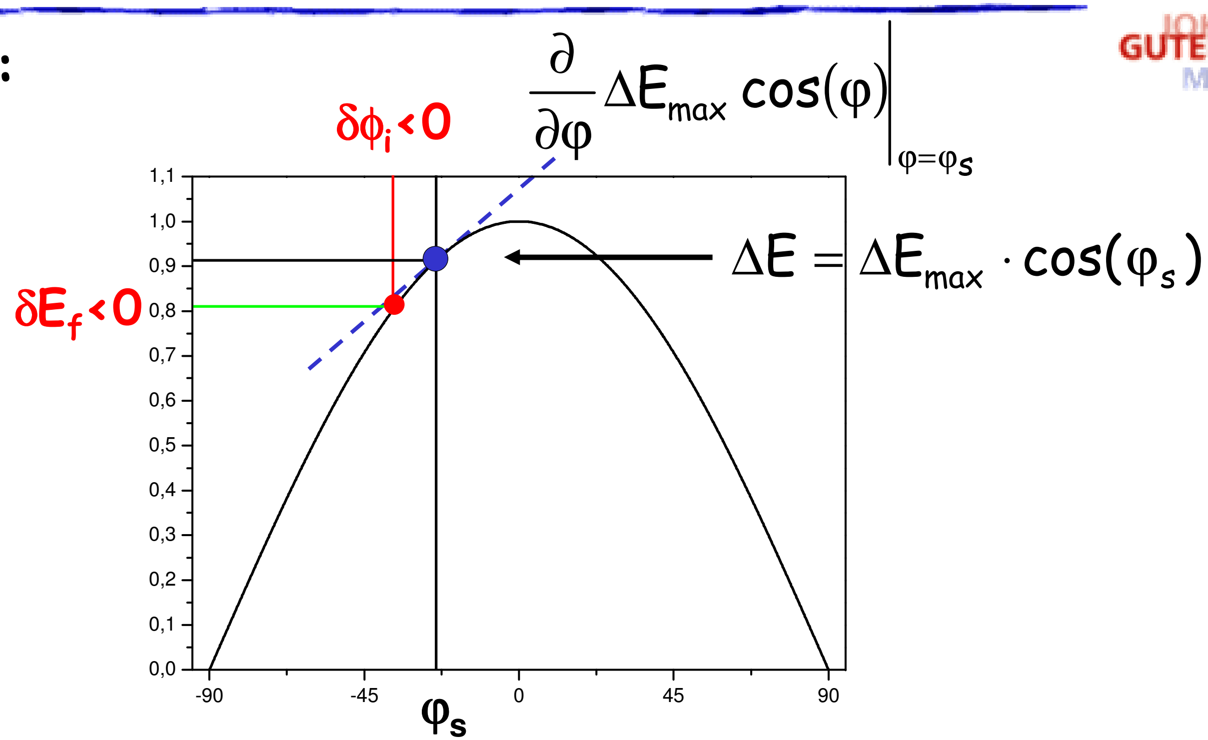

$$\delta\phi_f = \delta\phi_i \quad \text{(because } \beta\text{=const. =1)}$$

$$\delta E_f = \Delta E_{max}\cdot\big(\cos(\varphi_s+\delta\phi_i)-\cos(\varphi_s)\big)+\delta E_i$$

matrix notation (linear approximation of the cosine wave) :

$$\begin{pmatrix}\delta\phi_f\\ \delta E_f\end{pmatrix} = \underbrace{\begin{pmatrix}1 & 0\\ -\Delta E_{max}\sin(\varphi_s) & 1\end{pmatrix}}_{M_{Linac}}\cdot\begin{pmatrix}\delta\phi_i\\ \delta E_i\end{pmatrix}$$

One 360°- recirculation through dipoles:

$$\frac{2\pi}{e \cdot c \cdot B} \cdot \Delta E = n \cdot \lambda_{rf}$$

$$\Rightarrow$$

$$\frac{\delta E}{\Delta E} = \frac{\delta E}{\Delta E_{max} \cdot \cos(\varphi_s)} = -\frac{\delta s}{n \cdot \lambda_{rf}} = -\frac{\delta \phi}{n \cdot 2\pi}$$

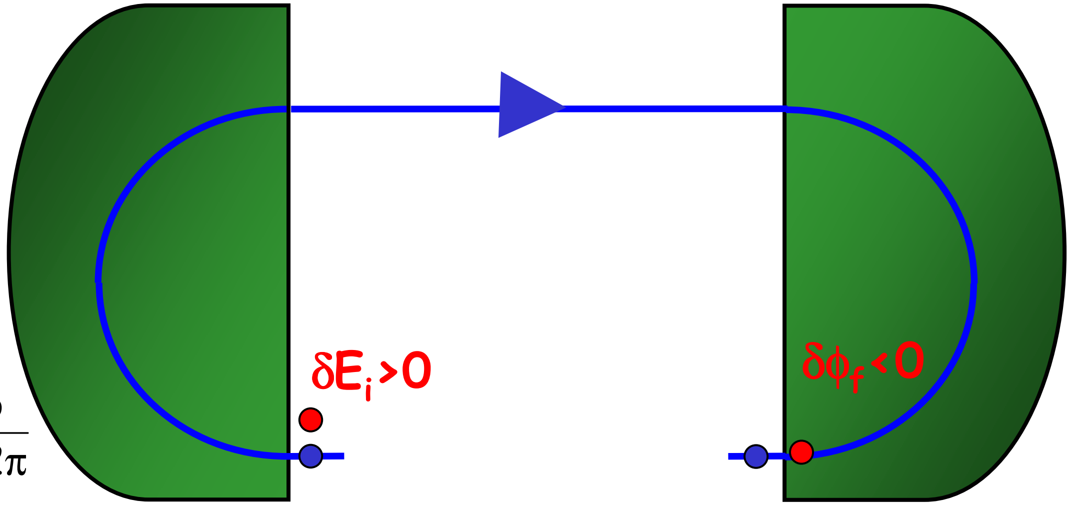

$$\delta\phi_f = \delta\phi_i - \frac{n \cdot 2\pi}{\Delta E_{max} \cdot \cos(\varphi_s)} \cdot \delta E_i$$

$$\delta E_f = \delta E_i$$ (because magnetic fields do not change energy)

<u>matrix notation:</u>

$$\begin{pmatrix} \delta\phi_f \\ \delta E_f \end{pmatrix} = \underbrace{\begin{pmatrix} 1 & -\frac{n \cdot 2\pi}{\Delta E_{max} \cdot \cos(\varphi_s)} \\ 0 & 1 \end{pmatrix}}_{M_{360°}} \cdot \begin{pmatrix} \delta\phi_i \\ \delta E_i \end{pmatrix}$$

Transfermatrix through RTM:

$$\boxed{M^{RTM} = M_{360^\circ} \cdot M_{Linac} = \begin{pmatrix} 1 + n \cdot 2\pi \cdot \tan(\varphi_s) & -\dfrac{n \cdot 2\pi}{\Delta E_{max} \cdot \cos(\varphi_s)} \\ -\Delta E_{max} \cdot \sin(\varphi_s) & 1 \end{pmatrix}}$$

$$RTM \approx \text{periodic system } (z - \text{recirculations}):$$

$$M(z) = M^{RTM} \cdot M^{RTM} \cdot \quad \ldots \quad \cdot M^{RTM} \cdot M^{RTM} = \left(M^{RTM}\right)^z$$

criterium for longitudinal stability:

$$-2 < Tr(M^{RTM}) < 2$$

$$\Leftrightarrow -2 < 2 + n \cdot 2\pi \cdot \tan(\varphi_s) < 2$$

n=1: $\boxed{\Leftrightarrow -32.48^\circ \quad < \quad \varphi_s \quad < \quad 0}$

n=2: $\Leftrightarrow -17.65^\circ \quad < \quad \varphi_s \quad < \quad 0$

Proof of the criterium for longitudinal stability [D]:

$$M^z \cdot \vec{x}_i = \vec{x}_f = \lambda^z \cdot \vec{x}_i \quad \text{with } \lambda \text{ eigenvalue and } \vec{x}_i \text{ eigenvector of } M$$

$$M = \begin{pmatrix} m_{11} & m_{12} \\ m_{21} & m_{22} \end{pmatrix} \qquad (M - \lambda \cdot I) \cdot \vec{x} = 0 \qquad I = \begin{pmatrix} 1 & 0 \\ 0 & 1 \end{pmatrix}$$

$$\det(M - \lambda \cdot I) = 0$$

$\det(M) = 1$
(for transfer matrices, Liouville)

$$\Rightarrow (m_{11} - \lambda) \cdot (m_{22} - \lambda) - m_{21} \cdot m_{12} = 0$$

$$\Rightarrow \lambda^2 - \lambda \cdot (m_{11} + m_{12}) + (m_{11} \cdot m_{22} - m_{21} \cdot m_{12}) = 0$$

$$\Rightarrow \lambda^2 - \lambda \cdot (m_{11} + m_{12}) + 1 = 0$$

$$\lambda_{1,2} = \frac{1}{2}(m_{11} + m_{22}) \pm \sqrt{\frac{1}{4}(m_{11} + m_{22})^2 - 1}$$

if $\quad \left| \frac{1}{2}(m_{11} + m_{22}) \right| < 1$ it is possible to write $\quad \frac{1}{2}(m_{11} + m_{22}) = \cos(\Psi)$

resulting in $\lambda_{1,2} = \cos(\Psi) \pm i \cdot \sin(\Psi) = e^{\pm i\Psi}$

$$\Rightarrow |m_{11} + m_{22}| = |Tr(M)| < 2$$

This is the required condition that ($M^z \vec{x}$) stays finite for z increasing indefinitely.

$$\underbrace{\begin{pmatrix} 1+n\cdot 2\pi\cdot\tan(\varphi_s) & -\dfrac{n\cdot 2\pi}{\Delta E_{max}\cdot\cos(\varphi_s)} \\ -\Delta E_{max}\cdot\sin(\varphi_s) & 1 \end{pmatrix}^z}_{\text{RTM elementary matrix}} = \underbrace{\begin{pmatrix} \cos(z\cdot\psi_Q)+\alpha\cdot\sin(z\cdot\psi_Q) & \beta\cdot\sin(z\cdot\psi_Q) \\ -\dfrac{1+\alpha^2}{\beta}\cdot\sin(z\cdot\psi_Q) & \cos(z\cdot\psi_Q)-\alpha\cdot\sin(z\cdot\psi_Q) \end{pmatrix}}_{\text{quadratic-form: ellipse}}$$

$$\gamma\cdot\delta\phi^2+2\cdot\alpha\cdot\delta E\cdot\delta\phi+\beta\cdot\delta E^2=\varepsilon \qquad \gamma=\frac{1+\alpha^2}{\beta}$$

By comparing the elements of both matrices for z=1
it is possible to calculate α, β and Ψ_q.

$$\alpha=\frac{\cos(\Psi_Q)-1}{\sin(\Psi_Q)}$$

$$\beta=-\frac{1}{\sin(\Psi_Q)}\cdot\frac{n\cdot 2\pi}{\Delta E_{max}\cdot\cos(\varphi_s)}$$

$$\boxed{\cos(\psi_Q)=1+n\cdot\pi\cdot\tan(\varphi_s) \quad \text{with} \quad Q_{long}=\frac{\Psi_Q}{2\pi}}$$

Ψ_Q=phase advance per turn, Q_{long}=number of oscillations per turn

Definition of the parameters of the beam ellipse: [C]

$$\gamma \cdot \delta\phi^2 + 2 \cdot \alpha \cdot \delta E \cdot \delta\phi + \beta \cdot \delta E^2 = \varepsilon$$

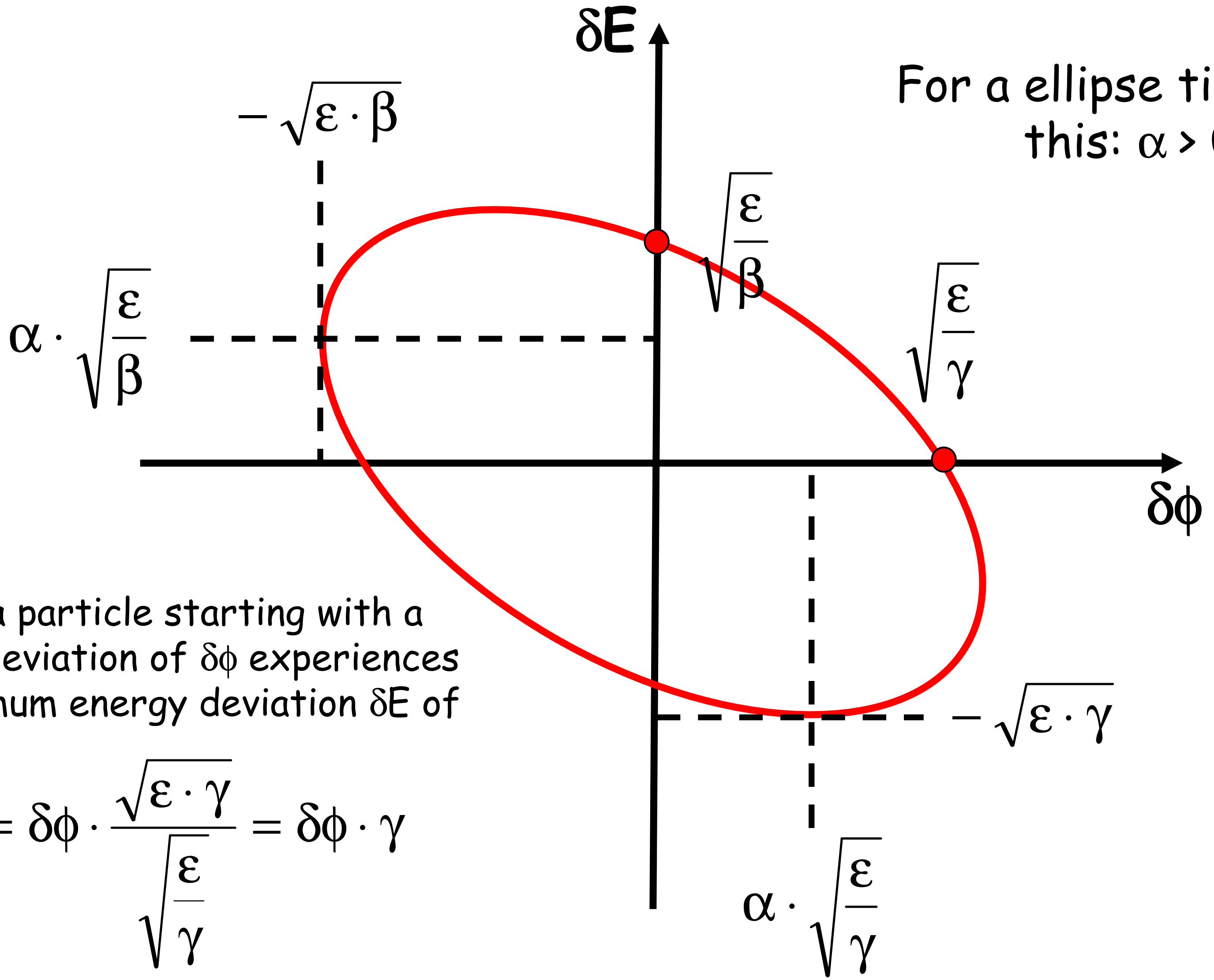

For a ellipse tilted like this: $\alpha > 0$!

e.g.: a particle starting with a phase deviation of $\delta\phi$ experiences a maximum energy deviation δE of

$$\delta E = \delta\phi \cdot \frac{\sqrt{\varepsilon \cdot \gamma}}{\sqrt{\frac{\varepsilon}{\gamma}}} = \delta\phi \cdot \gamma$$

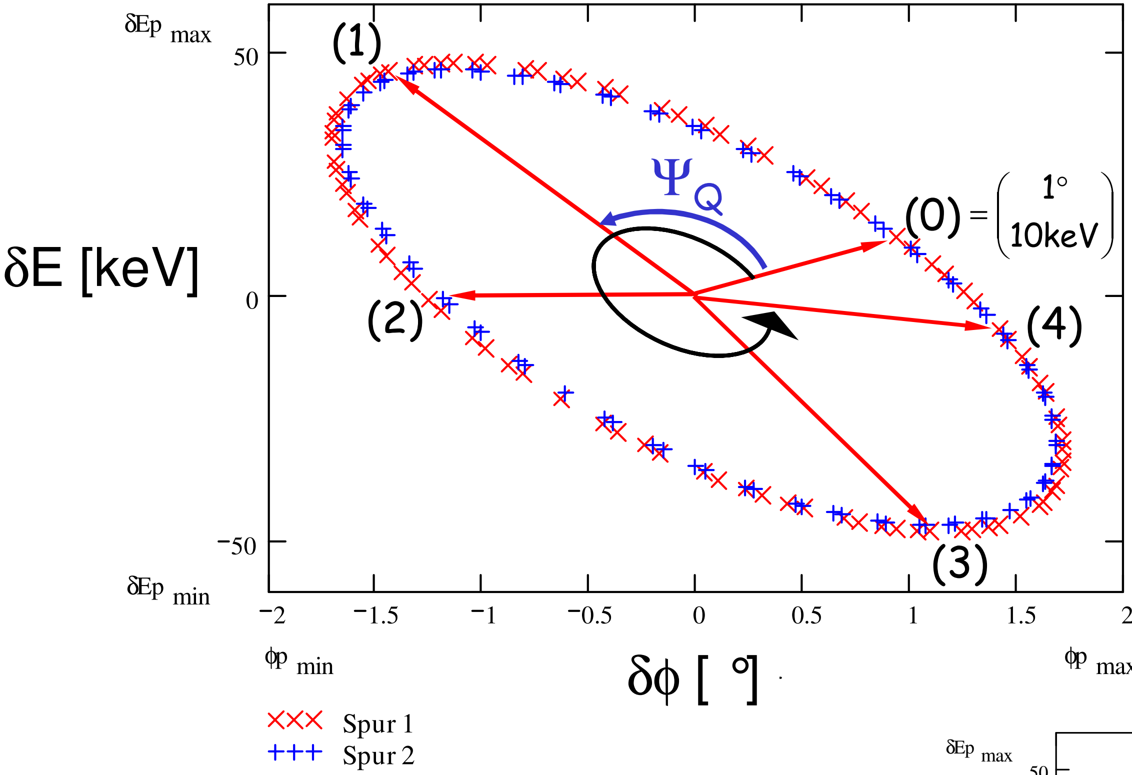

e.g.

φ_s=-16° / Ψ_Q=84.309°

n=1

ΔE=7.5MeV

z=90 turns

linear approximation (x)

versus

real cosine wave (+)

Q_{long}	φ_s RTM
1	-
1/2	-32,48°
1/3	-25,52°
1/4	-17,65°
1/5	-12,40°

strength

resonance

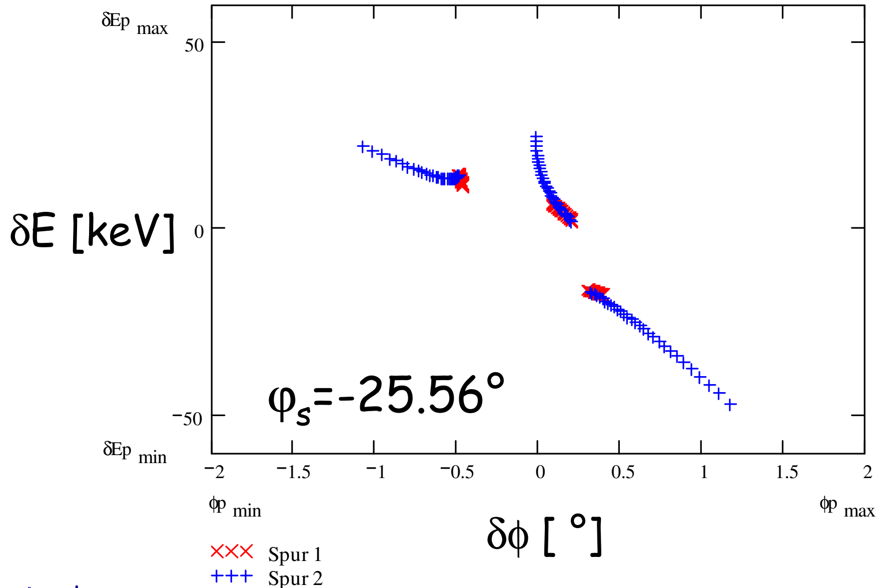

Simple tracking calculations (with real cosine wave):

n=1, φ_s=-16°, ΔE=7.5MeV, z=90

maximum acceptance

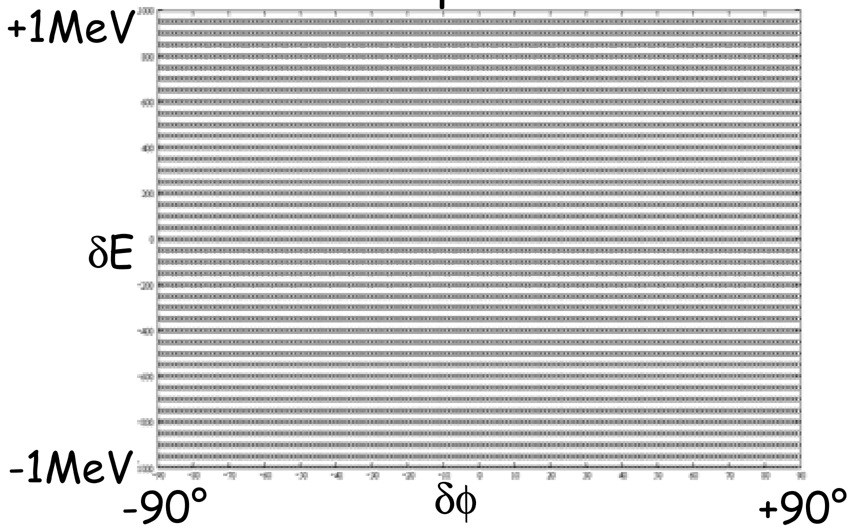

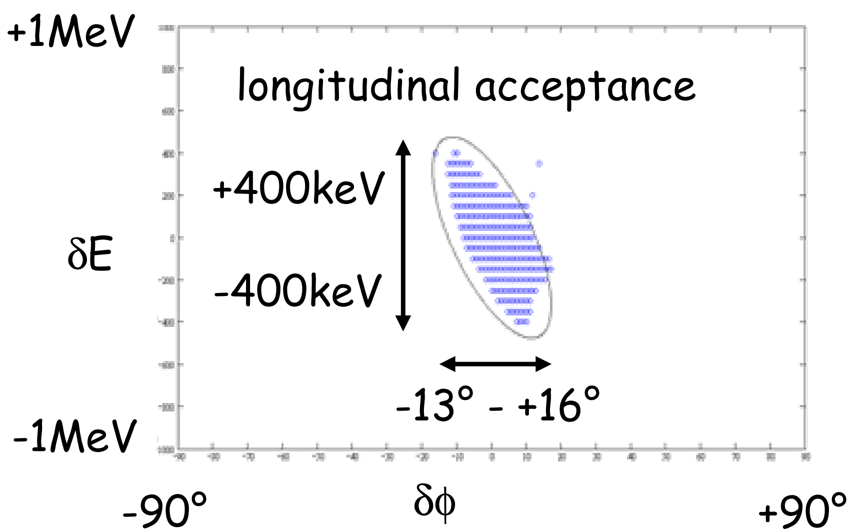

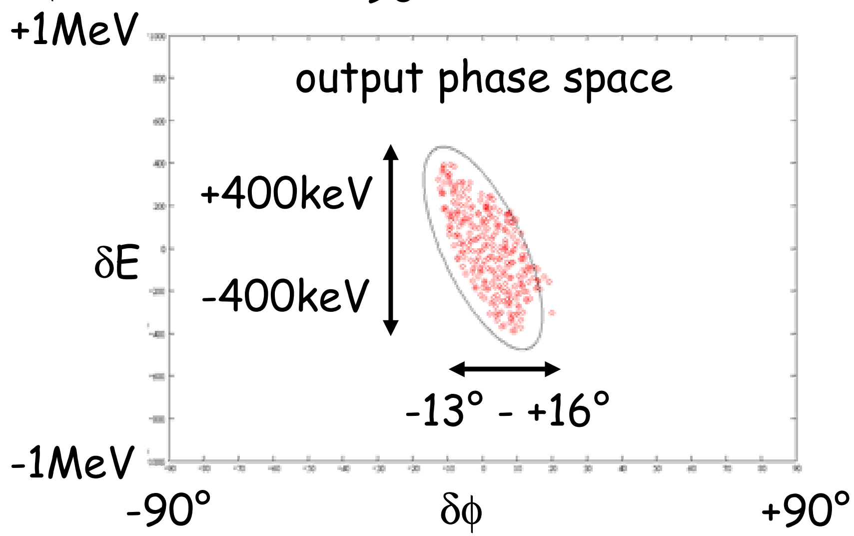

The Microtron acts like an "energy filter".
The relative energy spread $\sigma_{E,r}$ at extraction scales: $\sigma_{E,r} \sim \dfrac{\Delta E_{max}}{z}$
(for fixed reference phase)

$\delta\phi=2°$, $\varphi_s=-16°$, $\Delta E=7.5$MeV, 87 turns

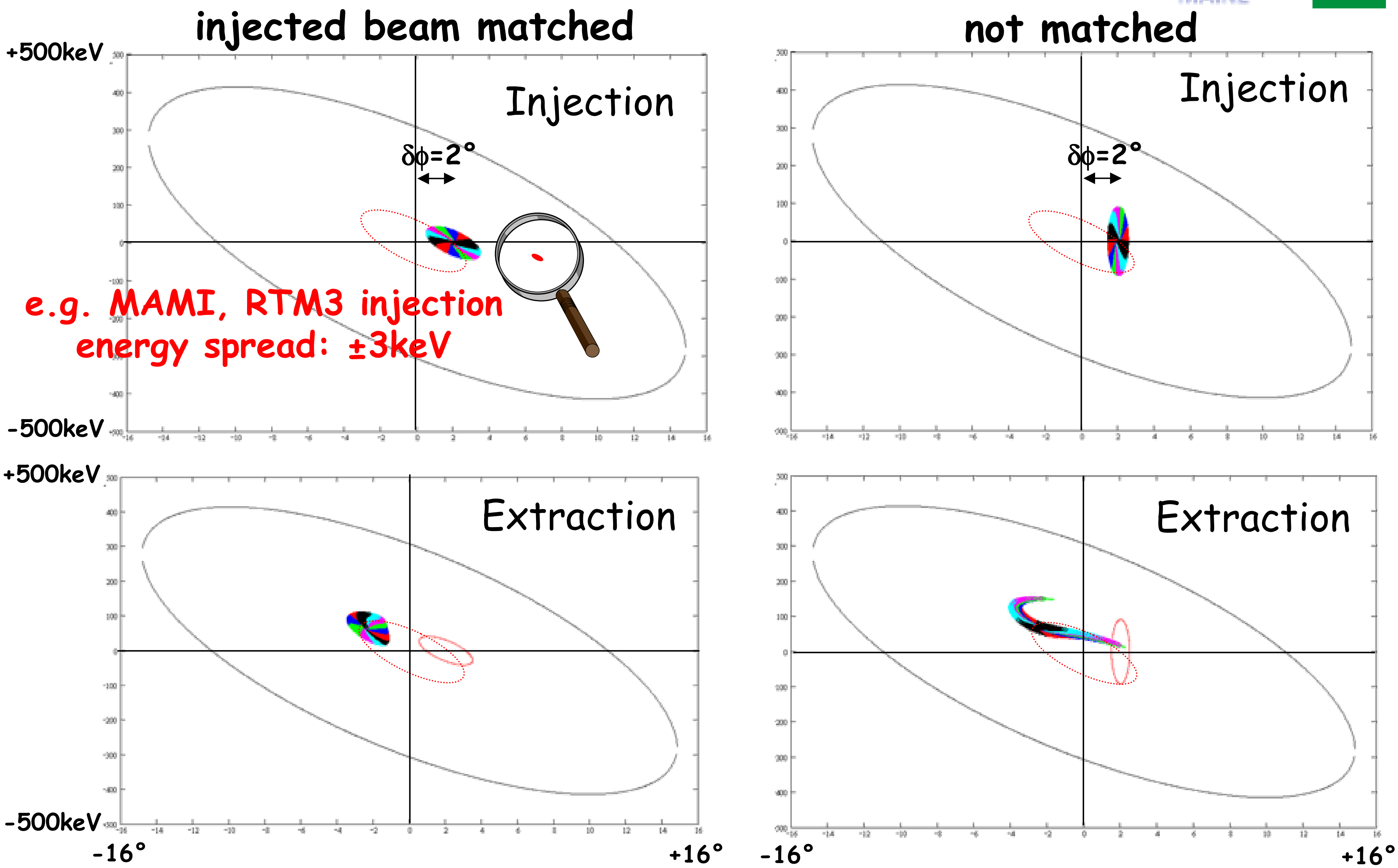

A beam with phase (energy) error at injection is bounded to the eigenellipse, which defines max. resulting energy error. Relative energy error decreases with increasing number of turns !

Influence of amplitude and phase jitter of the accelerating rf:

(normally slow enough, that for one pass through RTM amplitude and phase is constant!)

Amplitude jitter δE_{rf}:

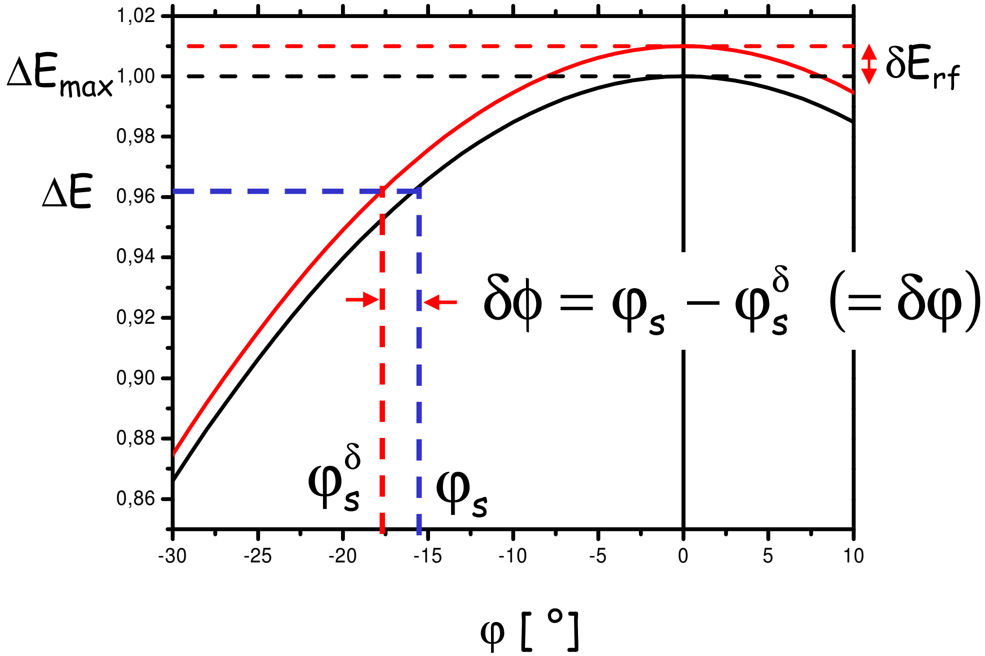

$$\delta E_{rf,rel.} = \frac{\delta E_{rf}}{\Delta E_{max}}$$

$$\Delta E = \Delta E_{max} \cdot \cos(\varphi_s) = (1 + \delta E_{rf,rel.}) \cdot \Delta E_{max} \cdot \cos(\varphi_s^\delta)$$

$$\Rightarrow \cos(\varphi_s^\delta) = \frac{\cos(\varphi_s)}{1 + \delta E_{rf,rel.}}$$

$$\delta\phi = \varphi_s - \varphi_s^\delta \sim -\delta E_{rf,rel.} \cdot \frac{\cos(\varphi_s)}{\sin(\varphi_s)}$$

e.g. φ_s=-16°, Q=0.2342:

$\delta E_{rf,rel.}$ =1%: φ_s^δ=-17.9°, Q=0.2520, $\delta\phi$=1.9°
$\delta E_{rf,rel.}$ =0.1%: φ_s^δ=-16.2°, Q=0.2360, $\delta\phi$=0.2°
$\delta E_{rf,rel.}$ =0.01%: φ_s^δ=-16.02°, Q=0.2344, $\delta\phi$=0.02°

Small amplitude jitter δE_{rf} results in a phase jitter $\delta\phi$ of the input beam and slightly changes the longitudinal tune.

Special choice of longitudinal tune Q_{long} (by setting φ_s):

$$\begin{pmatrix}\delta\phi_z\\ \delta E_z\end{pmatrix}=\begin{pmatrix}\cos(z\cdot\psi_Q)+\alpha\cdot\sin(z\cdot\psi_Q) & \beta\cdot\sin(z\cdot\psi_Q)\\ -\frac{1+\alpha^2}{\beta}\cdot\sin(z\cdot\psi_Q) & \cos(z\cdot\psi_Q)-\alpha\cdot\sin(z\cdot\psi_Q)\end{pmatrix}\cdot\begin{pmatrix}\delta\phi_0\\ \delta E_0\end{pmatrix}$$

$$\alpha=\frac{\cos(\Psi_Q)-1}{\sin(\Psi_Q)},\quad \beta=-\frac{1}{\sin(\Psi_Q)}\cdot\frac{n\cdot 2\pi}{\Delta E_{max}\cdot\cos(\varphi_s)},\quad \gamma=\frac{1+\alpha^2}{\beta},\quad \cos(\psi_Q)=1+n\cdot\pi\cdot\tan(\varphi_s)$$

$$\boxed{\delta E_z=-\frac{1+\alpha^2}{\beta}\cdot\underbrace{\sin(z\cdot\Psi_Q)}_{=\ 0}\cdot\delta\phi_0}$$

As we know in case of jitter δE_{rf} of the linac amplitude it follows that:

$$\delta\phi_0\sim-\delta E_{rf,rel.}\cdot\frac{\cos(\varphi_s)}{\sin(\varphi_s)}$$ (δ$E_{rf,rel.}$ < 1%) **and also a change of φ_s (and therefore Ψ_Q)**

By a proper setting of φ_s the resulting energy fluctuations can be suppressed very effectively !

ΔE=7.5MeV,
90 turns,
E_{out}=855MeV

δE_{out}:
10keV = $1 \cdot 10^{-5}$

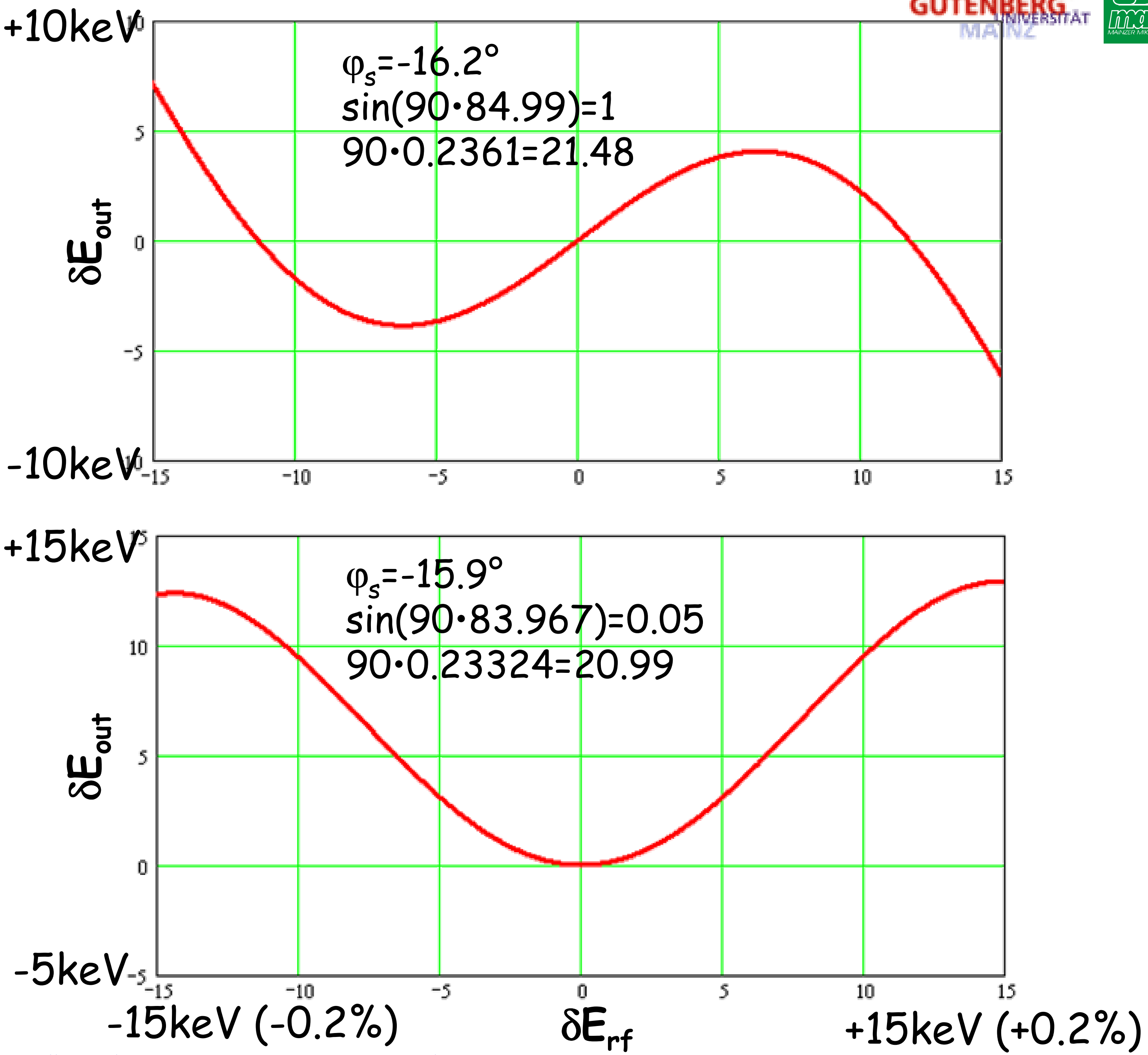

Transverse focussing in an RTM (only principles):

a) vertical focussing by reverse field stripe [12]

beam outside midplane of the dipole experiences vertical defocussing in the fringe field of the dipole.

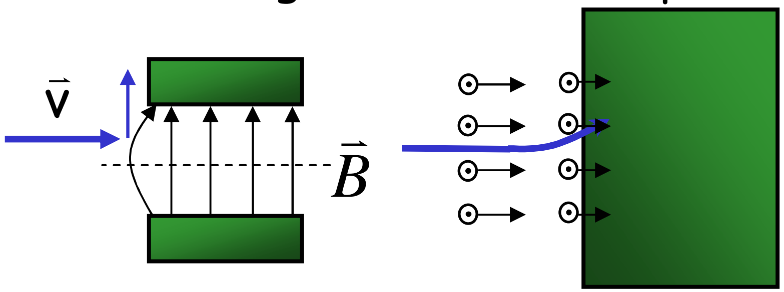

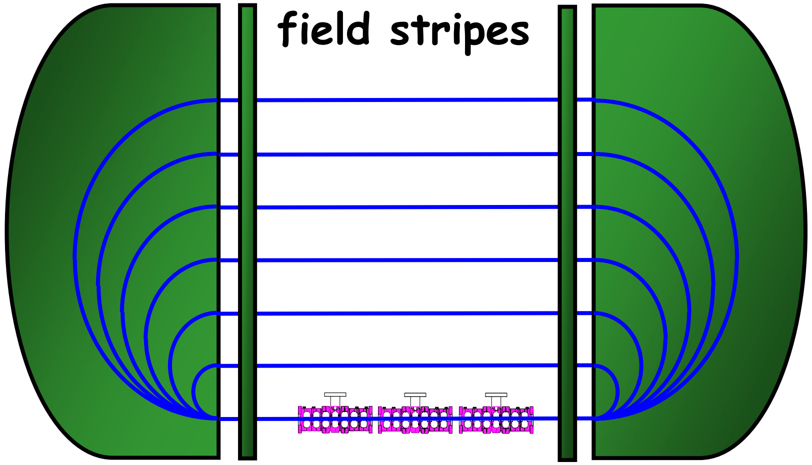

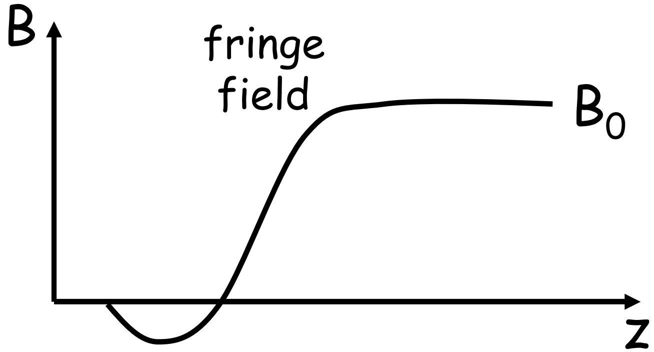

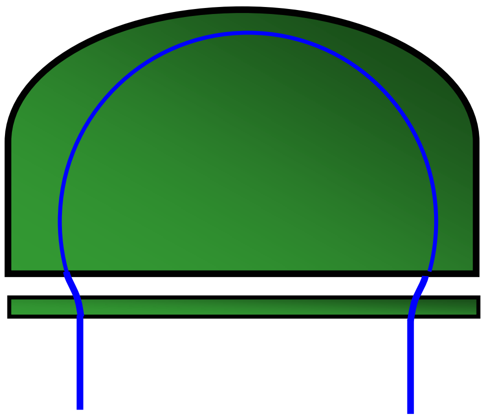

By adjusting the reverse field, vertical defocussing of the fringe field can be compensated or even vertical focussing can be introduced !

b) focussing on each return path:

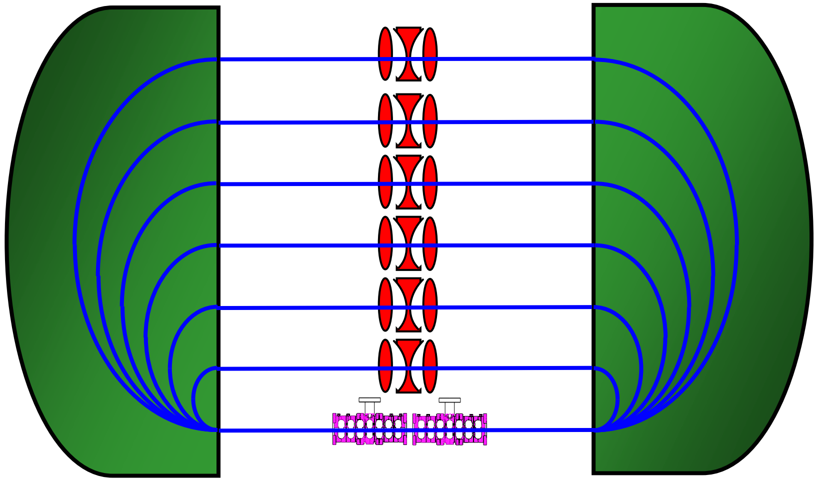

- individual focussing for each energy
- constant beta function → decreasing beam size

- big number of components (z×2, z×3)
- quadrupoles in dispersive section lead to coupling of longitudinal and horizontal motion
- alignment tolerances very small

c) focussing on linac axis:

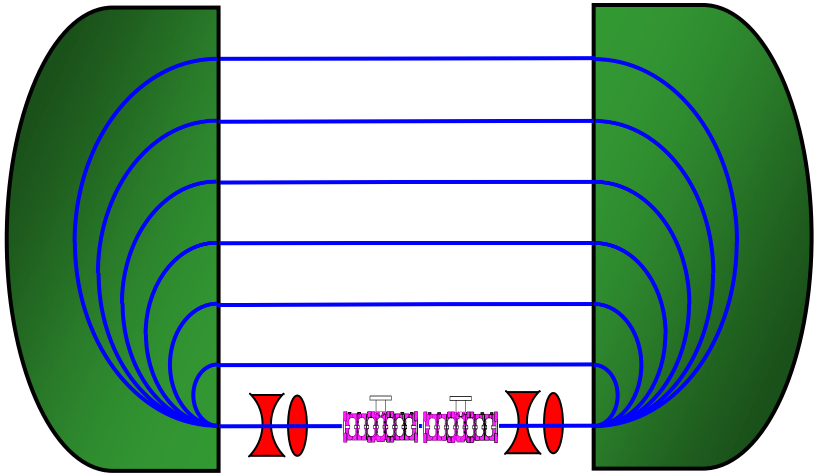

- only few components
- focussing only in dispersion free region, no coupling of hor. and long. motion

- focal length of quadrupole doublet [B] is $1/f_{doub} \sim 1/f^2$. Therefore the focussing strength decreases with $1/E^2$, which results in increasing beta functions.

Due to pseudo damping of beam emittance during acceleration

$$\varepsilon_{x,y} = \frac{1}{\beta \cdot \gamma} \cdot \varepsilon_{x,y}^{norm}$$

beam size stays nearly constant !

Example for quadrupole doublet focussing on linac axis (RTM3, MAMI, 90 turns):

development of horizontal and vertical beta-functions in the centre of the return paths

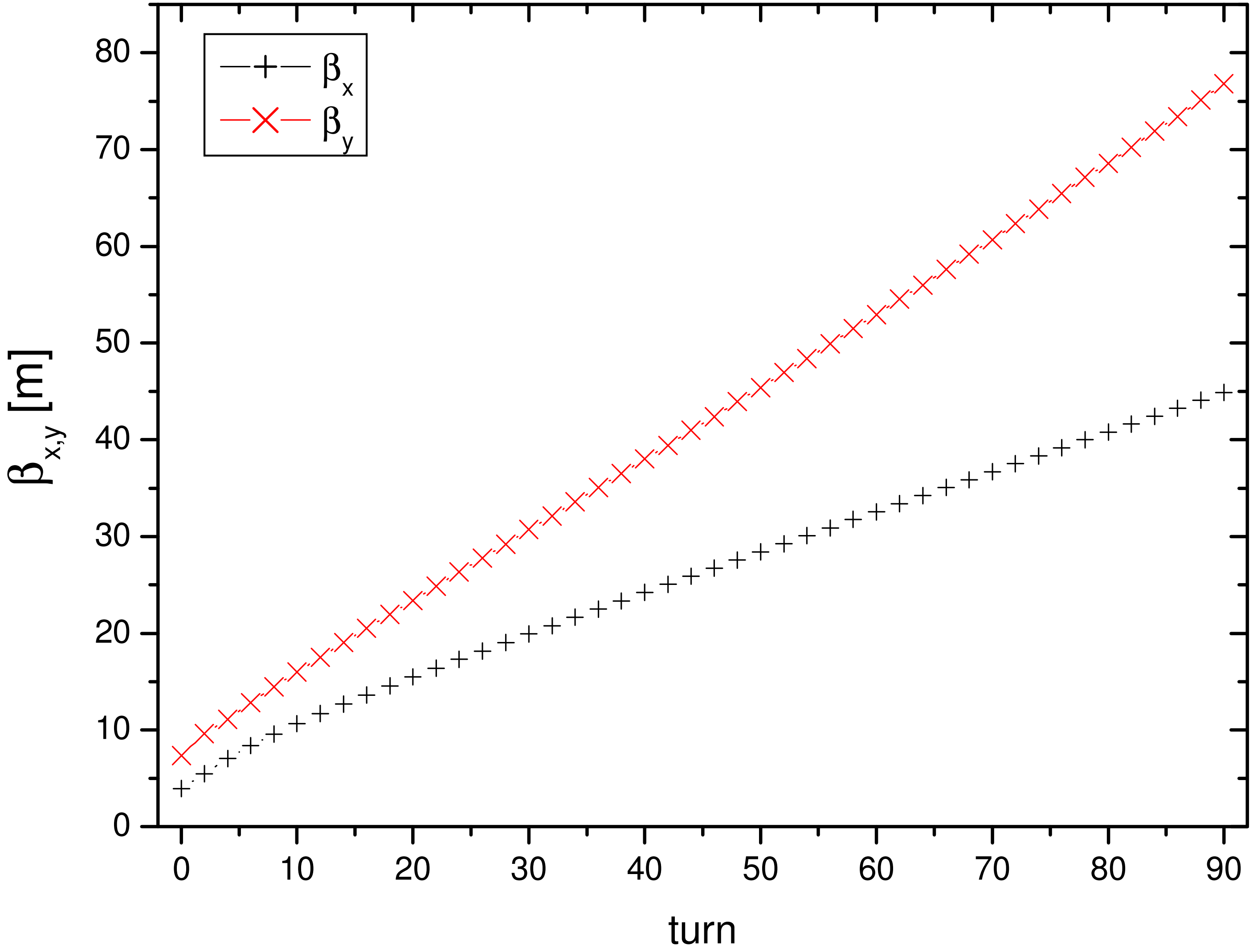

Example for quadrupole doublet focussing on linac axis (RTM3, MAMI, 90 turns):

horizontal beam ellipse each 10th turn:
(not taking into account synchrotron-radiation effects, see 4c))

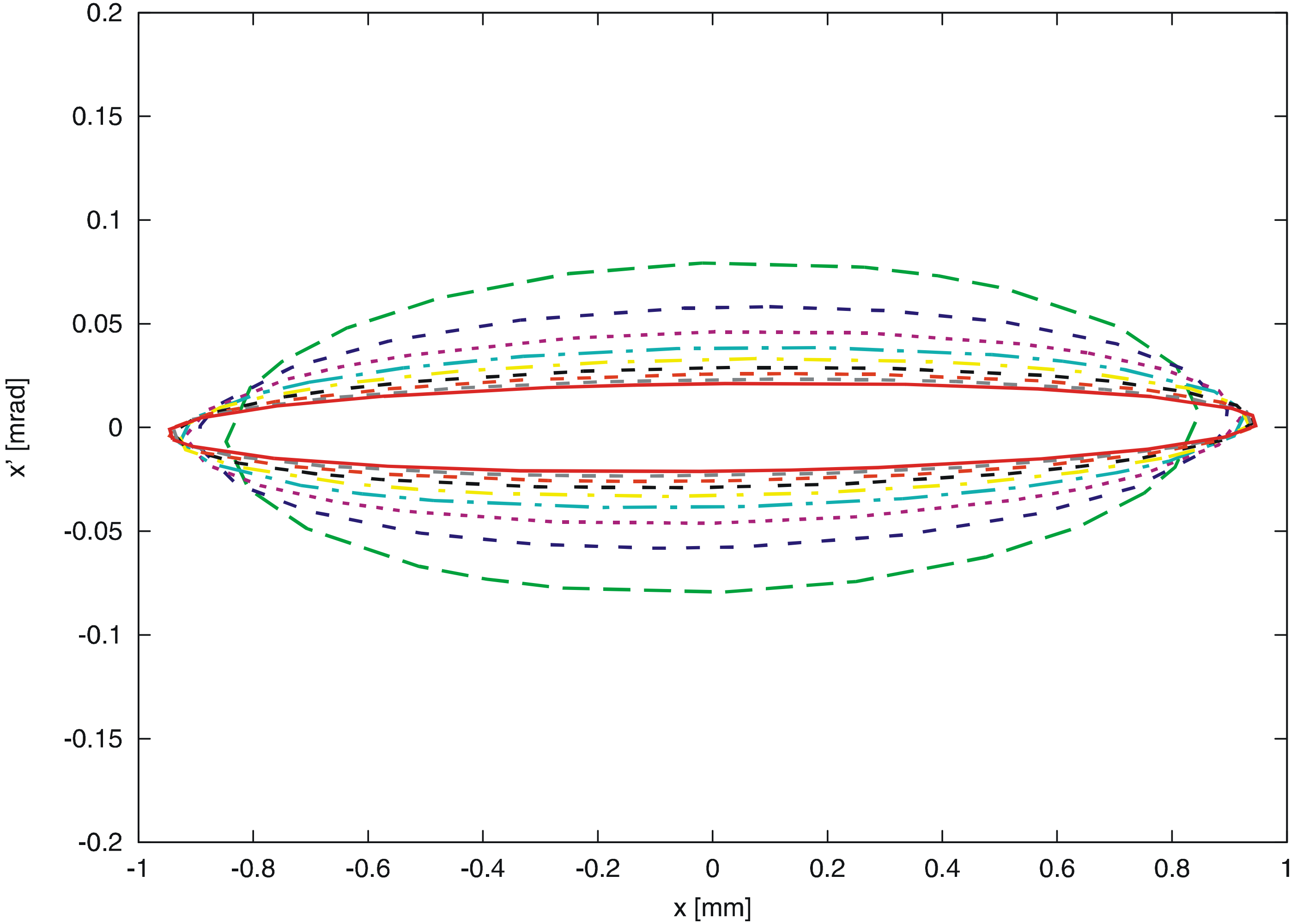

Due to pseudo damping horizontal beam size stays nearly constant !

General remarks on Race-Track-Microtrons:

- very flexible concerning extraction energies
- with long straight section cw-operation possible
- in pulsed mode very compact high energy accelerator
- excellent beam quality (energy spread, emittance)
- injected electrons must be relativistic (β~1), requires $E_{Inj.}$ some MeV
- "Herminghaus rule" [13] for RTMs: E_{out} / $E_{Inj.}$ < 10 (due to: beam path length in dipole fringe field, focussing on linac axis)
  requires cascading of RTMs to reach very high energies
- needs very homogenous bending magnet fields: $\Delta B/B < 10^{-4}$
  (for stable longitudinal beam dynamic, avoiding coupling of planes, feasible corrector strengths on return paths)
- at fixed magnetic field, weight of 180°-dipole magnets scale like E^3 !
- energies up to several 100MeV (up to GeV, see e.g. 4c)) possible
  (big number of turns)
- widely used for:
  radiotherapy, injector for synchrotrons,
  "big" cw machines especially for nuclear physics coincidence exp. [14]

2c) Recirculators = Recirculating Linacs

First publications: Stanford University High Energy Physics Laboratory (HEPL), Superconducting Linear Accelerator (SCA) [15,16,17]

Simplified sketch of principle

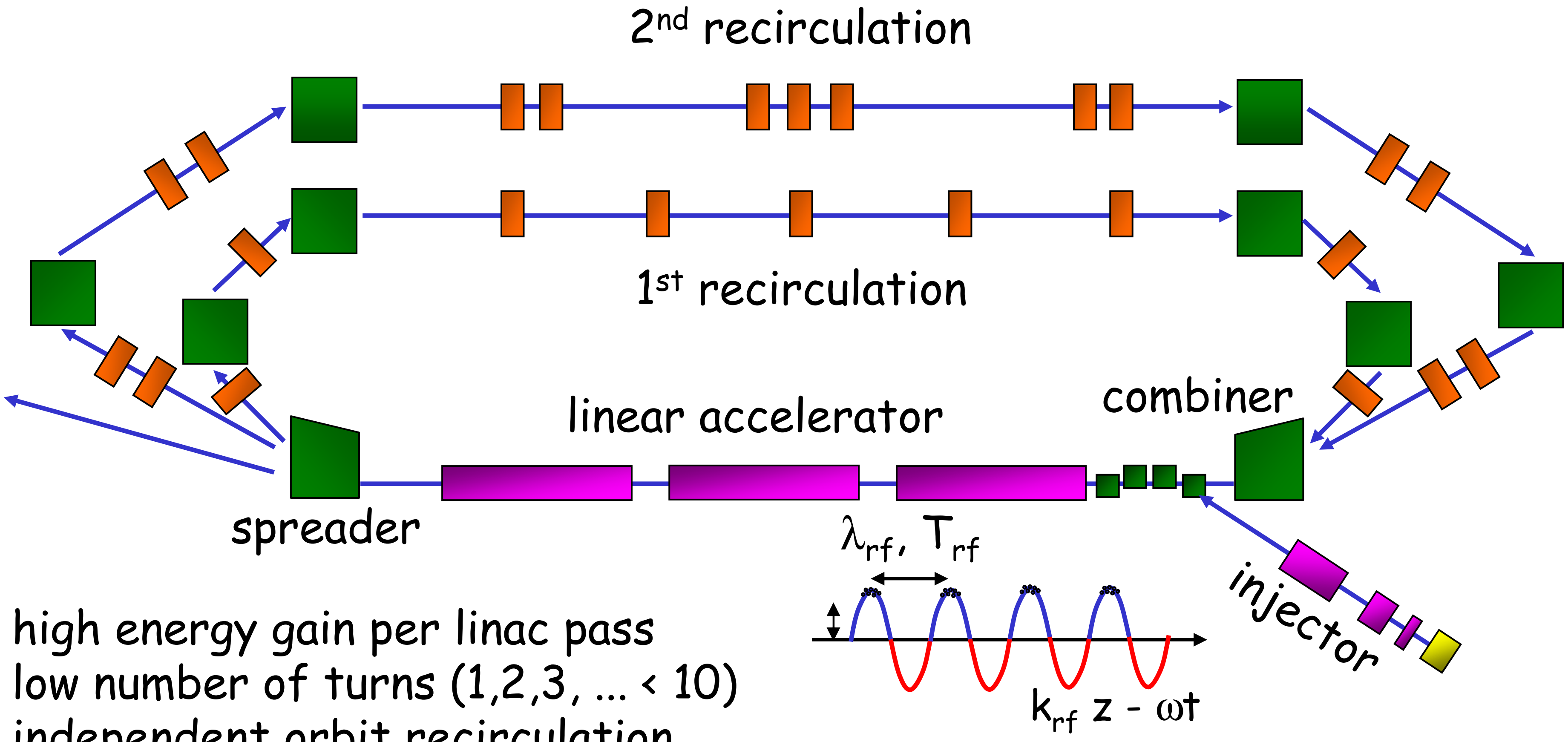

- high energy gain per linac pass
- low number of turns (1,2,3, ... < 10)
- independent orbit recirculation (no "big" 180°-dipoles; each orbit can have individual matched beam optics)

The beam optics of recirculating linacs:

The full six by six transfer matrix for a beam optics system with midplane symmetry (no coupling between x-y):

$$\begin{pmatrix} x_f \\ x'_f \\ y_f \\ y'_f \\ \delta\phi_f \\ \delta E_f \end{pmatrix} = \begin{pmatrix} R_{1,1} & R_{1,2} & 0 & 0 & 0 & \cancel{R_{1,6}} \\ R_{2,1} & R_{2,2} & 0 & 0 & 0 & \cancel{R_{2,6}} \\ 0 & 0 & R_{3,3} & R_{3,4} & 0 & 0 \\ 0 & 0 & R_{4,3} & R_{4,4} & 0 & 0 \\ R_{5,1} & R_{5,2} & 0 & 0 & 1 & \cancel{R_{5,6}} \\ 0 & 0 & 0 & 0 & 0 & 1 \end{pmatrix} \cdot \begin{pmatrix} x_i \\ x'_i \\ y_i \\ y'_i \\ \delta\phi_i \\ \delta E_i \end{pmatrix}$$

In most cases it is desired, that the beam optics of each recirculating line should be:

achromatic ⟺ Independent of energy, beam always comes back to the centre of the linac axis.

and

isochronous ⟺ The time to pass one recirculation is independent of beam energy.

N.B. isochronous systems are always achromatic ! [B]

Realising the recirculating arcs isochronous the recirculator acts like one long straight linac*) with max. energy gain ΔE_{max}

The **final beam properties** like phase length $\sigma\phi_f$ and energy spread σE_f are **mainly determined by the injector parameters $\sigma\phi_i$ and σE_i** !
(and the phase and amplitude jitter of the main linac)

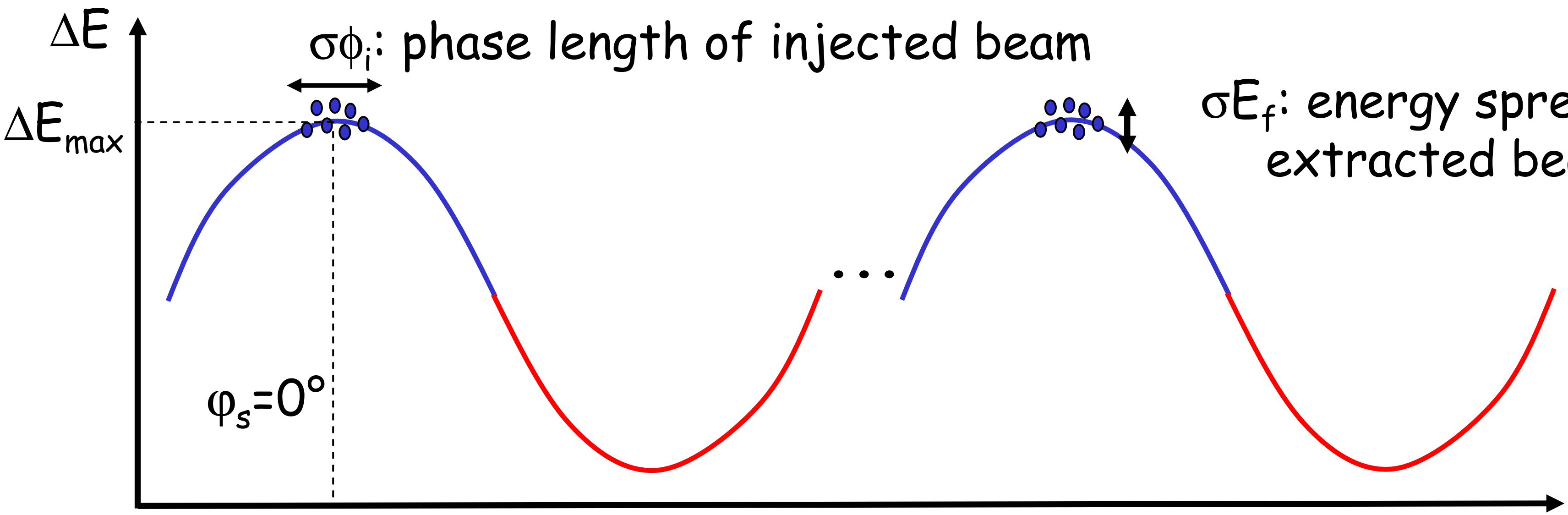

$\sigma\phi_f = \sigma\phi_i$ (definition of being isochronous)

$$\sigma E_f = \Delta E_{max} \cdot \left(1 - \cos(\sigma\phi_i / 2)\right) \sim \Delta E_{max} \cdot \sigma\phi_i^{\,2} / 8 \quad \text{(assumed: } \sigma E_i \sim 0\text{)}$$

e.g.: $\sigma\phi_i = 2° \rightarrow \sigma E_{f,rel} = \sigma E_f / \Delta E_{max} \sim 1.5 \cdot 10^{-4}$
$\sigma\phi_i = 10° \rightarrow \sigma E_{f,rel} = \sigma E_f / \Delta E_{max} \sim 3.8 \cdot 10^{-3}$

*) Not taking into account effects of e.g. synchrotron radiation.

Influence of phase $\delta\varphi_{rf}$ and amplitude δE_{rf} jitter:

(assuming here $\sigma E_i \sim 0$)

$$\delta E_{rf,rel.} = \frac{\delta E}{\Delta E_{max}}$$

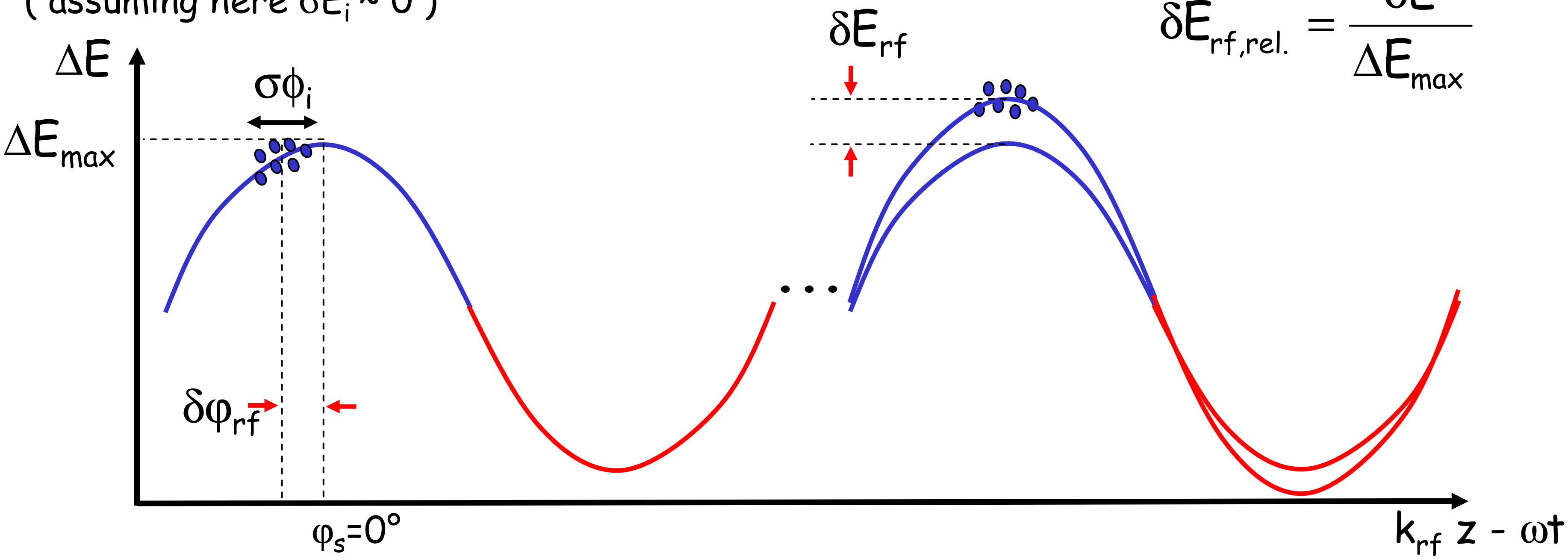

phase jitter $\delta\varphi_{rf}$: $\quad \delta E_f = \Delta E_{max} \cdot [1 - \cos(\delta\varphi_{rf})] \;\sim\; -\Delta E_{max} \cdot \delta\varphi_{rf}^{\,2} / 2$

(δE_f: energy deviation of bunch centre at output)

$$\sigma E_f = \Delta E_{max} \cdot |\cos(\delta\varphi_{rf} + \sigma\phi_i/2) - \cos(\delta\varphi_{rf} - \sigma\phi_i/2)|$$

$$= 2 \cdot \Delta E_{max} \cdot \sin(\delta\varphi_{rf}) \cdot \sin(\sigma\phi_i/2) \sim \Delta E_{max} \cdot \delta\varphi_{rf} \cdot \sigma\phi_i$$

(σE_f: energy spread of bunch at output)

amplitude jitter δE_{rf} : $\quad \delta E_f = (1 + \delta E_{rf,rel.}) \cdot \Delta E_{max}$

Phase and amplitude jitter directly transform to output energy jitter !

e.g.: ΔE_{max}=40MeV, 3 passes: E_{out}=120MeV, isochronous rec.

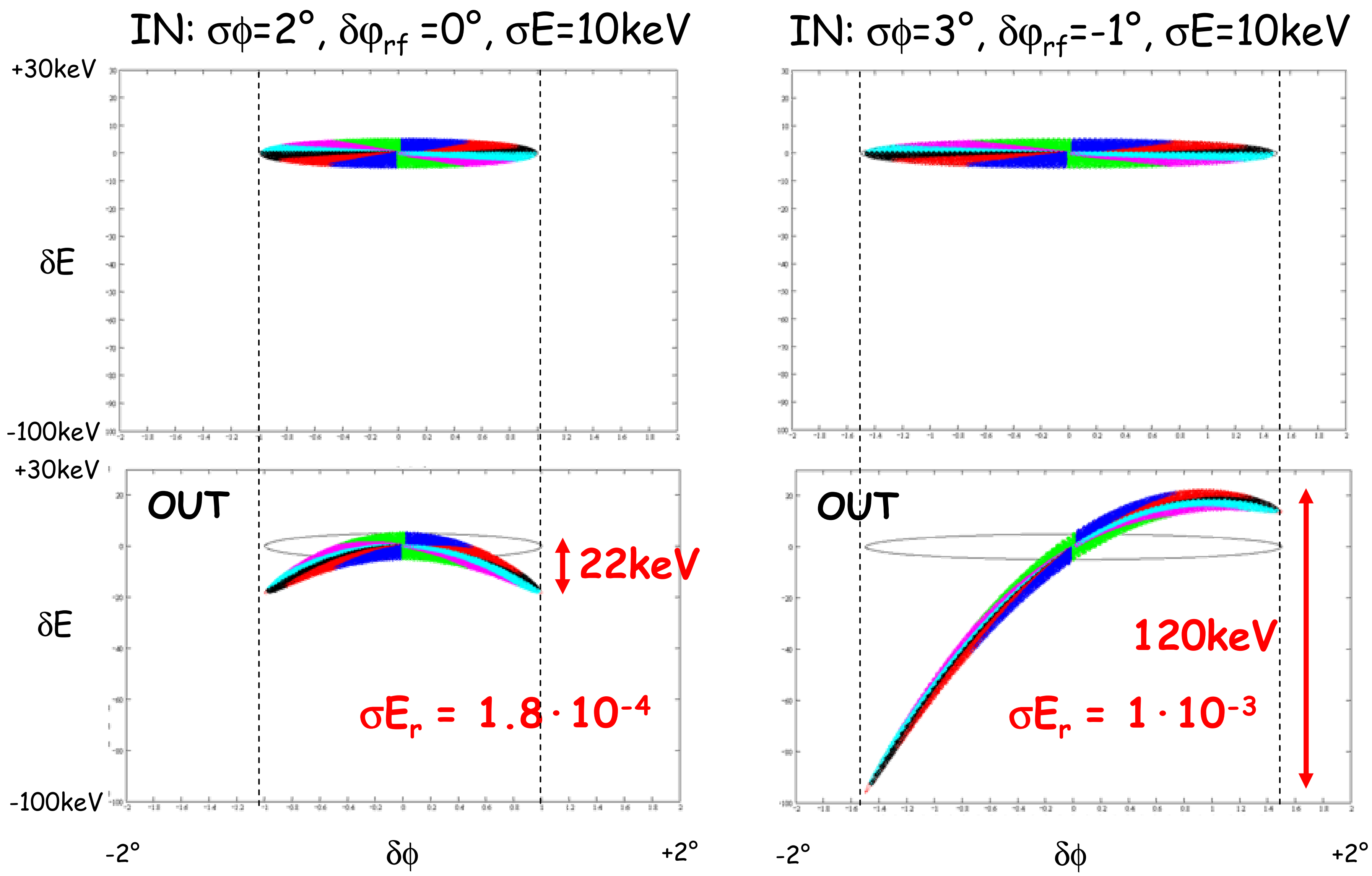

Under certain conditions it could be interesting to operate a recirculator in a non-isochronous mode with special tune value [18]

From RTM longitudinal dynamics we know:

amplitude jitter δE_{rf} of the linac transforms to phase jitter $\delta\varphi$!

(and to changes of the longitudinal tune value Q_{long} !)

e.g.: for a recirculator with **5 turns** select **Q_{long}=1 / 5**

(by choice of φ_s < 0)

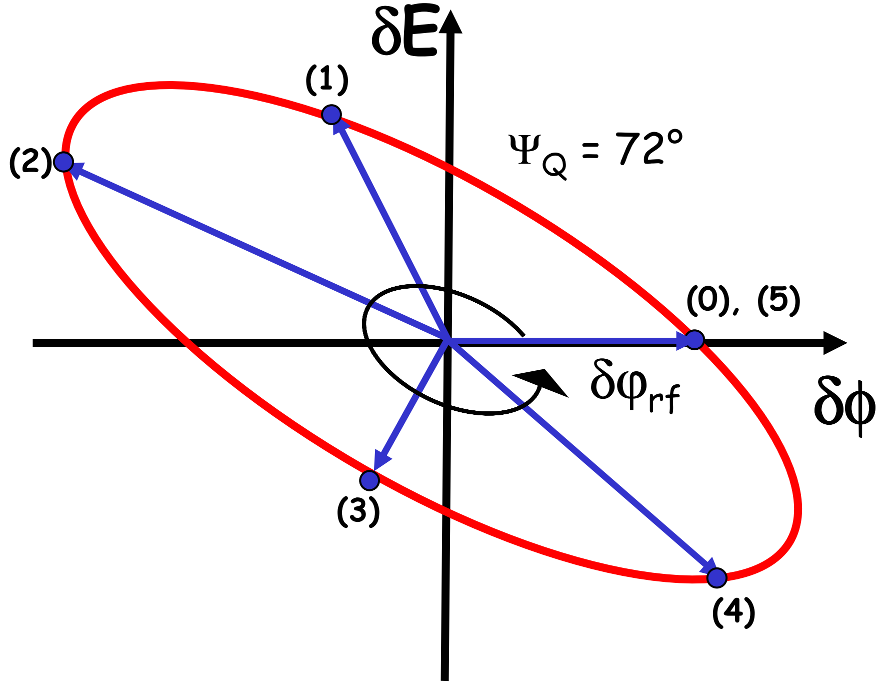

As a result each phase deviation at the input just transforms to an phase deviation at the output without introducing (much) energy jitter !

(as long as the amplitude jitter is small enough ($\delta E_{rf.rel.}$ < 1%) and does not change Q_{long} too much !)

General remarks on recirculating linacs:

- high energy gain per turn (long linac section)
- cw-operation possible
- low number of turns (z = 1, 2, … 10)
- independent-orbit recirculation allows individual adaptation of beam optics for each individual turn
- complex spreader and combiner design
- optics mostly isochronous and achromatic (operation on crest of the rf and therefore most efficient use of rf-power)
- no big 180° bending magnets necessary
- excellent beam quality possible (especially very short bunches)
- needs excellent amplitude and phase stabilisation for the linac-rf
- beam quality of extracted beam concerning bunch length and energy spread strongly depends on the beam quality of the injector
- very high electron energies possible, up to several GeV
- allows “easy” and cost-effective upgrade of existing linacs
- widely used for:
  nuclear physics research, FEL driver, proposed as future light source (see 5))

3) Rf-systems

Normal conducting ("room temperature", T=300k) rf, cw ↔ pulsed

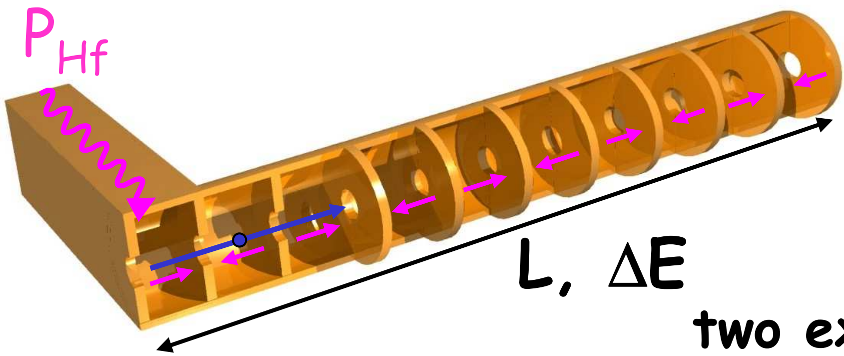

$$\Delta E = e \cdot \sqrt{R_s \cdot L \cdot P_{rf}}$$

R_s [Ω/m]: shunt-impedance

two examples:

cw: MAMI section [19]:
standing wave, 2.45GHz,
bi-periodic, π/2-mode
R_s=67MΩ/m, L=1.8m, P_{rf}=25kW
ΔE=1.74MeV

1MeV/m @ 14kW/m

This is a suitable power level which allow stable and reliable operation*) !

pulsed: DESY S-Band section [20]
travelling wave, 3GHz,
single periodic, 2π/3-mode
R_s=51MΩ/m, L=5.2m, P_{rf}=35MW **)
ΔE=96MeV

20MeV/m @ 7MW/m

(pulse length e.g.: 5µs, 100Hz,
duty cycle: 0.05%
→ **$P_{av.}$=3.5kW/m**)

Remember: This rf-power is necessary just to generate the accelerating fields even if only a single electron is accelerated !

*) In tests values of 210kW/m = 3.5MeV/m were reached [21] but only small demo sections !

**) 35MW pulse klystrons are standard.

Superconducting rf, mostly cw (or long pulse ~ ms)

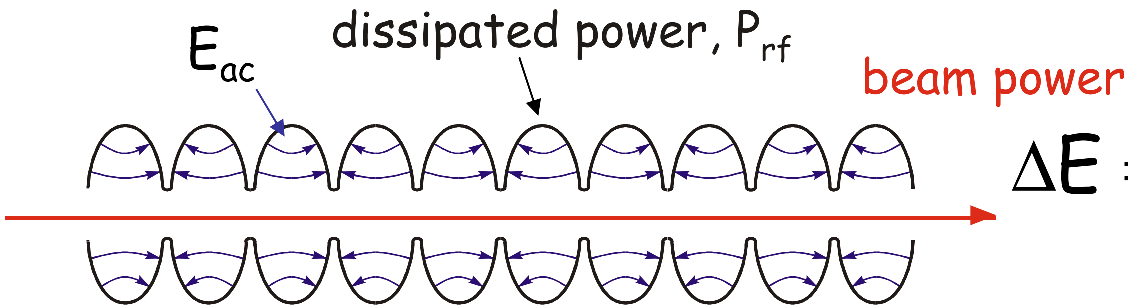

$$\Delta E = e \cdot \sqrt{(R/Q) \cdot Q \cdot L \cdot P_{rf}}$$

$$P_{rf} = P_{diss} = \frac{(\Delta E / e)^2}{(R/Q) \cdot Q \cdot L}$$

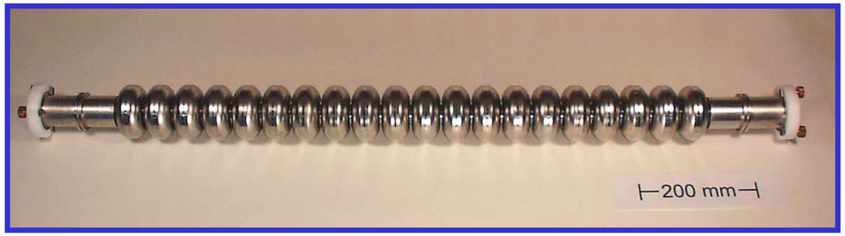

cw S-DALINAC section [22]**:**
standing wave, 3GHz,π-mode, 20-cells
$R/Q=2k\Omega/m$, $Q=3 \cdot 10^9$, $L=1m$
($Q_L=Q \cdot (1+\kappa)^{-1}=3 \cdot 10^7$: loaded Q-value)

$\Delta E=5MeV/m^{*)}$ @ $P_{rf}=4W/m$

3dB-bandwidth of the resonator:
$\delta f_{3dB} = 3GHz/Q_L = 100Hz$
(MAMI nc: 320kHz)

frequency versus length variation:
$\delta f / \delta l = 500Hz/\mu m$
$\Rightarrow$ phase versus length variation:
$\delta\varphi/\delta l = 0.6°/nm$

In sc-cavities the available rf-power goes mostly to the beam. But: the small amount of dissipated rf-power must be removed from a cryogenic environment @ 2K (cooling away 1W@2K needs approx. 500W@300K power) !

*) 5MeV/m is today a rather conservative value. For the energy upgrade of CEBAF, Jefferson Lab., cavities with 19.2MeV/m and $Q=8 \cdot 10^9$ (@1.5GHz) under cw-operation are already tested [23]. Theor. limit @ 1.3GHz: 50MeV/m [24].

Efficiency of nc and sc recirculators:

Will use the following definition (and normalize per linac-meter):

$$\eta_{electricity} = \frac{P_{beam}}{P_{electricity}}$$

nc-linac:

rf-power to generate acc. fields

beam power

needs rf-power

$$\eta_{nc} = \frac{z \cdot \Delta U_{acc} \cdot I_{beam}}{\frac{1}{\eta_{rf}} \cdot \left(\frac{\Delta U_{acc}^2}{R_s \cdot \cos(\varphi_s)} + z \cdot \Delta U_{acc} \cdot I_{beam} \right)} = \frac{\eta_{rf} \cdot z \cdot \Delta U_{acc} \cdot I_{beam}}{\frac{\Delta U_{acc}^2}{(R_s/Q) \cdot Q \cdot \cos(\varphi_s)} + z \cdot \Delta U_{acc} \cdot I_{beam}}$$

2.45GHz, z: number of turns, $\Delta U_{acc}=(\Delta E/e)/L=0.83$MV/m, $R_s/Q=4.4$kΩ/m, $Q=15200$, $\eta_{rf}=50\%$ (efficiency of rf-generation)

sc-linac:

and here additionally: rf-power needs to be cooled away @2K

$$\eta_{sc} = \frac{z \cdot \Delta U_{acc} \cdot I_{beam}}{\frac{\Delta U_{acc}^2}{R_s \cdot \cos(\varphi_s)} \cdot \left(\frac{1}{\eta_{rf}} + \frac{1}{\eta_{cool}} \right) + \frac{1}{\eta_{rf}} \cdot z \cdot \Delta U_{acc} \cdot I_{beam}} = \frac{\eta_{rf} \cdot z \cdot \Delta U_{acc} \cdot I_{beam}}{\frac{\Delta U_{acc}^2}{(R_s/Q) \cdot Q \cdot \cos(\varphi_s)} \cdot \left(1 + \frac{\eta_{rf}}{\eta_{cool}} \right) + z \cdot \Delta U_{acc} \cdot I_{beam}}$$

3GHz, z: number of turns, $\Delta U_{acc}=(\Delta E/e)/L=5$MV/m, $R_s/Q=2$kΩ/m, $Q=3 \cdot 10^9$, $\eta_{rf}=50\%$ (efficiency of rf-generation), $\eta_{cool}=0.2\%$ (efficiency of cryogenic system)

Efficiency of nc and sc recirculators:

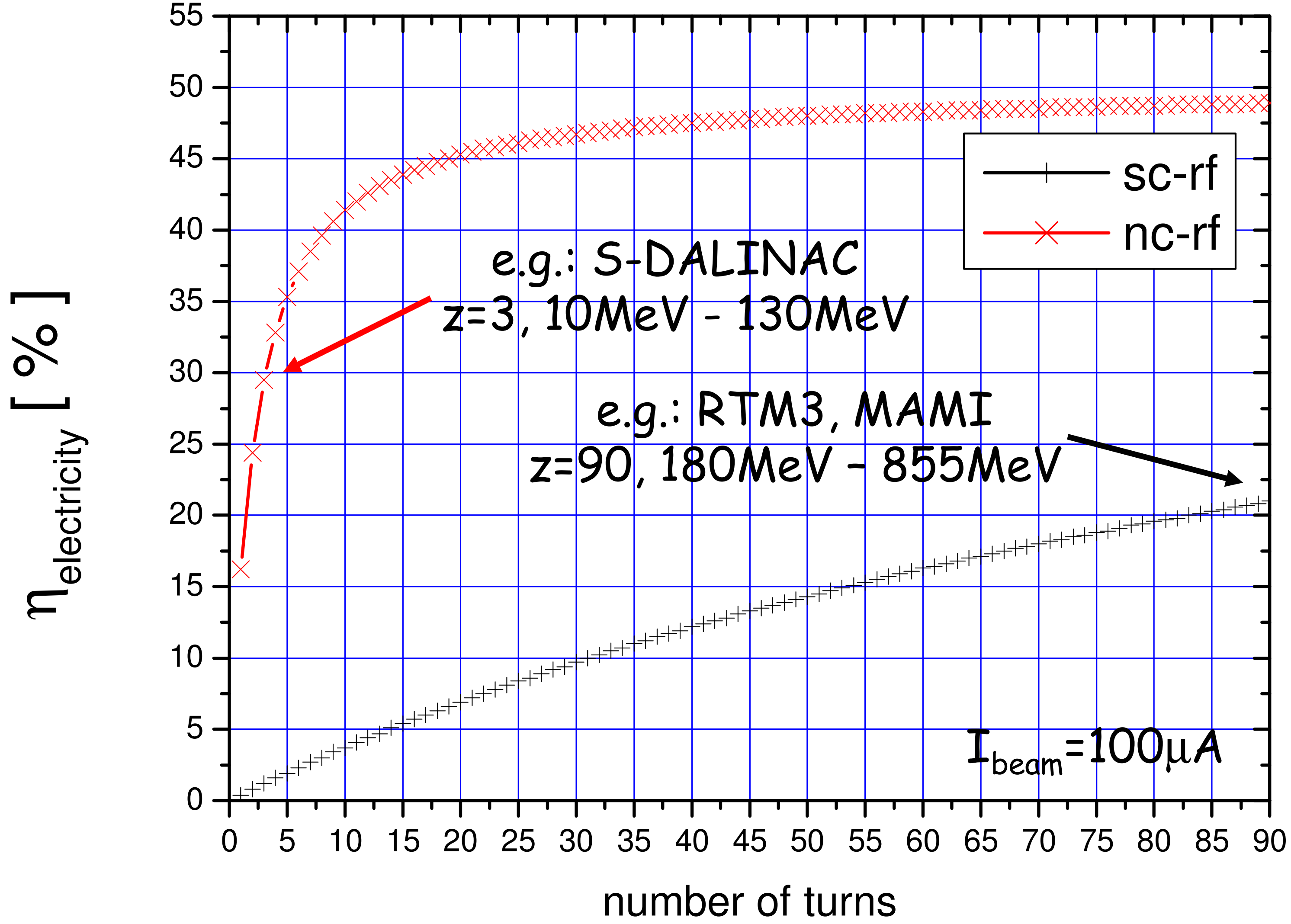

General remarks nc-rf ↔ sc-rf:

nc-rf:

- very reliable and well approved technology
- in pulsed operation very high gradients (>> 25MeV/m) achievable
- requirements concerning phase and amplitude stability easy to fulfil
- for highest shunt impedance R_s (efficient use of rf) the apertures need to be small (design: trade-off between beam transmission, wake fields, transverse higher modes and R_s)
- rule of thumb: in cw mode 1MeV/m @ 15kW/m (only for the acc. fields)
- at low beam loading rather inefficient: 100μA single pass beam current at 1MeV/m needs only additional 100W rf-power

sc-rf:

- rapid development and progress during the last years (e.g. TESLA [24]) This will go on: International Linear Collider technology decision: **sc** ! [25]
- 10MeV/m up to 20MeV/m accessible with very low rf-power
- high efficiency possible even at low number of recirculations
- big apertures possible (because no need for optimisation of R_s/Q)
- very high requirements for the rf-regulation loops concerning phase and amplitude stability
- complex technology (surface treatment, clean rooms, cryogenics)

Scanditronix 100MeV RTM (similar to the old MAX-LAB injector*)) [26,27]

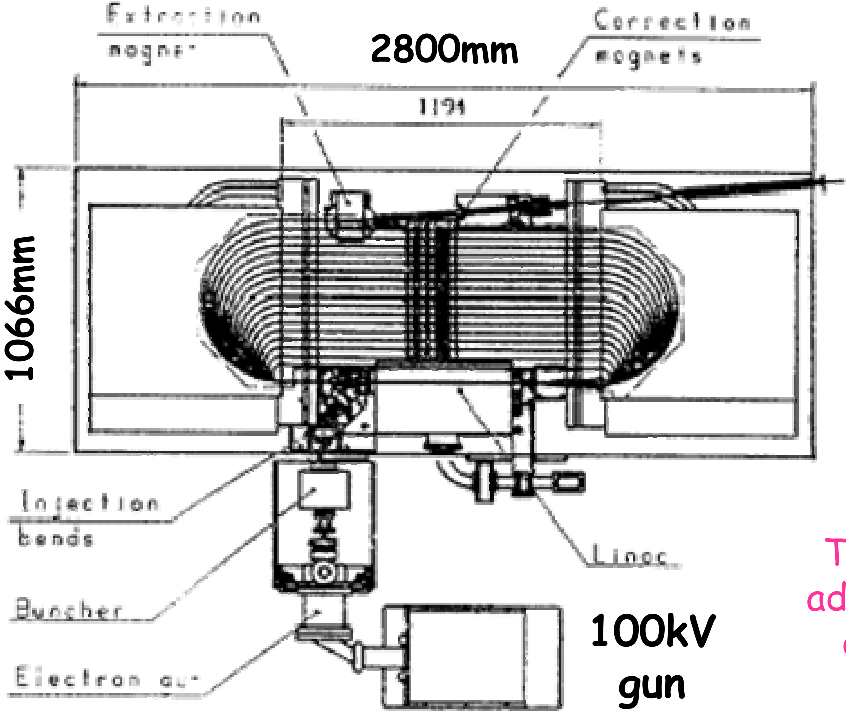

MAX-LAB:

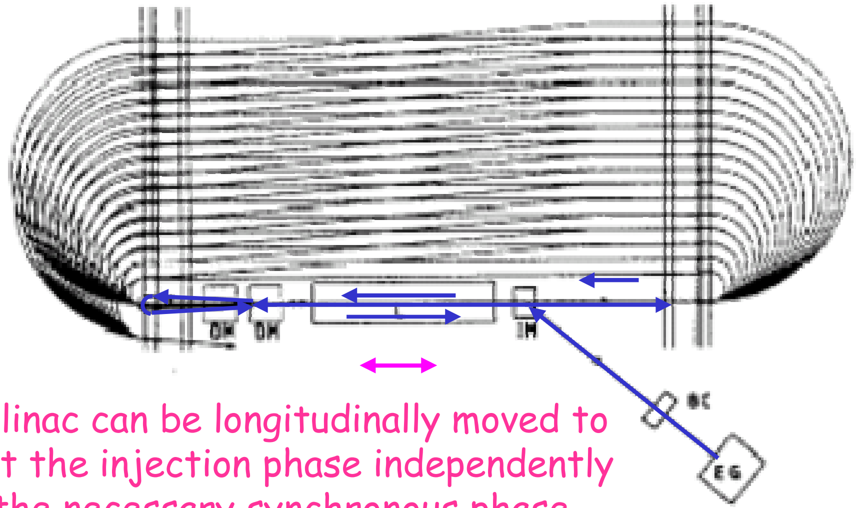

The linac can be longitudinally moved to adjust the injection phase independently of the necessary synchronous phase.

rf-system: 3GHz, 5MW pulse klystron $\rightarrow \Delta E$=5.3MeV/turn (B=1.1T)

injection: reversed orbit geometry [28] (two linac passes: E_{Inj}= 12.6MeV)

focussing: with reverse field stripe and focussing on linac axis (rf + quad.)

beam parameters: 100MeV (MaxLab: 10MeV – 100MeV), z=19 turns, σE=0.1% (100keV), pulse length: 0.1 – 2μs, rep. rate: 0.1 – 10Hz, beam pulse current: 15 – 30mA

*) Similar machines are used as injectors for synchrotrons (ANKA, BESSY I+II). Some Scanditronix RTMs (RTM50, 10-50MeV) were built for radio-therapy.

Eindhoven University 75MeV RTM [29]

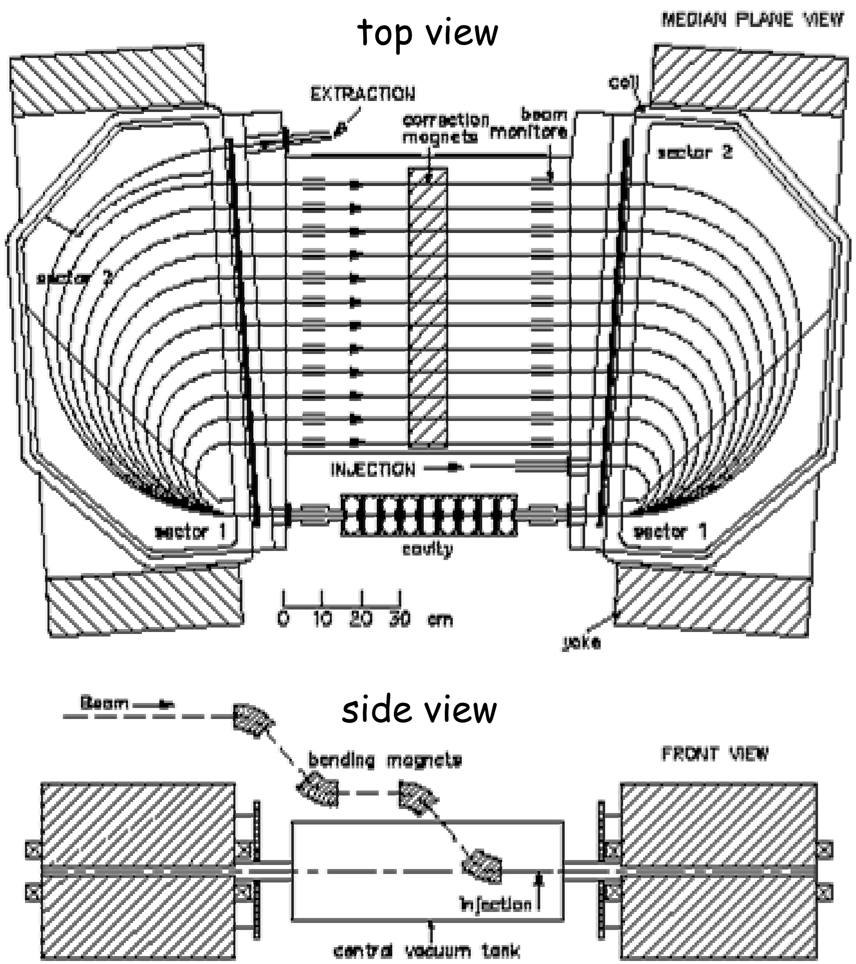

rf-system:
3GHz, 2.2MW phase-locked, pulsed magnetrons $\rightarrow$ ΔE=5MeV/turn (B=0.5-0.6T)

injection:
injector linac with 10MeV (refurbished medical linac)

focussing:
by segmented dipoles and quadrupoles on linac axis

beam parameters:
75MeV, z=13 turns, σE=0.15%
special: n=2 operation mode (2 x λ_{rf} phase advance per turn, φ_s=-9°) for bigger orbit separation = 60.6mm
By variation of $E_{Inj.}$, ΔE and B a continuous variation of the output energy from 45MeV up to 90MeV is possible [30].

Originally this machine should have served as the injector for the EUTERPE project, a 400MeV e^- -storage ring for accelerator physics studies and sr-application. Now itself is used as a testbed for accelerator physics developments.

Permanent Magnet Dipoles 70MeV RTM [31]

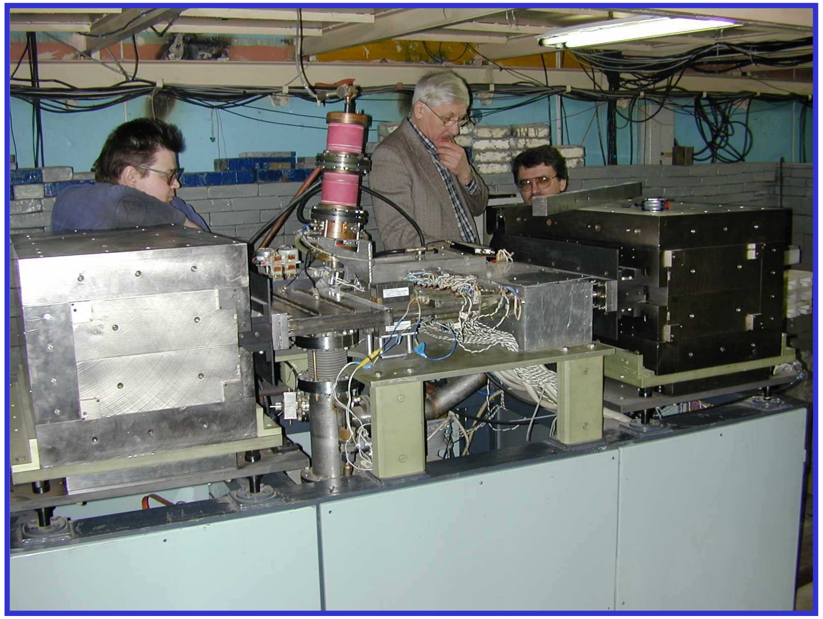

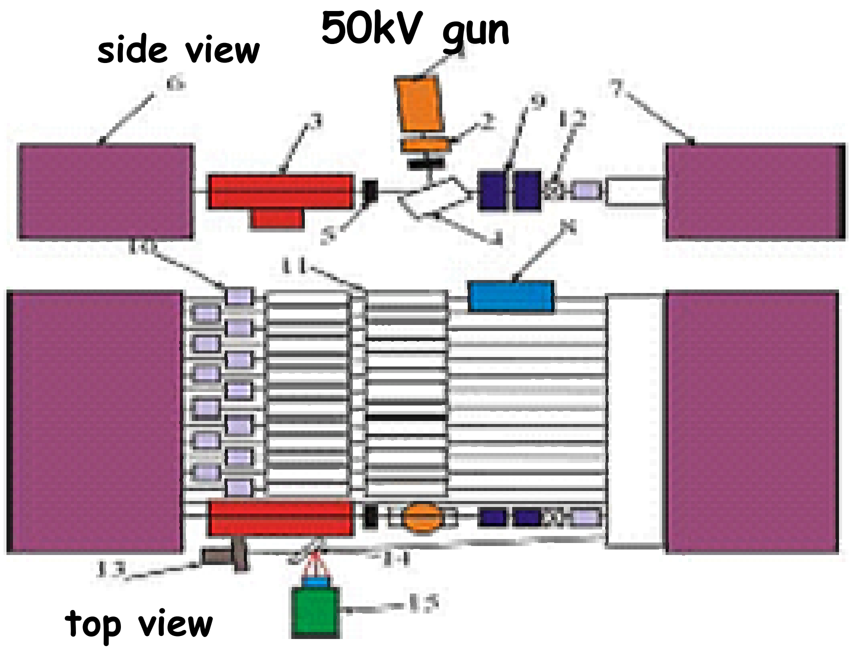

rf-system: 2.856GHz, 6MW multi-beam (low high-voltage), PPM-focussed*) klystron
$\rightarrow \Delta E$=5MeV/turn (B=1.0T)
injection: by alpha magnet directly in the linac axis (one linac pass: E_{Inj}= 5MeV)
focussing: on linac axis; horizontally by linac section apertures, vertically by single quadrupole
beam parameters: 10MeV-70MeV, z=12 turns, pulse length: max. 10µs, rep. rate: max. 250Hz, beam pulse current: max. 40mA

*) Periodic Permanent Magnet focussing.

4b) nc pulsed Recirculating-Linacs

MIT Bates Linear Accelerator [32,33]

- originally designed as a high duty factor, single pass linac for nuclear physics experiments; regular operation starts: mid 1974
- consisting of 24 linac sections, powered by 10 klystrons (2856MHz, max. 4MW each)
- beam parameters: e.g. 15μs pulse length, 300Hz, duty cycle: 0.45%, 25μA av. current, 320MeV output energy, 0.3% energy spread (defined by collimators)

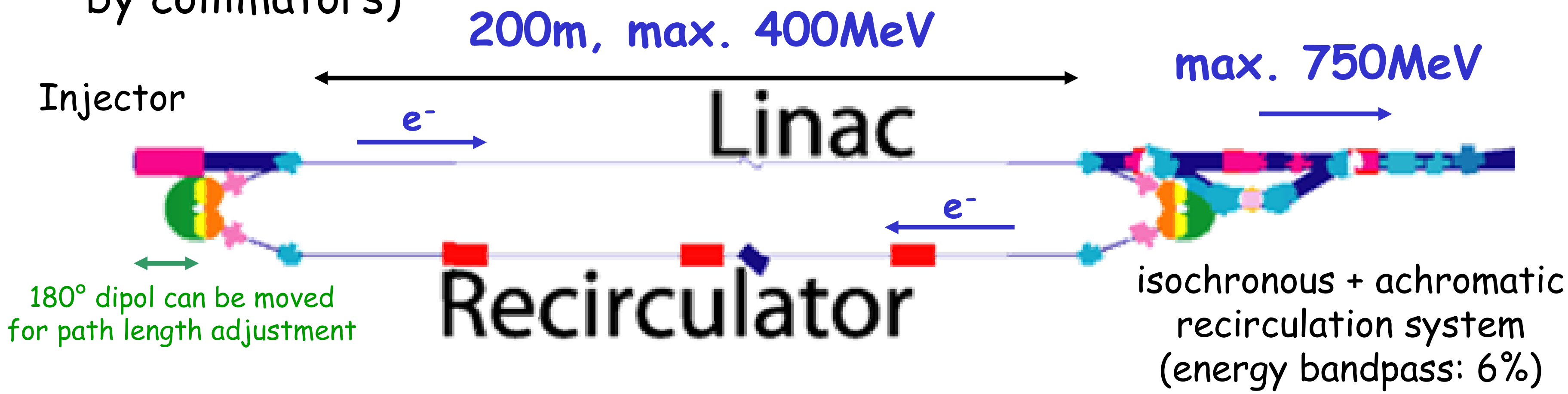

- a one turn isochronous (and highly achromatic) recirculation system was added and operation starts in 1983 [34]
- complication: energy deviation over the beam pulse length due to transient beam loading effects (needs big acceptance of recir. system)

The 500MeV Injector for MAX-LAB, University of Lund

- replaces the over 20 years old injector-RTM (heavily radiation damaged)
- gains more flexibility for the injection into the 3 MAX-LAB storage rings

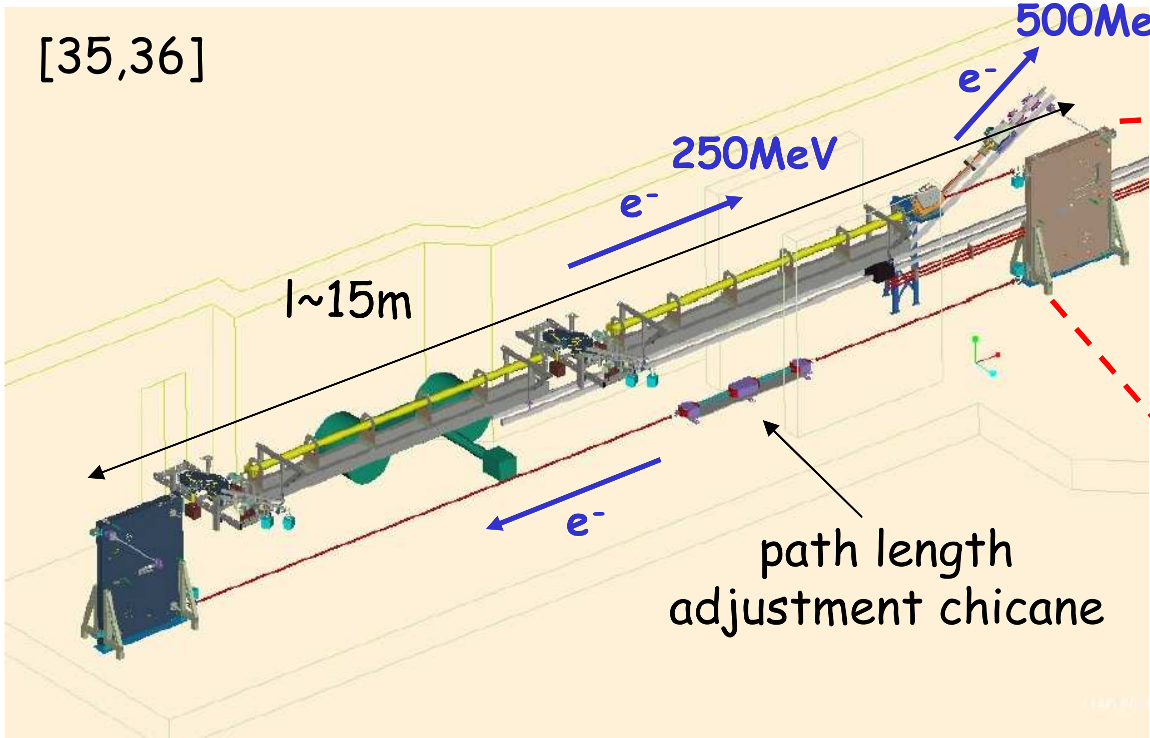

"recirculation block":

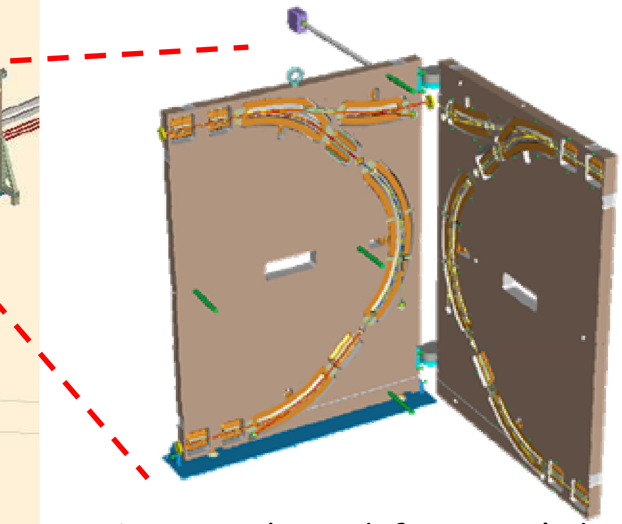

CNC machined from solid iron
(high alignment precision)
"put in coils, close door"

rf-system: two S-band (3GHz) sections (l=5.2m), each powered by one 35MW pulse klystron (additionally equipped with a SLED*) system) → 250MeV energy gain (25MeV/m)
injector: photo rf-gun (2MeV, pulse current >100mA, bunch length: ~3ps)
recirculation system: two isochronous "recirculation blocks" with path length chicane in the connecting straight section for phase adjustment
beam parameters: 100ns pulse length, 40mA pulse current, 10Hz, 0.033% energy spread

*) Stanford Linac Energy Doubler: Rf-energy storage cavities (increased rf-power on the expense of decreased pulse length).

4c) cw Race-Track-Microtrons

Microtron Using a Superconducting Linac (MUSL), University of Illinois Nuclear Physics Group [37,38]

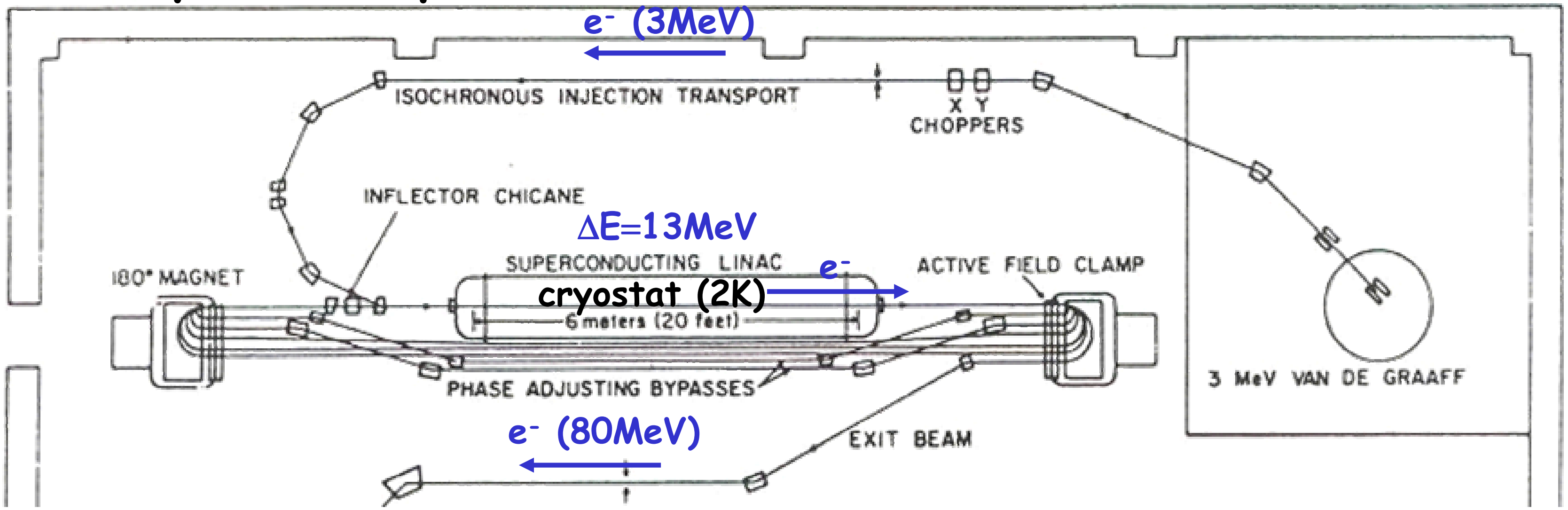

- design of RTMs with sc-linacs started as early as 1967 !
- the sc-cavities were built in collaboration with the Stanford HEPL / SCA group
- a first machine (MUSL-1) was built and operated beginning of 1970 (1.3GHz, T_{op}=4.2K, gradient: 2MeV/m, z=6 passes → E_{out}=19MeV)
- in the mid of 1970 a second machine, MUSL-2 was built using magnets of MUSL-1 (1.3GHz, T_{op}=2K, ΔE/turn=13MeV@10W rf power, z=6 passes → E_{out}=80MeV, n=2 operation mode for sufficient orbit separation)
- it was planned to install a cascade of sc-RTMs to reach ~ 750MeV output energy
- MUSL-2 was limited to 1µA beam current due to Regenerative Beam Blow Up (BBU) (after modifications of the sc-structures: 3µA) [39]

Regenerative Beam Blow Up (BBU) (short introduction):

[40,41,42]

e.g. TM_{11}-mode

E-Field, B-Field

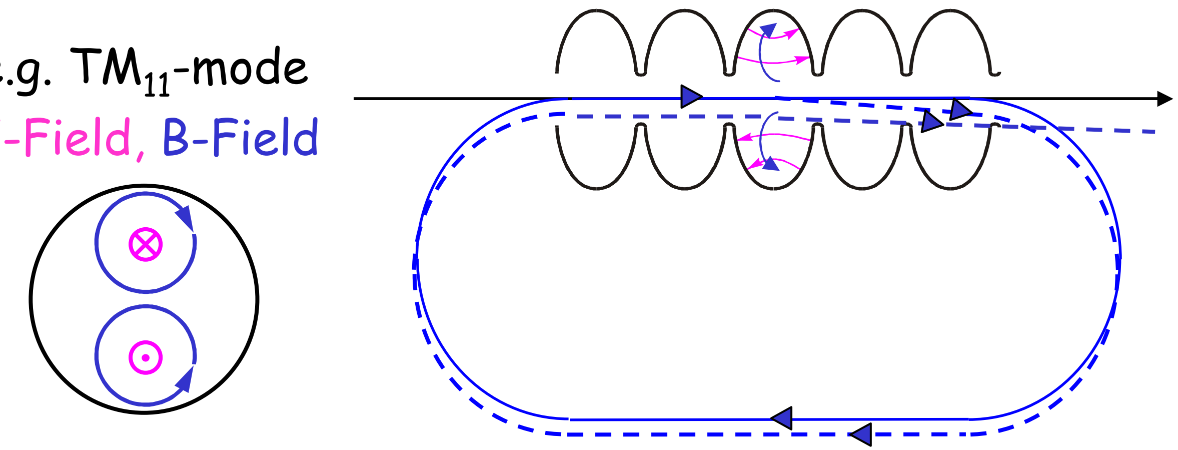

Beam enters cavity slightly off axis and excites + gets a transverse kick from TM_{11}-mode (B-field). Beam starts betatron-oscillations on recirculation path and enters cavity again. If betatron phase and rf-phase of deflecting mode are "in phase", beam is more and more kicked and energy from the beam is transferred to the mode (via E-field).

Short cavity model by Herminghaus/Euteneuer ("worst case approx."):

[41]

$$I_S \sim \frac{1}{(R_S/Q)_{BBU} \cdot Q_{BBU}} \cdot \frac{E_z \cdot \lambda_{BBU}}{\beta} \cdot \frac{1}{z \cdot \ln(E_{Out}/E_{In})}$$

I_s: threshold current
$\ldots_{BBU}$: parameters related to the BBU mode
E_z: accelerating field strength
β: average beta-function of the recirculation
z: number of turns
R_s/Q: here in $[\Omega]$, and not normalized to length

Transverse optics of the recirculation plays an important role (more complex as included in this approximation) !

That´s the reason why BBU was at first a concern for sc-accelerators like MUSL . Countermeasures: damping/detuning of modes.

The Mainz Microtron MAMI, University of Mainz [13,43]

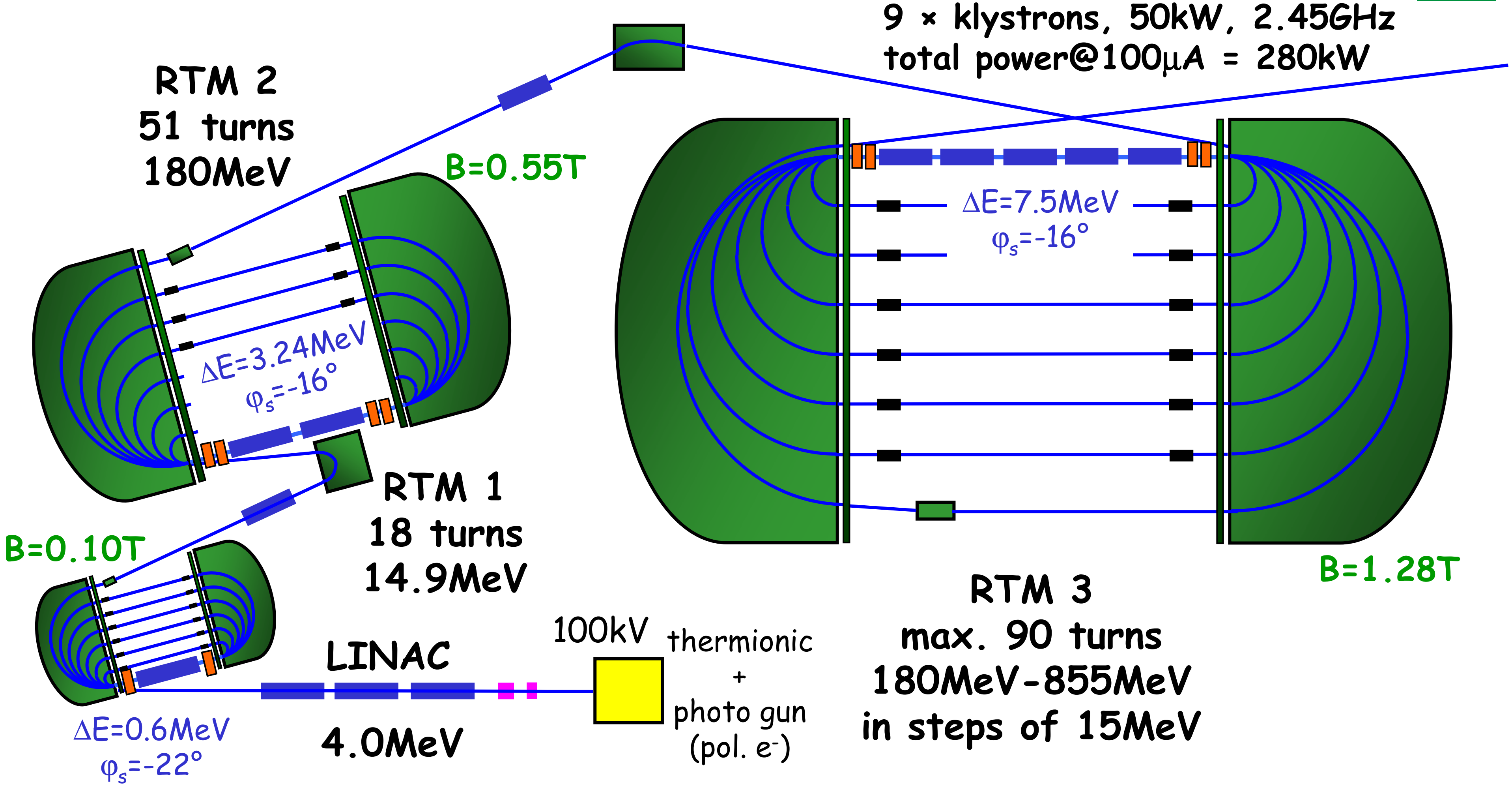

beam parameters: 100µA max cw current (86kW beam power)

injector linac:	RTM 1:	RTM 2:	*) RTM 3:
σE=1.2keV ($3\cdot10^{-4}$)	σE=1.2keV ($8\cdot10^{-5}$)	σE=2.8keV ($1.5\cdot10^{-5}$)	σE=13keV ($1.5\cdot10^{-5}$)
$\varepsilon_{x,n}=0.05\cdot10^{-6}$ m rad	$\varepsilon_{x,n}=0.07\cdot10^{-6}$ m rad	$\varepsilon_{x,n}=0.25\cdot10^{-6}$ m rad	$\varepsilon_{x,n}=13\cdot10^{-6}$ m rad
			$\varepsilon_{x,abs}=8\cdot10^{-9}$ m rad

*) Increase in energy spread and emittance due to sr-effects (see next page).

Increase of energy spread σ_E and horizontal emittance ε_x due to quantum excitation of synchrotron radiation photons emitted when a e$^-$ -beam with energy γ passes a horizontal (x-plane) 360°-bending system (R) ! [44]

$$\Delta\sigma_E^2 = \frac{55\cdot(\hbar\cdot c)^2}{48\cdot\sqrt{3}}\cdot\gamma^7\cdot\int_0^L \frac{1}{|R(s)|^3}ds$$

Integration along the path through the bending magnet.

r_e: classical e$^-$ radius, m_e: e$^-$-mass

$$\Delta\varepsilon_x = \frac{55\cdot r_e\cdot\hbar\cdot c}{48\cdot\sqrt{3}\cdot m_e\cdot c^2}\cdot\gamma^5\cdot\int_0^L \frac{H_x(s)}{|R(s)|^3}ds$$

$$H_x = \beta_x\cdot D_x'^2 + 2\cdot\alpha_x\cdot D_x\cdot D_x' + \gamma_x\cdot D_x^2$$

(α, β, γ: optical functions, D: dispersion)

RTM 3: comparison of measured and calculated emittances [45]

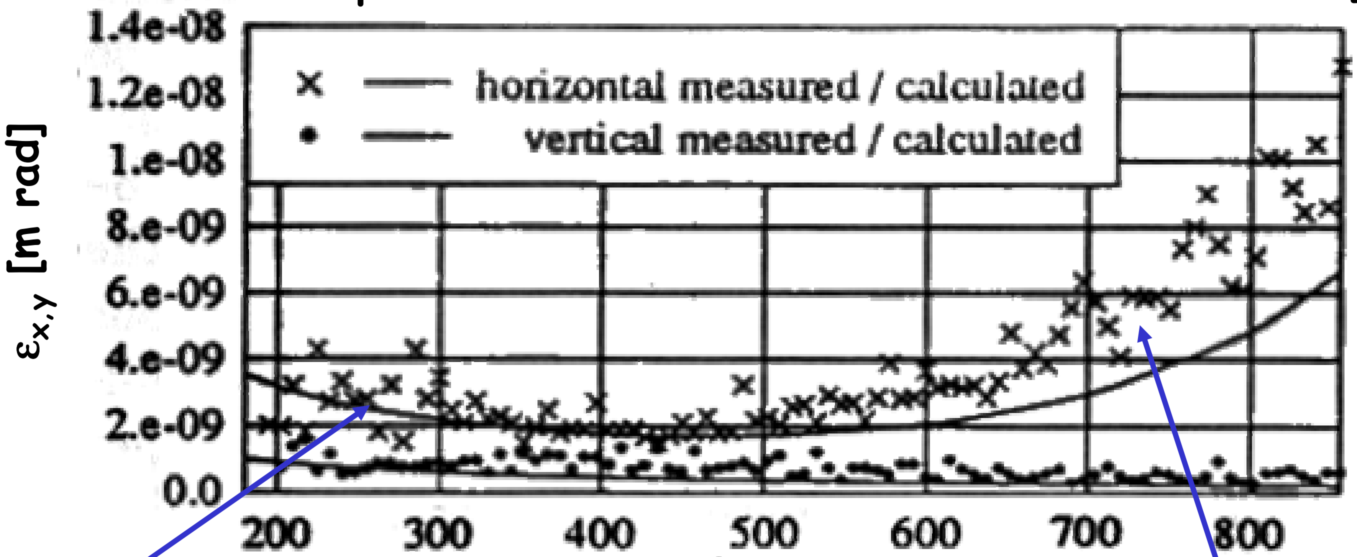

adiabatic damping:
(in x and y) $\varepsilon = \frac{1}{\beta\cdot\gamma}\cdot\varepsilon_{norm}$

quantum excitation: only in x
(without coupling of planes)

Precision energy stabilization RTM 3 [46]

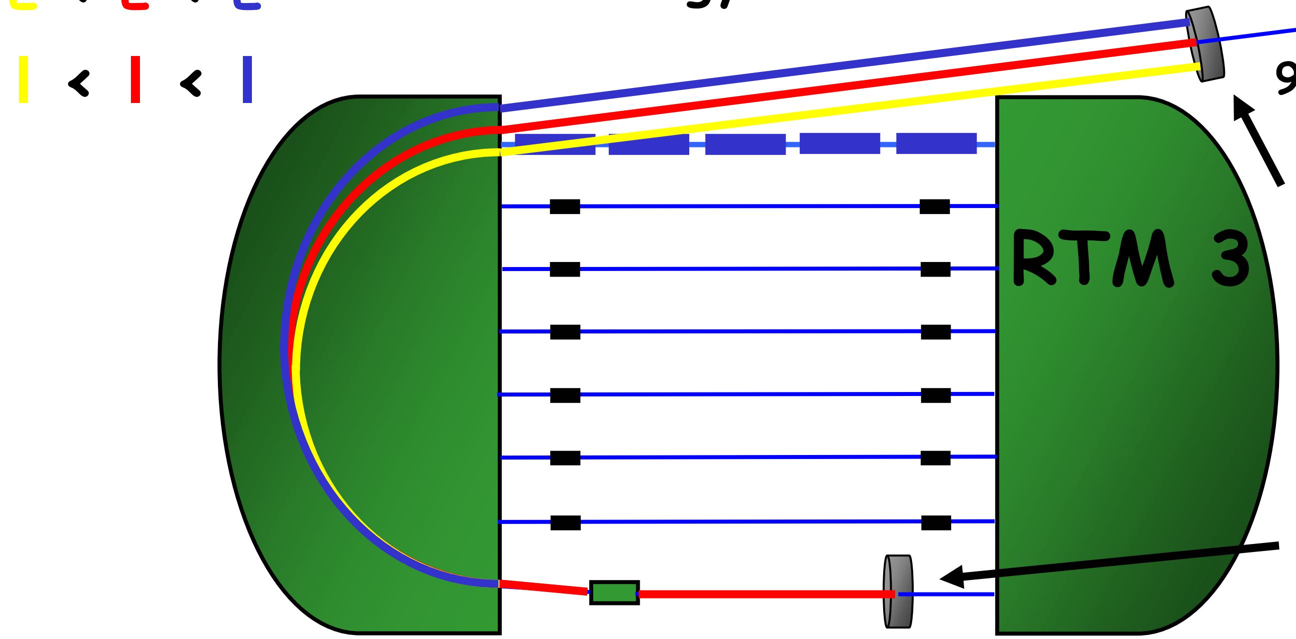

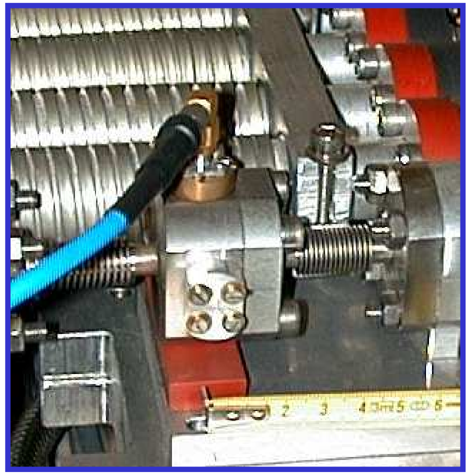

Time of flight measurement in the last 180° extraction turn via relative phase measurement between two 9.80GHz resonators (TM_{010}). By selecting a proper longitudinal Q-value it is possible to steer the RTM 3 injection phase to stabilize the output energy !

Longitudinal dispersion of 180°-dipole in terms of the 9.80GHz resonators is:

$$\frac{\lambda_{rf}/2}{\Delta E} = \frac{2 \cdot \lambda_{9.80GHz}}{7.5\text{MeV}} = 8.16\,\text{mm/MeV} = 96°/\text{MeV}$$

With a phase resolution of 0.1° we get an energy stabilization of:

~ 1keV @ 855MeV = $1.2 \cdot 10^{-6}$

Hall A: Injector Linac, RTM 1 + RTM 2

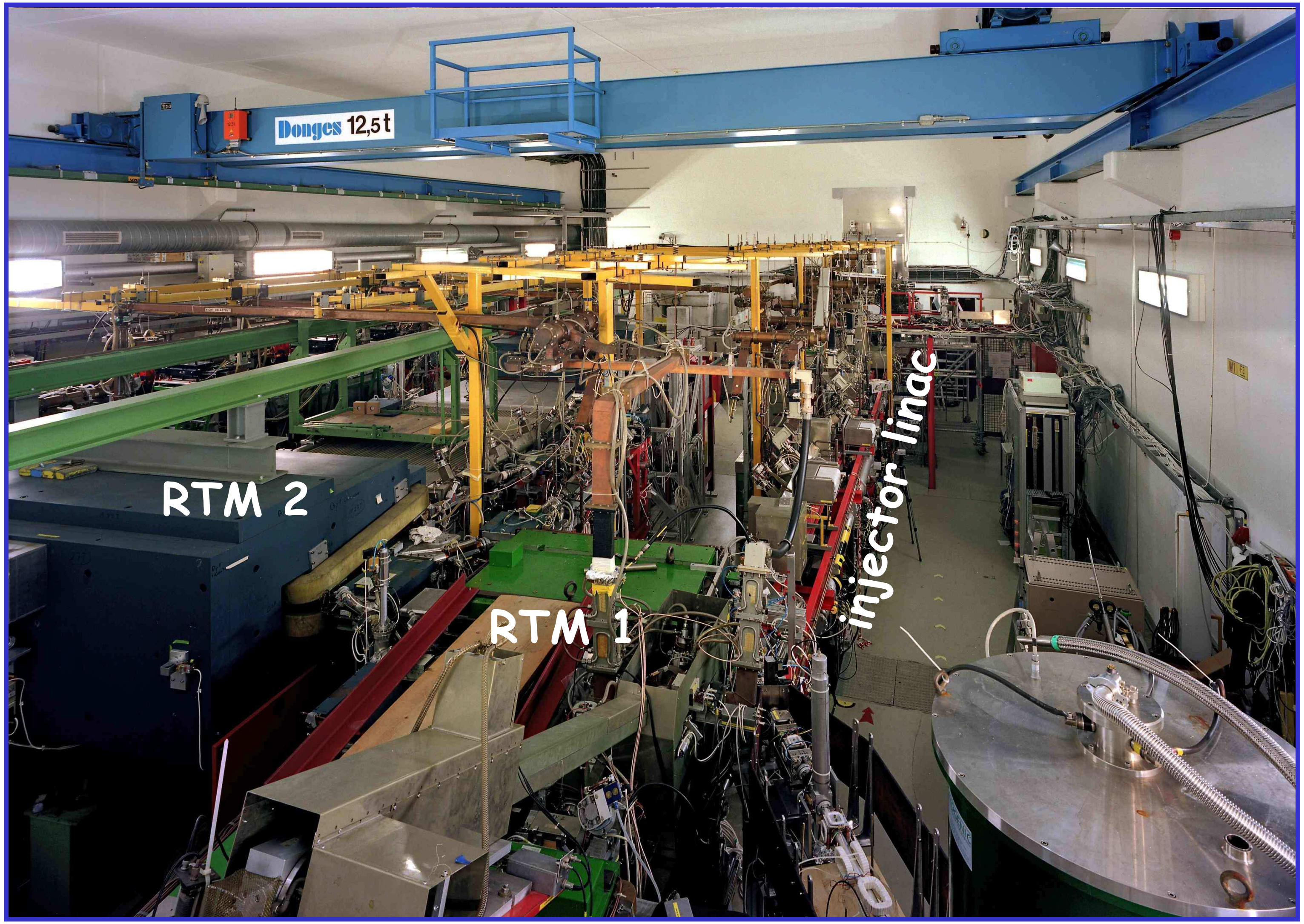

Hall B: RTM 3

Floorplan of MAMI B

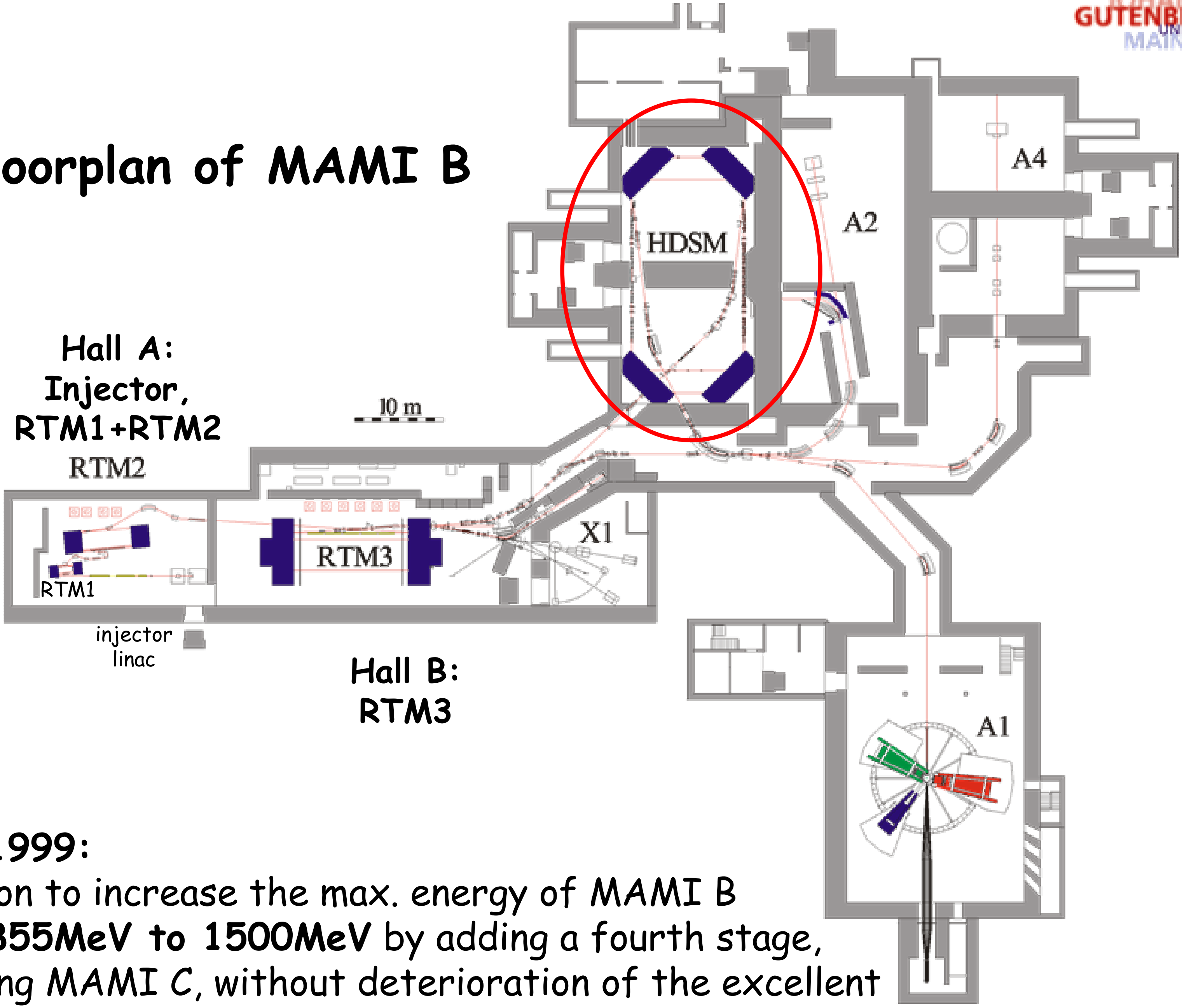

year 1999:
Decision to increase the max. energy of MAMI B from **855MeV to 1500MeV** by adding a fourth stage, realising MAMI C, without deterioration of the excellent beam quality, using the expertise (nc-recirculators) of the institute.

A fourth microtron ?

E=855MeV **E=1500MeV**

(B = 1.28 T = const.)

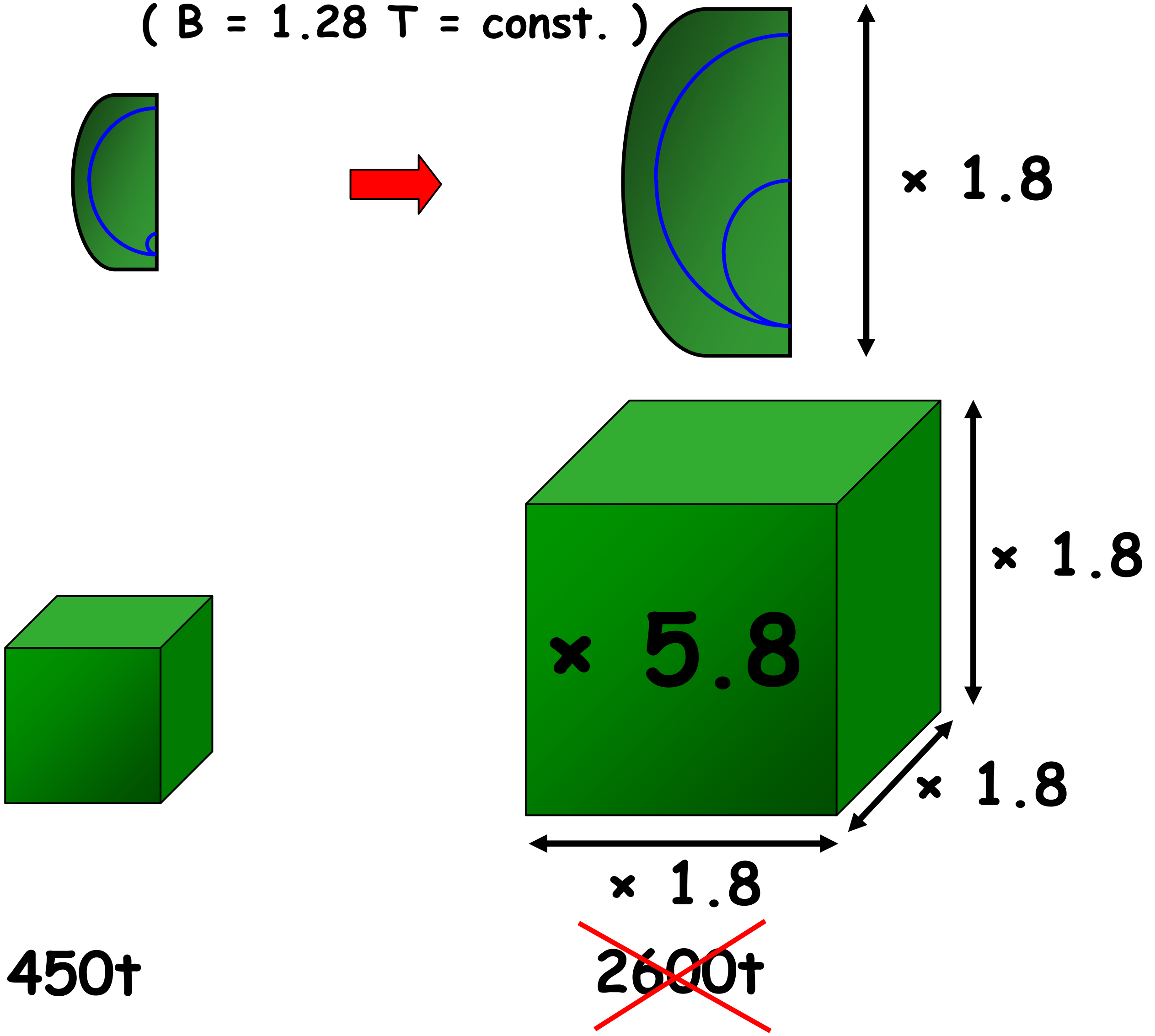

Harmonic Double Sided Microtron (HDSM) (next higher polytron) [47,48,49]

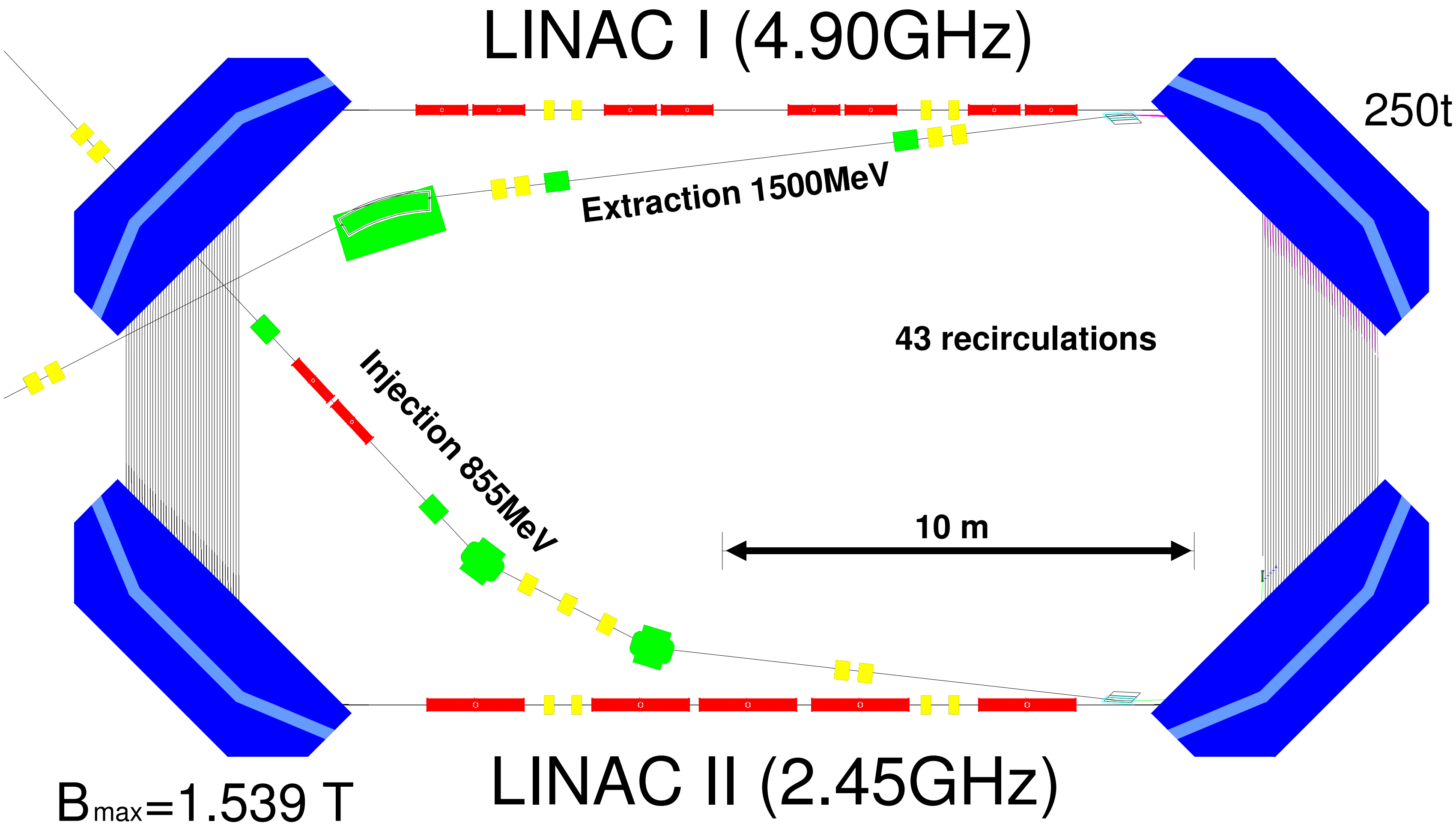

Coherence condition of a Double-Sided-Microtron:

per magnet

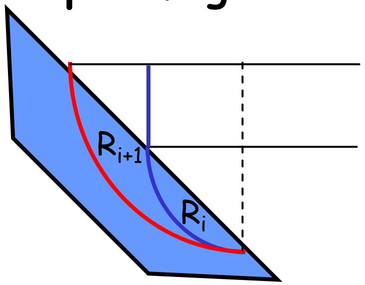

$$\Delta E = \lambda \cdot \frac{e \cdot c \cdot B}{\pi - 2}$$

$$\left\{\frac{2\pi}{4}(R_{i+1} - R_i) - (R_{i+1} - R_i)\right\} \cdot 4 = 2\cdot(\pi-2)\cdot\Delta R = 2\cdot\lambda$$

phase advance / turn
must be $2\times 2\pi$ in a DSM !

e.g.: B=1.28T, λ=0.1224m $\Rightarrow$ ΔE=41.1MeV
(with cw-sections: linac ~~~ 45m)~~

Therefore here: λ_{DSM}=0.5 · 0.1224m $\Rightarrow$ ΔE=20.5MeV

The fundamental frequency of the HDSM is
4.90GHz instead of 2.45GHz !

compensation of fringe-field defocussing ?

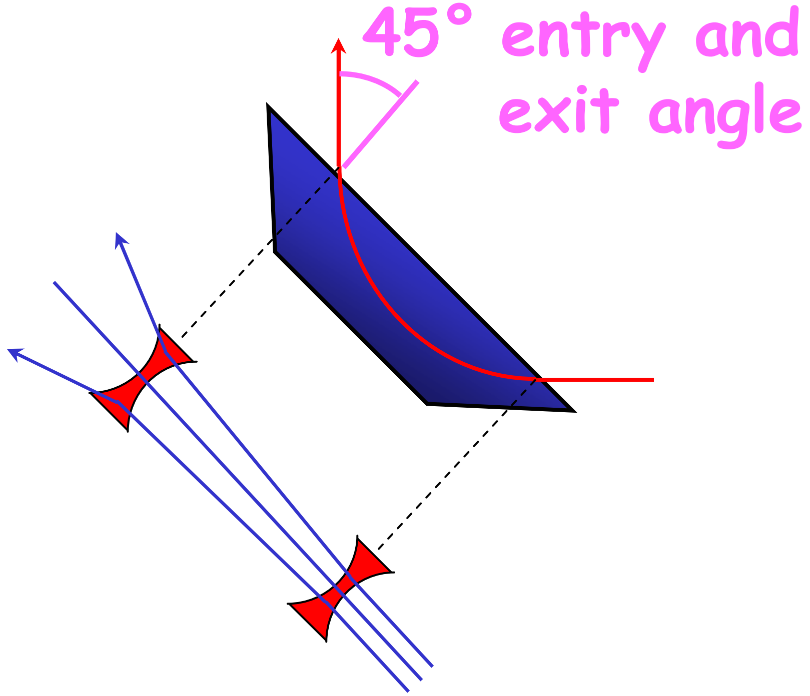

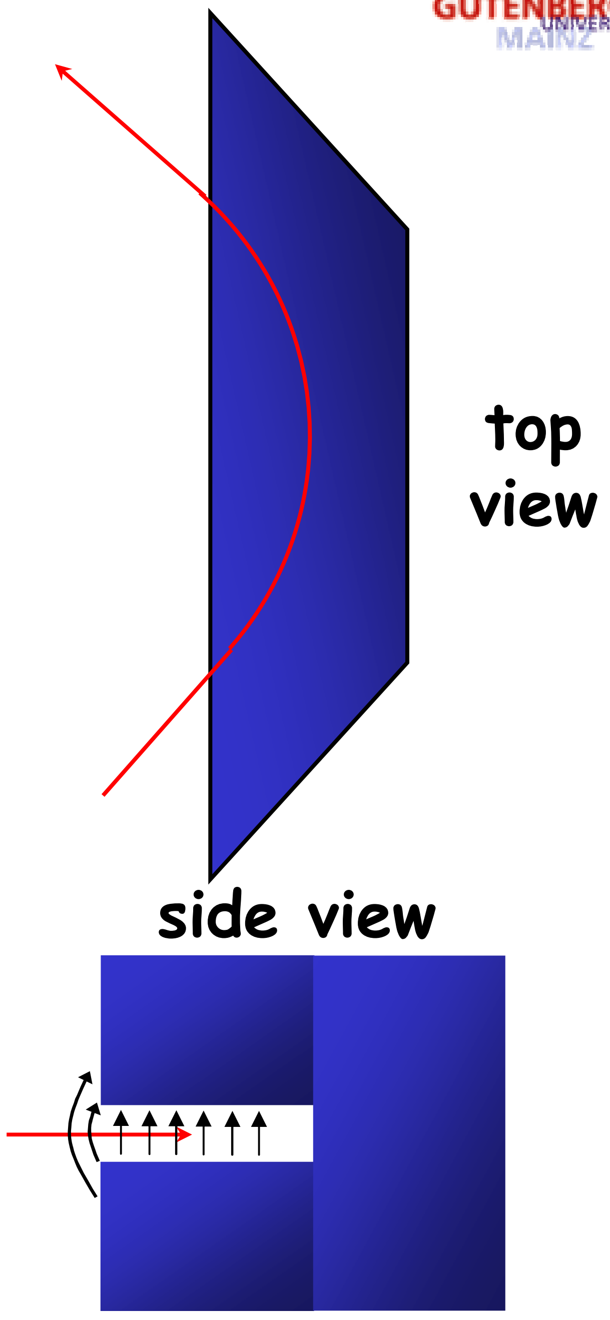

dipole with field-gradient

compensation of fringe-field defocussing !

45° entry and exit angle

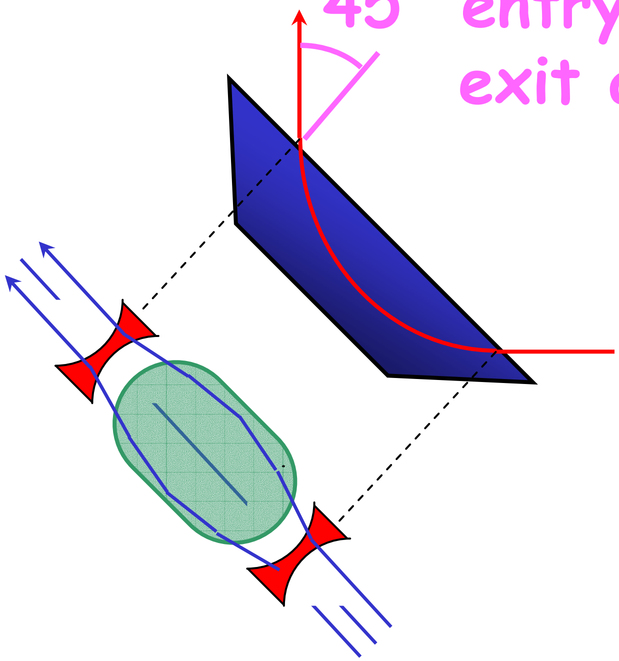

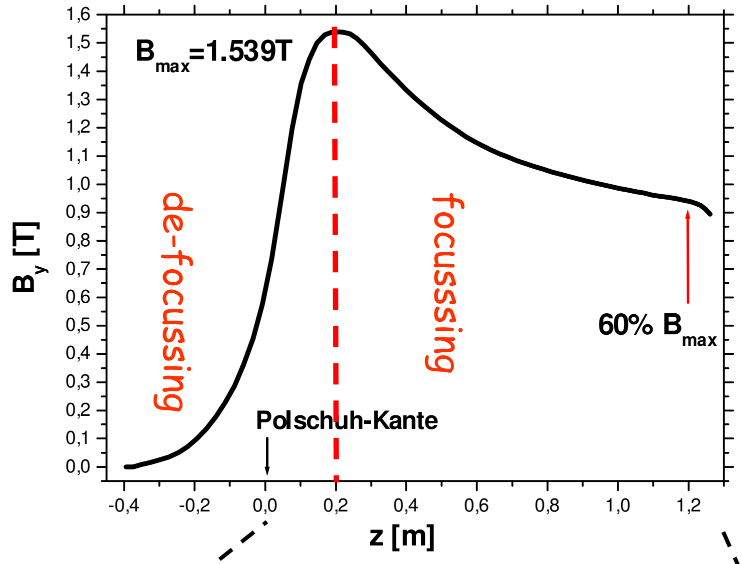

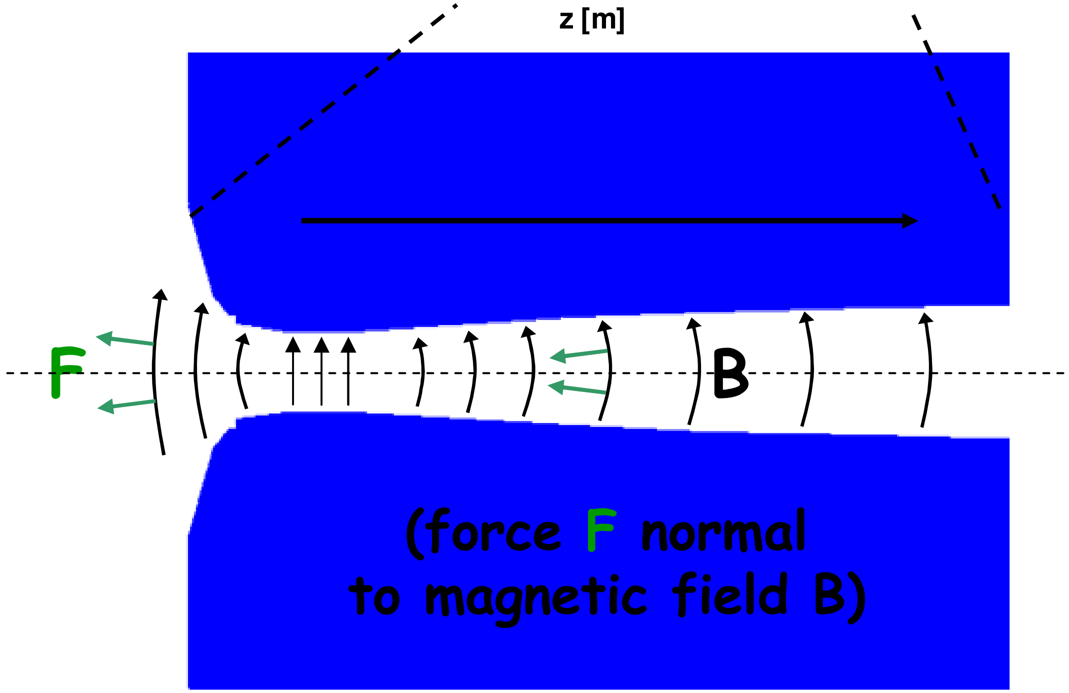

Consequences of the field gradient for the longitudinal dynamic:

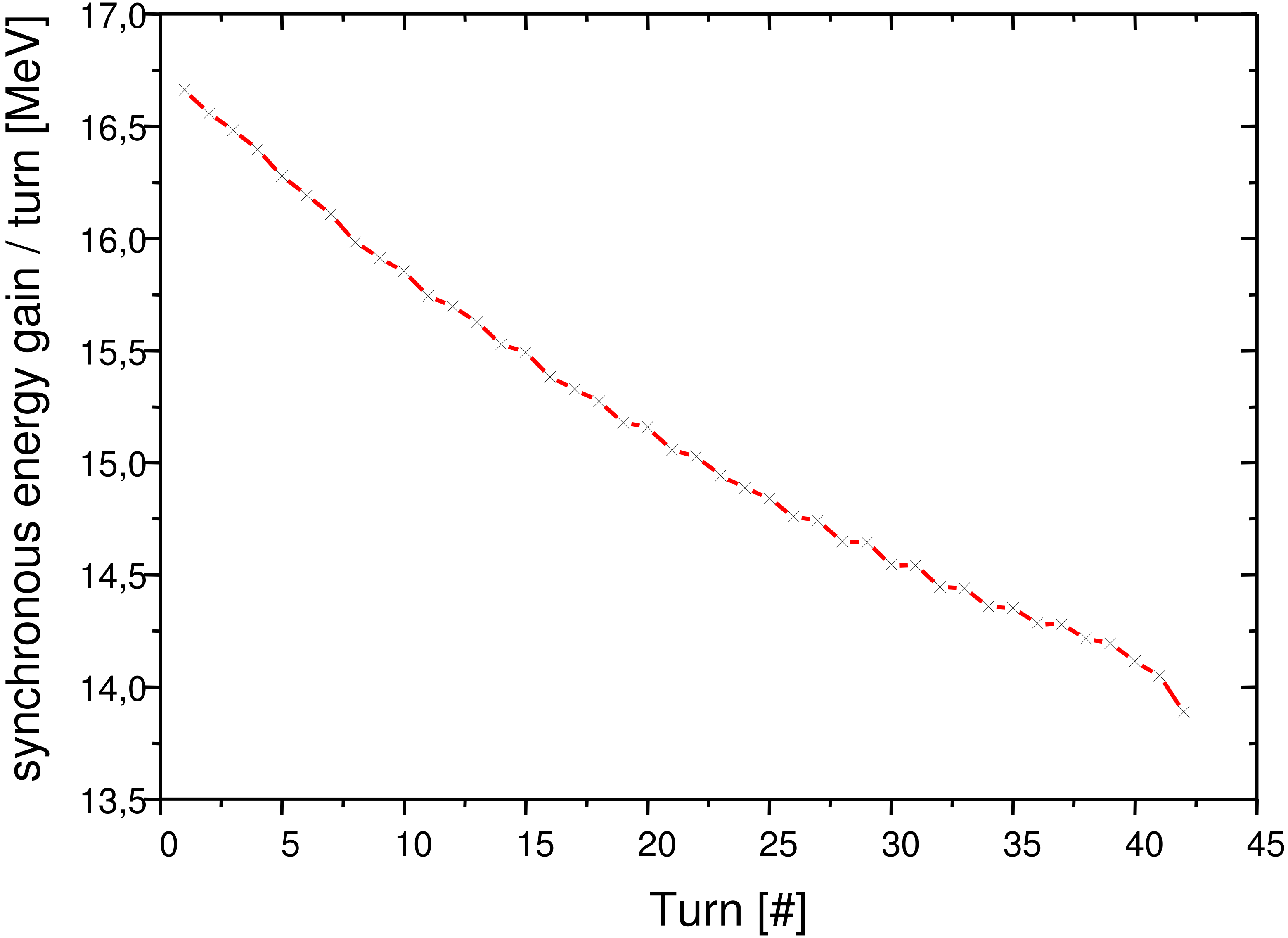

With increasing energy the beam intrudes deeper and deeper in the 90° dipoles and experiences turn by turn a relatively decreasing field-integral, which requires less energy gain per turn to fulfil the dynamic coherence condition.

less steep gradient of 2.45GHz wave
avoids reaching instable area

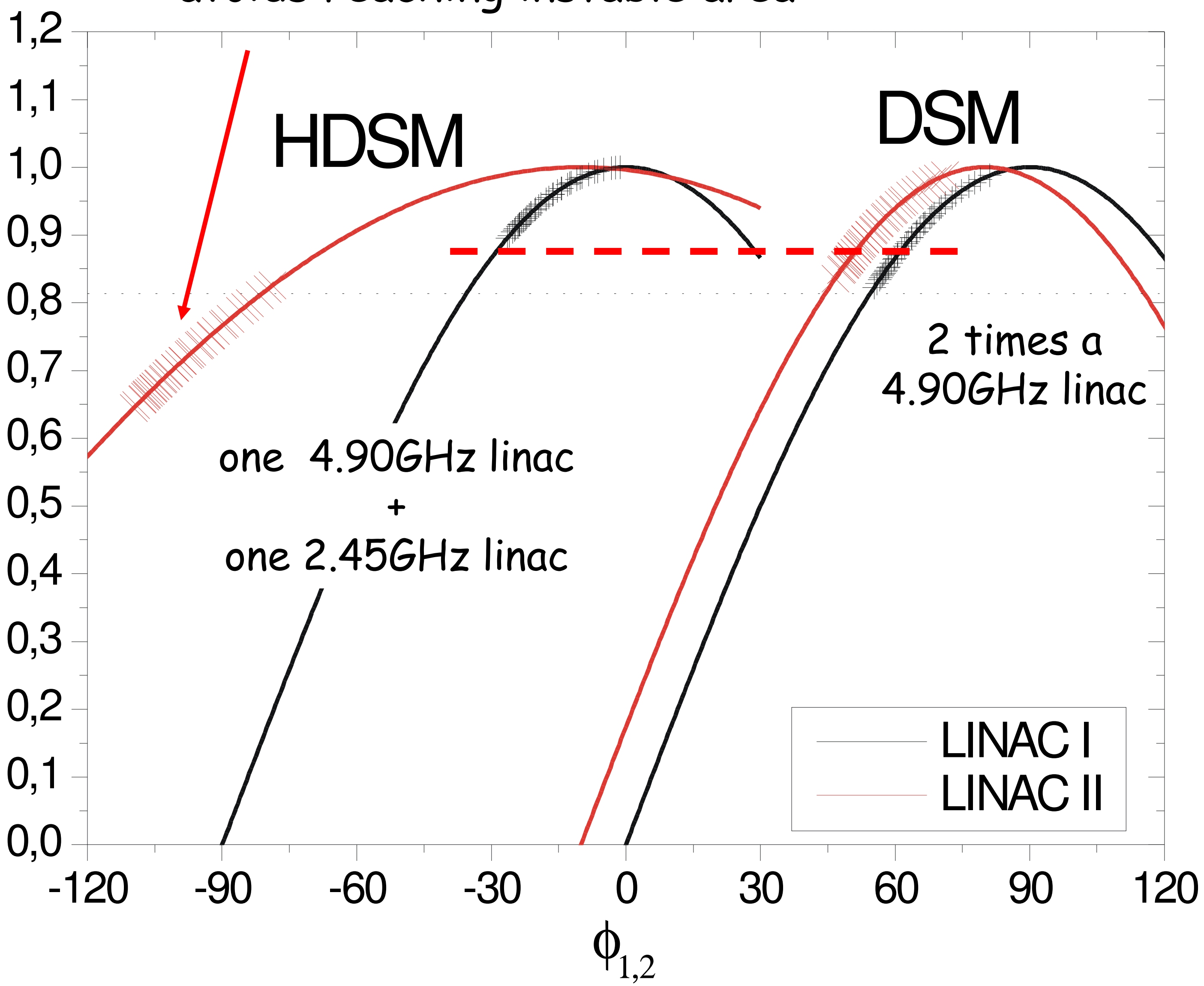

– – – instable region of longitudinal motion for 4.90GHz wave

Harmonic-operation
(for highest longitudinal beam stability)

DSM, 2 x 4.90GHz linac

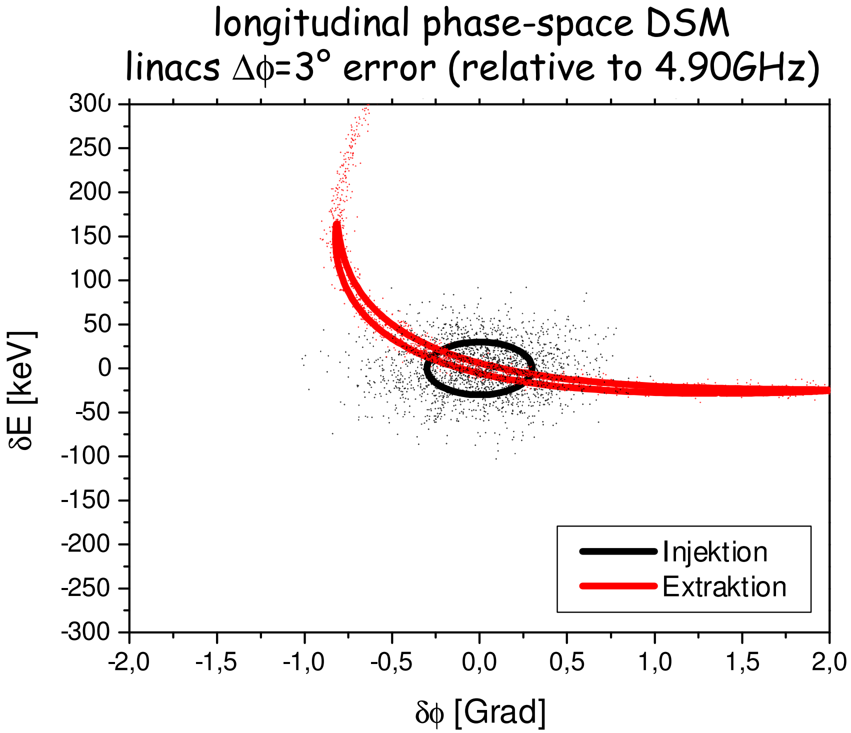

HDSM, 4.90GHz + 2.45GHz Linac

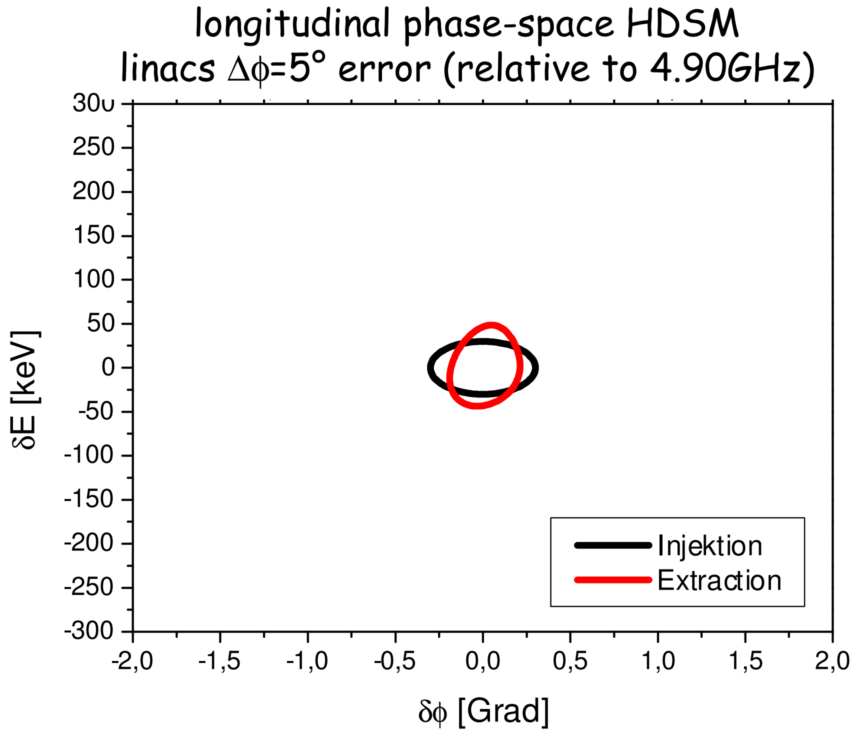

4d) sc cw Recirculating-Linacs

S-DALINAC, Technical University of Darmstadt [22,50,51]

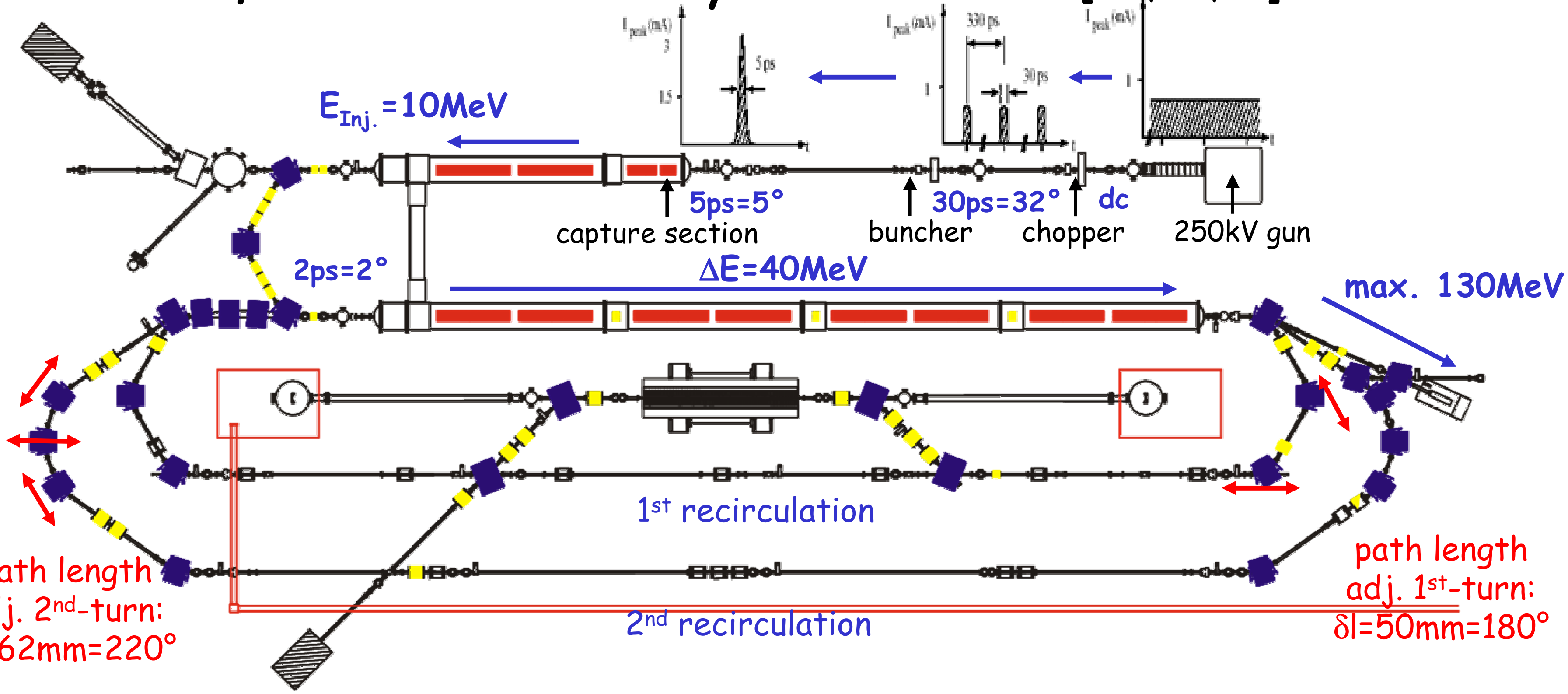

rf-system: 8 S-Band (3GHz) sc π–mode standing wave structures (see 3)) powered by 8 500W klystrons → max. 40MeV energy gain (5MeV/m)
injector: 250keV gun, max. 2mA dc-current, chopper+buncher-section (nc) followed by capture section (sc) + 2 standard modules (sc) delivers 10MeV, 2ps=2° bunch length
recirculation system: two isochronous recirculation lines with path length adjustment by moving dipoles and quadrupoles
beam parameters: cw-operation, 100MeV, 10μA (120MeV, 60μA @ 33% duty cycle), $\delta E/E \sim 2.5 \cdot 10^{-4}$ (only in "non-isochronous" mode, limited due to rf-control of phase and amplitude)

S-DALINAC is mainly used for nuclear physics experiments.

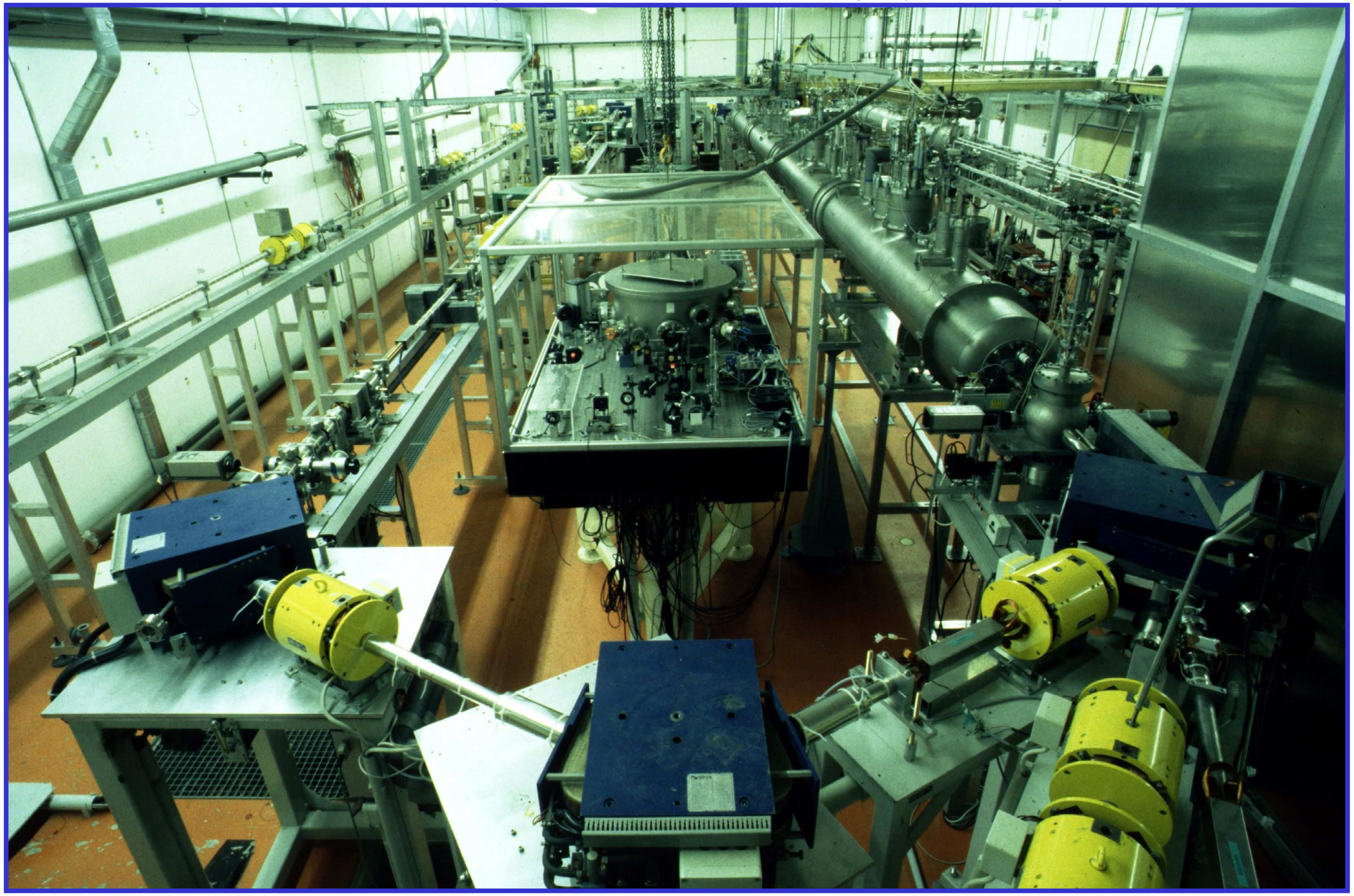

S-DALINAC also successfully serves as a driver for an infrared (λ=7-8μm) Free-Electron-Laser [50] which requires short pulses (> 1.5A peak bunch current).

Continuous Electron Beam Accelerator Facility, Jefferson Lab.

"not really" a small accelerator

[52]

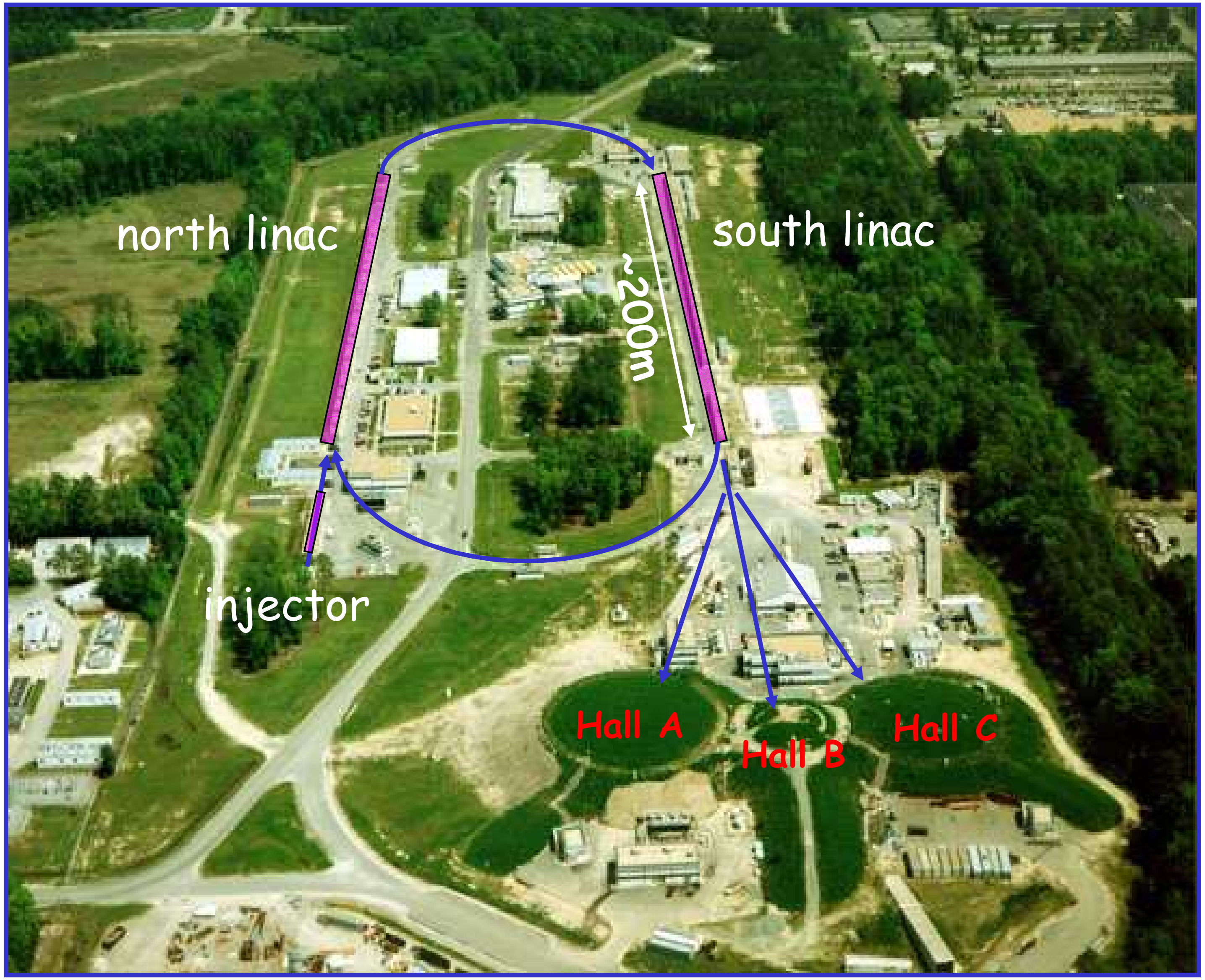

- 338 sc accelerating cavities in two linacs + injector (338 × 5kW cw klystron)
- 1.5GHz, 5 cells/cavity, 0.5m length
- $R/Q = 980\Omega$, $Q = 4\cdot10^{9}$ (T=2k) → 7.5MeV/m

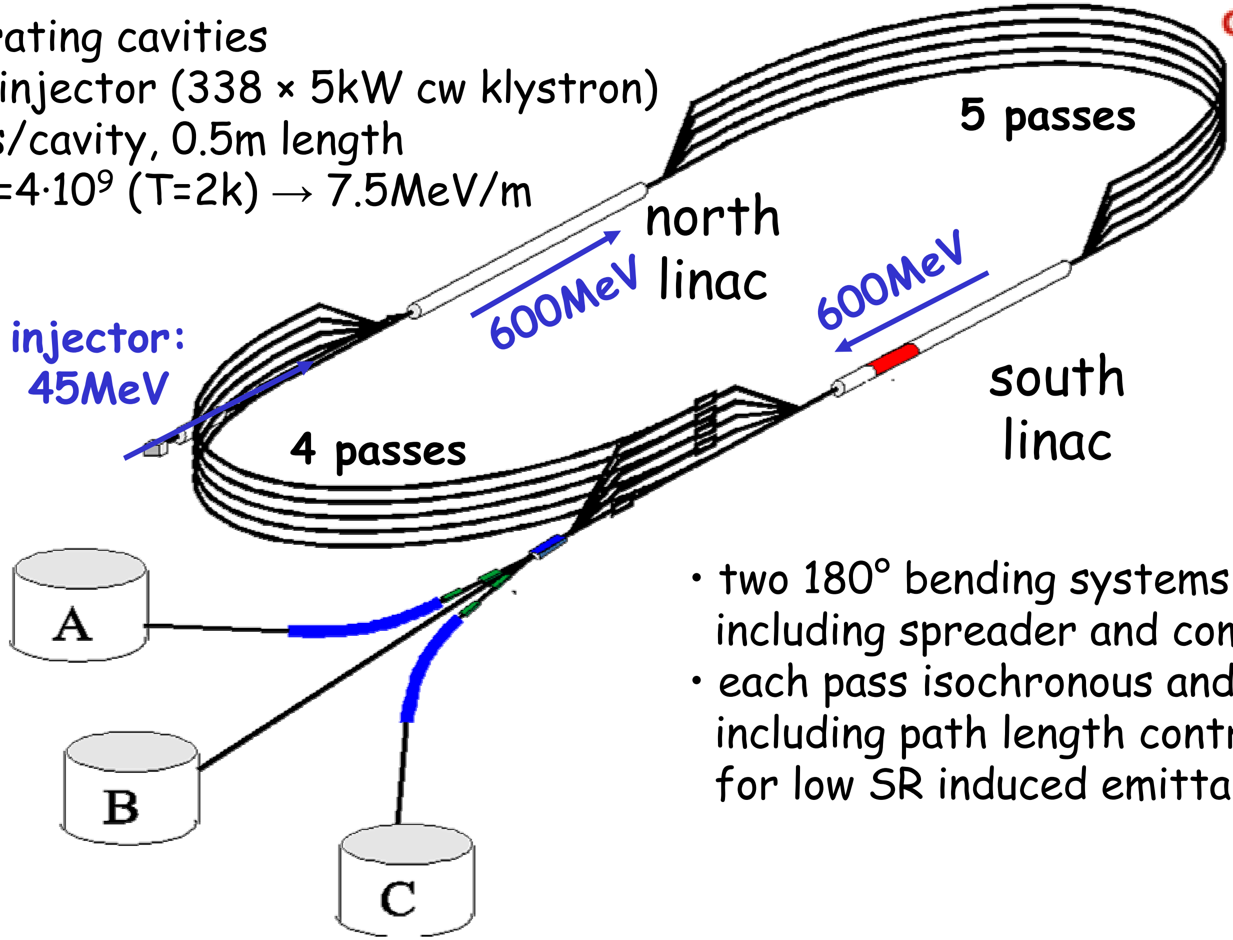

- two 180° bending systems (4 and 5 passes) including spreader and combiner
- each pass isochronous and achromatic including path length control and optimised for low SR induced emittance degradation

By using a **photo-gun** driven by **three independent laser systems** and a **sub-harmonic (500MHz) rf-separator** based extraction, it is possible to deliver **three different beam energies** into the three experimental halls with **current ratios approaching 10^6** !

ultimate beam parameters:

6GeV*), 150μA (900kW), bunch length 300fs (0.16°), $\delta E/E \sim 2.5\cdot10^{-5}$ **)

*) A program is under way to increase the energy to 12GeV [23] by adding 10 new cryomodules with 17.5MV/m gradient, each supplying additional 100MV (1GV in total) to the linacs.

**) This defines strict requirements for the injector performance, amplitude/phase control of all cavities and control of the arc optics.

5) Energy Recovering Linacs (ERL) [53]

A very hot topic! Lot's of work is done on this field and many projects are under development (ERL as the 4thgeneration light source) ! Here only some very basic ideas and one example.

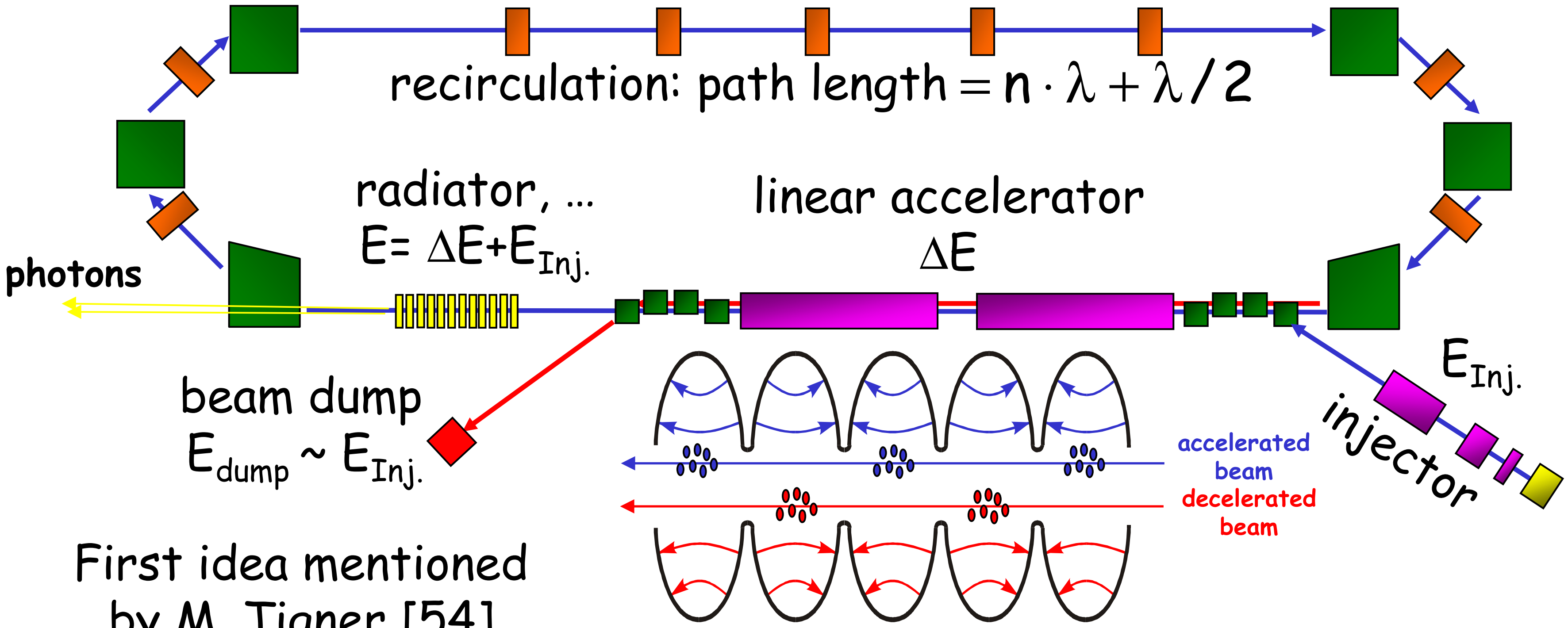

First idea mentioned by M. Tigner [54]

By setting the recirculation path length to be an integer wavelength plus half a wavelength, the beam re-enters the linac, when the electrical fields decelerate the beam. By that energy is back-transferred to the rf-fields in the cavity and the accelerating fields are self-preserving by the closed loop of the recirculated-beam !

First demonstration*) of energy recovering at Stanford SCA/FEL (sc) [55].
Some preliminary tests at MIT-BATES linac (nc) [34].

Parameter to quantify the efficiency of energy-recovery:

"rf to beam multiplication factor"

$$\kappa = \frac{I_{beam} \cdot (\Delta E + E_{Inj})}{I_{beam} \cdot E_{Inj.} + P_{rf,linac}} \sim \frac{P_{beam}}{P_{Rf}}$$

the energy of the injector,
which can not be recovered

$\kappa \sim 0.1$ or less (nc) / $\kappa \gg 1$ (up to some 100 seems possible) (sc)
(for single pass linacs always $\kappa < 1$)

Hold in mind: P_{beam} is some kind of "virtual" beam power. It is not available as external beam power, but it can be used e.g. in radiators (wiggler/undulator-magnets) to produce synchrotron radiation ! (like storage ring synchrotron radiation sources with e.g. 300mA@2.4GeV = 720MW "beam power")

*) First realisation (without drawing attention to it) in a reflexotron called linac for medical applications designed at Chalk River Nuclear Labs. [56].

The Jefferson Lab. IR Demo FEL [57]

sc cavities based on CEBAF technology

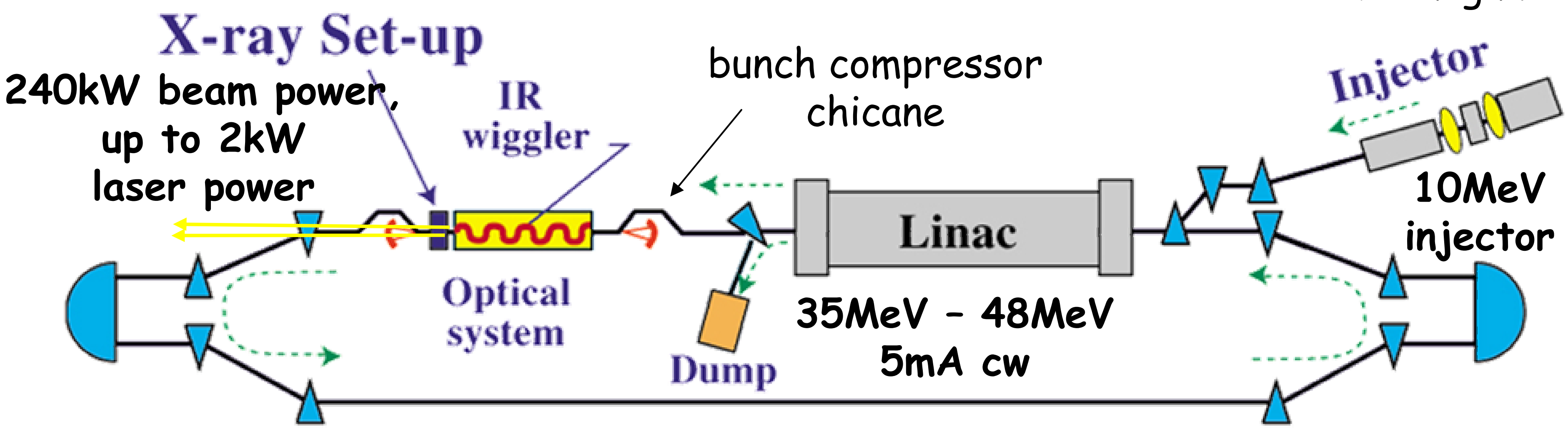

$\kappa \cong 16$!

(not taking into account the injector power)

bunch length before wiggler:
0.4ps = 60A peak bunch current

challenges:

After FEL interaction the beam energy spread reaches 6-8%. This beam must be transported isochronous through the recirculation system and decelerate through the linac. This requires to control also the higher order contributions to the longitudinal dispersion !

The IR-FEL was upgraded to 10kW laser power:
This requires 150MeV beam energy with 5mA current (750kW beam power).

Demonstration of energy recovery: drive power signal

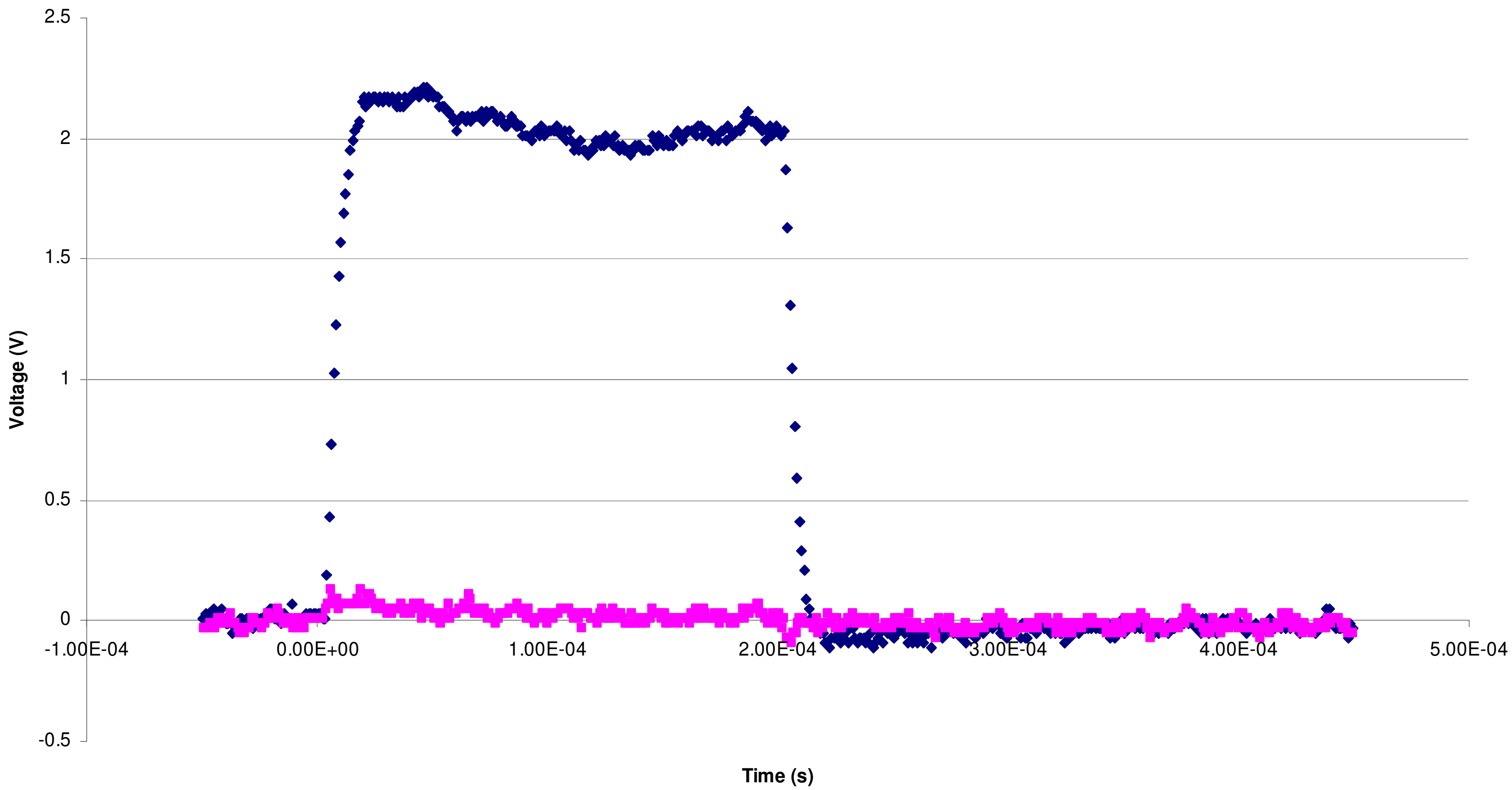

Courtesy:
Lia Merminga, JLab

The future: ERL based light sources [58,59]
e.g. Cornell University Phase II X-ray SR Source Conceptual Layout

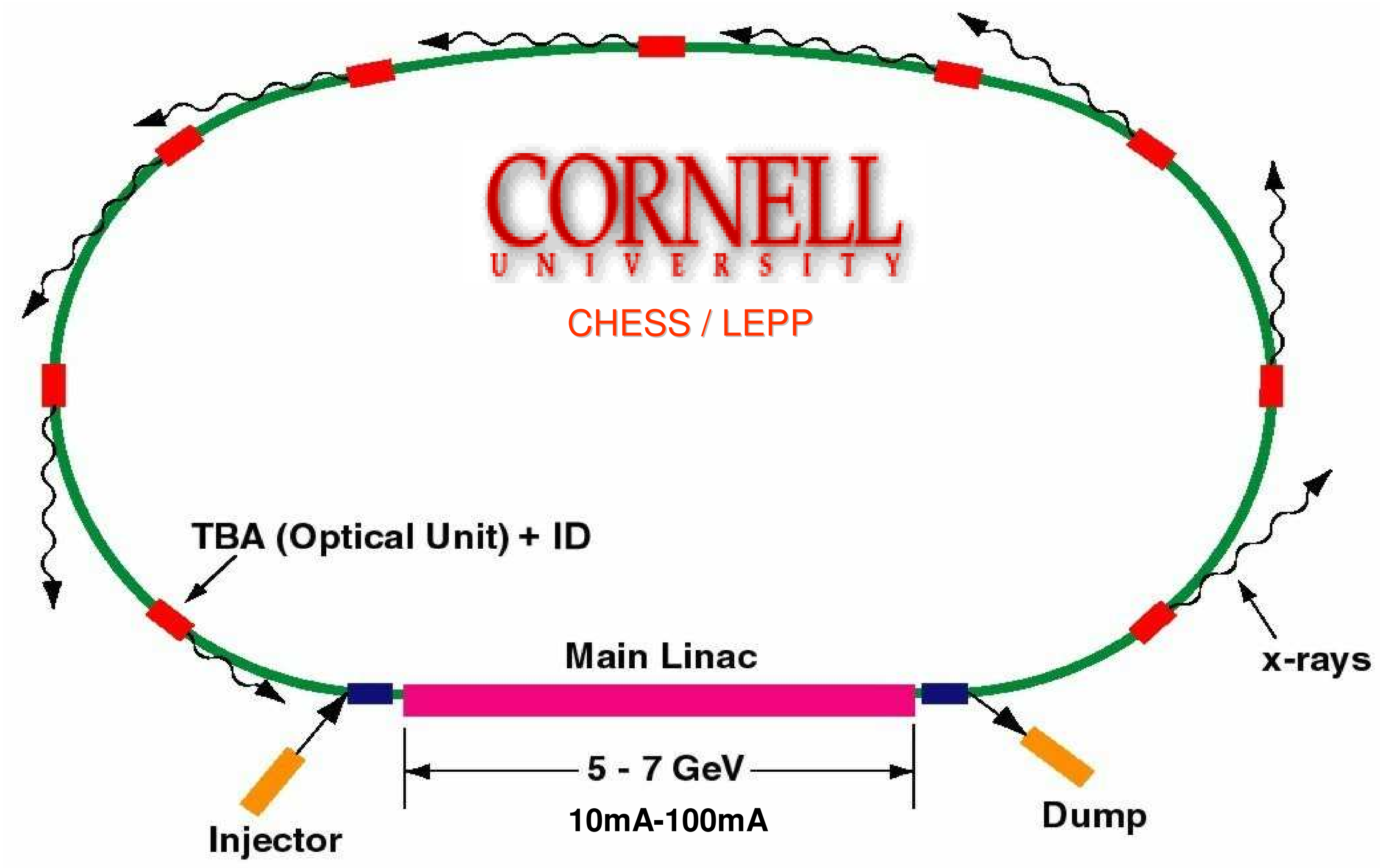

General remarks on energy recovering linacs:

- modern light sources are mainly limited due to their rather "large" natural bunch length and transverse horizontal emittance (sr-quantum excitation, collective effects)
- modern linacs are superior concerning their beam quality because their injectors (guns) can deliver beams with very small emittances and the bunch-length can be controlled by bunch compressors (aside coherent-synchrotron-radiation (csr) - effects)
- with a single pass linac the average beam power of a storage ring in the order of several 100MW is beyond any reach
  $\rightarrow$ energy recovering is mandatory
- in energy recovering linacs beam powers exceeding a factor of 100 of the rf-drive power are possible
- an energy recovering linac needs typically a very powerful injector (~10MeV, ~100mA = ~1MW), which is also capable to deliver a beam with very short ($<$ ps) pulse lengths and transverse emittance ~ π mm mrad
- the isochronous recirculation arc needs to be able to handle a beam, which after the interaction with the radiators has typically an energy-spread in the order of several %. This needs a tight control of beam optical parameters even in higher orders.
- high beam energies need long linacs, which raises the problem to design a linac axis beam optics which allows to transport beams with big energy differences (E_{out}/E_{in} ~ some 100)

Bibliography

Related Monographs

[A] Roy. E. Rand, "Recirculating Electron Accelerators", Harwood Academic Puplishers, Chur, CH, 1984

[B] David C. Carey, "The Optics of Charged Particle Beams", Harwood Academic Puplishers, Chur, CH, 1992

[C] Klaus Wille, "Physik der Teilchenbeschleuniger und Synchrotronstrahlungsquellen", 2. Auflage, Teubner, Stuttgart, D, 1996 and Klaus Wille, "The Physics of Particle Accelerators", Oxford University Press, USA, 2001

[D] H. Wiedemann, "Particle Accelerator Physics" Vol. I+Vol. II, Springer Berlin Heidelberg (1993, 1995)

Microtron

Basic Idea:

[1] W.J. Veksler, Dokl.Ak.Nauk., 43, 346 (1944) (in russian) and "A new method of acceleration of relativistic particles", Jour.Phys. USSR., 9, p.153 (1945)

[2] E.M. McMillan, "The synchrotron – a proposed high energy particle accelerator", Phys.Rev., 68, p.143 (1945)

[3] L.I. Schiff, "Production of particle energies beyond 200MeV", Rev.Sci.Instrum., 12, p.6 (1946)

[4] J. Itho et al., "Harmonic resonance accelerator-microtron", Sci.Papers Osaka U., No. 12 (1949)

First operating microtron:

[5] W.J. Henderson et al., "A magnetic resonance accelerator for electrons", Nature, 162, p.699 (1948)

Improvement of classical microtron

[6] S.P. Kapitza, V.N. Melekhin et al., Zh. Eksp. Teor. Fiz., 41, 368 (1961) and Sov.Phys.JETP, 14, p.268 (1962)

Standard reference microtron:

[7] S.P. Kapitza and V.N. Melekhin, "The microtron", Harwood Academic Puplishers, London (1978)

[8] S.P. Kapitza, "The microtron and its fields of Application", Journal of Nuclear Energy Part C, 8, p.183 (1966)

Race-Track-Microtron

[9] E.M. Moroz, "A cyclotron with sectional magnets", Sov.Phys.Doklady, 1, p.326 (1956)

[10] A. Roberts, "The microtron as a high-energy, high current particle accelerator", Ann. of Phys., 4, p.115 (1958)

[11] E. Brannen, H.R. Froehlich, "Preliminary operation of a four-sector racetrack microtron", J.Appl.Phys., 32, p.1179 (1961) and also H.R. Froehlich, E. Brannen, "Four-sector racetrack microtrons", IEEE Trans.Nucl.Sci., NS-14, p.756 (1967)

[12] H. Babic, M. Sedlacek, Nucl.Instr.&Meth., 56, p.170 (1967)

[13] H. Herminghaus et al., "The design of a cascaded 800MeV normal conducting c.w. race track microtron", Nucl.Instr.&Meth., 138, p.1 (1976)

[14] M.A.D. Wilson, "cw racetrack microtrons", Proc. PAC1991, London, UK, p.71 (1991)

Recirculating Linac
[15] T.I. Smith et al., Los Alamos Conf. LA-3609, TID4500, p.491 (1966)
[16] E. Jones, Stanford Publication, HEPL 609 (1969)
[17] R.E. Rand, IEEE Trans. NS-20, No. 3, p.938 (1973)
[18] H. Herminghaus, "On the inherent stability of non-isochronous recirculating accelerators", Nucl.Instr.&Meth. in Ph.Res., A314, p.209 (1992)

Rf-system
[19] H. Euteneuer et al., "Experiences in fabricating and testing the rf-sections of the mainz microtron", Proc. LINAC1986, Stanford, USA, SLAC Report-303, p.508 (1986)
[20] M. Schmitz, "The S-band linear collider test facility at DESY", Proc. PAC1997, Vancouver, Canada, p.569 (1997)
[21] J. Labrie et al., "Power handling capability of water cooled cw linac structures", Nucl.Instr.&Meth. in Ph.Res., A247, p.281 (1986)
[22] A. Richter, "Operational experience at the S-DALINAC", Proc. EPAC1996, Sitges, Spain (1996)
[23] L. Harwood, "Upgrading CEBAF to 12GeV", Proc. PAC2003, Portland, Oregon, USA p.586 (2003)
[24] R. Brinkmann et al. (editors), "TESLA – technical design report", Vol. II, DESY, ECFA 2001-209, TESLA Report 2001-23 (2001)
[25] B. Barish et al., "International technology recommendation panel (ITRP) final report", www.ligo.caltech.edu/~skammer/ITRP_Home.htm

Examples
[26] P. Lidbjörk et al., "A 100MeV racetrack-microtron", PAC1983, IEEE Trans. NS-30, No. 4, p.2068 (1983)
[27] M. Eriksson, "A 100MeV injector race-track microtron for the MAX strorage-ring/pulse stretcher", PAC1983, IEEE Trans. NS-30, No. 4, p.2070 (1983)
[28] R. Alvinsson, M. Eriksson, Royal Inst. of Tech., Stockholm, Report TRITA-EPP-76-07 (1976)
[29] G.A. Webers et al., "Optical design of the 75MeV Eindhoven racetrack microtron", Proc. PAC1993, London, GB, p.2062 (1993)
[30] W.H.C. Theuws et al., "Continous electron-energy variation of the Eindhoven racetrack microtron", Proc. EPAC1998, Stockholm, Sweden, p.1036 (1998)
[31] V.I. Shvedunov, "70MeV electron racetrack microtron commissioning", Proc. PAC2001, Chicago, USA, p.2596 (2001)

[32] J. Haimson, "A high duty factor 400MeV high resolution electron linear accelerator", Proc. High Energy Acc., Yerevan, Vol. 1, p.244 (1970)
[33] J. Haimson, "Initial operation of the MIT electron linear accelerator", IEEE Trans. Nucl. Sci., NS-20, No.3, p.914 (1973)
[34] J.B. Flanz et al., "Tests with an isochronous recirculation system", IEEE Trans. Nucl. Sci., NS-32, No.5, p.3213 (1985)
[35] Â. Andersson et al., "Status of the new injector for MAX-LAB", Proc. EPAC2002, Paris, France, p.772 (2002)
[36] S. Werin et al., "Commissioning of the 500MeV injector for MAX-LAB", Proc. EPAC2004, Lucerne, Switzerland, p.219 (2004)
[37] L.M. Young, IEEE Trans. Nucl. Sci., NS-20, No.3, p.81 (1973)
[38] P. Axel et al., IEEE Trans. Nucl. Sci., NS-24, No.3, p.1133 (1977)
[39] O. Hanson, Charlottesville Conf. Paper Q (1979)
[40] V.A. Volodin et al., IEEE Trans. Nucl. Sci., NS-22, No.3, p.1194 (1975)
[41] H. Herminghaus et al., "Beam blow up in race track microtrons", Nucl.Instr.&Meth., 163, p.299 (1979)
[42] G.A. Krafft, "Two dimensional simulations of multipass beam breakup", Proc. PAC1987, Washington, USA, p.1356 (1987)
[43] H. Euteneuer et al., "Experiences with the 855MeV RTM-cascade MAMI", Proc. EPAC1992, Berlin, Germany, p.418 (1992)
[44] A.W. Chao, M. Tigner (editors), "Handbook of accelerator physics and engineering", World Scientific, Singapore (1998)
[45] H. Euteneuer et al., "Beam measurements and operating experience at MAMI", Proc. EPAC1994, London, GB, p.506 (1994)
[46] M. Seidel et al., "High precision beam energy stabilisation of the Mainz Microtron MAMI", Proc. EPAC2000, Wien, Austria, p.1930 (2000)
[47] H. Herminghaus, "From MAMI to the polytrons – microtrons in the 10 GeV range", Proc. EPAC1992, Berlin, Germany, p.247 (1992)
[48] S. Ratschow, "Strahldynamische Untersuchungen zu einem Doppelseitigen Mikrotron als vierte Stufe von MAMI", Ph.D. thesis, Institut für Kernphysik, Universität Mainz, Mainz, Germany (2000) in german
[49] A. Jankowiak et al., "Design and status of the 1.5GeV-harmonic double sided microtron for MAMI", Proc. EPAC2002, Paris, France, p.1085 (2002)

[50] M. Brunken et al., "Latest developments from the S-DALINAC and its free-electron-laser", Proc. EPAC1998, Stockholm, Sweden, p.403 (1998)
[51] S. Watzlawik et al., "Latest Developments at the S-DALINAC", Proc. LINAC2002, Gyeongju, Korea, p.323 (2002)
[52] Ch. Leemann et al., "The continous electron beam facility: CEBAF at the Jefferson Laboratory", Annual Review of Nuclear and Particle Science, 51, p.413 (2001)

Energy recovering linacs

[53] L. Merminga et al., "High-current energy-recovering electron linacs", Annual Reviews of Nuclear and Particle Science, 53, p.387 (2003)
[54] M. Tigner, Nuovo Cim., 37, p.1228 (1965)
[55] T.I. Smith, "Development of the SCA/FEL for use in biomedical and materials science experiments", Nucl.Instr.&Meth., NIMA259, p.1 (1987)
[56] S.O. Schriber et al., IEEE Trans.Nucl.Sci., NS-24, p.1061 (1977)
[57] M. Shinn et al., Proc. SPIE3902, p.355 (2000)
[58] L. Merminga, "Physics challenges for ERL light sources", Proc. EPAC2004, Lucerne, Switzerland, p.16 (2004)
[59] G.H. Hoffstaetter et al., "ERL upgrade of an existing x-ray facility: CHESS at CESR", Proc. EPAC2004, Lucerne, Switzerland, p.497 (2004)

Especially many thanks to
H.-D. Gräf, S-DALINAC, TU-Darmstadt and G.A. Krafft, Jefferson Lab.
for providing many useful informations and graphs,
H. Euteneuer for carefully reading the manuscript.